ARMY RESEARCH LABORATORY

Interior Ballistics Modeling: Extensions to the One-Dimensional XKTC Code and Analytical Studies of Pressure Gradient for Lumped Parameter Codes

by Paul S. Gough

ARL-CR-460 February 2001

prepared by

Paul S. Gough
Paul Gough Associates
1048 South Street
Portsmouth, NH 03801-5423

Under contract

DAAK11-85-D-0002

The findings in this report are not to be construed as an official Department of the Army position unless so designated by other authorized documents.

Citation of manufacturer's or trade names does not constitute an official endorsement or approval of the use thereof.

Destroy this report when it is no longer needed. Do not return it to the originator.

Army Research Laboratory
Aberdeen Proving Ground, MD 21005-5066

ARL-CR-460 **February 2001**

Interior Ballistics Modeling: Extensions to the One-Dimensional XKTC Code and Analytical Studies of Pressure Gradient for Lumped Parameter Codes

Paul S. Gough
Paul Gough Associates

Abstract

We describe a number of extensions to the XNOVAKTC (XKTC) Code, a model of interior ballistic phenomena based on a numerical solution of the governing equations for one-dimensional, multi-phase flow. We also present some analytical formulations for the pressure gradient in a gun in a form suitable for incorporation into a lumped parameter interior ballistics model.

In XKTC, the flow resistance formula for stacked granular propellant is extended to account for the increase in drag due to tumbling of the grains as the bed expands. The code is also extended to permit the analysis of the consequences of propellant fracture, with fracture taken to be dependent on the local maximum intergranular stress. An explicit representation of the impact induced granular compaction wave as a surface of discontinuity is encoded to support the fracture analysis.

The analytical formulas for the pressure gradient include the effects of tube geometry and several aspects of the structure of the two-phase flow. The results are in a closed form with the breech and base pressure explicitly related to the spacemean pressure. Results are presented for both granular and stick propelling charges.

Preface

The enclosed report is presented in its original form as received from the contractor and without editorial change.

INTENTIONALLY LEFT BLANK.

Table of Contents

		Page
	Preface	iii
	List of Figures	vii
	List of Tables	vii
1.	**Introduction**	1
2.	**Revisions to XKTC Governing Equations**	3
2.1	Flow Resistance of Stacked Granular Propellant	3
2.2	Analysis of Grain Fracture	5
2.2.1	*Balance Equations for a Two-Phase Lumped Parameter Region*	6
2.2.2	*Constitutive Relations*	8
2.2.3	*Coding Considerations*	12
3.	**Pressure Gradient in Gun Propelling Charges**	14
3.1	Non-Uniform Bore Area	18
3.2	Propellant Velocity Lag	25
3.3	Area a Function of Position and Time	39
3.4	Combined Effects of Area and Propellant Lag	42
	References	49
	Appendix A: XNOVAKTC (XKTC)—Structure and Use	51
	Distribution List	161
	Report Documentation Page	171

INTENTIONALLY LEFT BLANK.

List of Figures

Figure		Page
A.1	Nomenclature for Definition of Charge Configuration in XKTC With MODET = 0	59
A.2	Nomenclature for Definition of Charge Configuration in XNOVAT With MODET = 1	60
A.3	Example of a Hybrid Charge Consisting of Conventional and Traveling Charge Increments	61
A.4	Example of Hybrid Charge Consisting of Traveling Liquid Propellant and Solid Propellant Booster	62

List of Tables

Table		Page
A.1	Summary of Routines and Linkages	68
A.2	Summary of XKTC "Mandatory" Input Files	86
A.3	Summary of XKTC Contingent Input Files	87
A.4	Summary of XKTC Traveling Charge Input Files	91
A.5	Summary of XKTC Traveling Liquid Charge Input Files	92
A.6	Description of Input Files	93

INTENTIONALLY LEFT BLANK.

1.0 INTRODUCTION

A first objective of this report is to document certain extensions which have been made to the XNOVAKTC (XKTC) Code (Gough, 1990). The XKTC Code is intended to provide digital simulations of the interior ballistics of a wide range of gun propelling charges with particular emphasis on the influence of propellant packaging and distribution on the processes of flamespreading and pressure wave formation. Like all versions of the NOVA Code, (Gough, 1980a) from which it is derived, XKTC is based on a numerical solution of the governing equations for the macroscopic, quasi-one-dimensional flow defined by the solid propellant and its products of combustion. A second objective of this report is to document certain closed form analytical results which describe the effects of tube geometry, and the structure of the two-phase flow, on the pressure gradient in the gun. These results which relate the breech, base and spacemean pressures are intended to be of use in lumped parameter models of interior ballistics.

The analytical results pertaining to the pressure gradient are presented in Section 3.0. The balance of this introduction is concerned with the XKTC Code.

The XKTC Code is based on the balance equations for macroscopically one-dimensional two-phase flow. The state variables are to be thought of as averages of the local values or microproperties. Intractable microflow details such as drag, heat transfer and propellant combustion are assumed to be related to the macroscopic variables by means of empirical correlations. The resulting equations for each of the two phases -- the solid propellant and its products of combustion -- resemble the equations for unsteady flow through a duct of variable cross-sectional area. The effective cross-section for each phase incorporates the porosity or fraction of a unit volume occupied by the gas-phase. The governing equations are solved by the method of finite differences with an explicit allowance for the discontinuities in the state variables at the internal boundaries defined by the ends of the increments. Appendix A may be consulted for details of the scope of application of the Code.

The XKTC Code is the latest in a series of codes in the NOVA family of which that of Gough (1980a), may be taken as the first generally available version. The XNOVA Code (Gough, 1983) was developed to take advantage of more efficient computational procedures which had been developed in related studies. XNOVA was intended as an express version of NOVA and deleted a number of little-used options. The XNOVAK Code (Gough, 1984) was an extension of XNOVA to include finite-rate chemistry in the gas-phase. XNOVAK was itself extended to become first XNOVAT (Gough, 1985), which included various features pertinent to the tank gun, but not linked to the chemistry model, and subsequently XKTC (Gough, 1990), which included additional details pertinent to tank charges and provided a full linkage of the tank gun and chemistry options. The current version of XKTC includes

certain additional features as discussed in Section 2.0. Moreover, it includes features developed under other contracts, namely the modeling of in-bore rockets (Gough, 1988a); the modeling of a traveling liquid charge (Gough, 1988b); the modeling of electrothermal guns (Gough, 1992, 1993); and alternative representations of the thermochemistry of the propellant to model near-field combustion (Gough, 1995).

Reference may be made to Gough (1990) for a statement of the balance equations for XKTC and to other sources for details of revisions to the various code options (Gough, 1998b, 1991, 1992, 1993).

The code description given in Appendix A is comprehensive and includes the contributions of all studies to date.

2.0 REVISIONS TO XKTC GOVERNING EQUATIONS

Two topics require documentation here. In Section 2.1 we discuss revisions to the analysis of flow resistance in a bed of stacked granular propellant. In Section 2.2 we review the analysis of grain fracture with emphasis on the representation of the compression wave formed by impact on the projectile base as an explicit surface of discontinuity.

2.1 Flow Resistance of Stacked Granular Propellant

Ordinarily, granular propellant is loaded in a randomly packed fashion with the result that the flow resistance is large and the probability of pressure wave anomalies is increased. A stacked granular propellant bed involves a careful arrangement of the grains so that well defined axial flow channels are created. Such an arrangement allows charges of highly progressive multiperforated grains to have the low flow resistance typical of stick propellant while avoiding the possibility of propellant rupture due to overpressurization of the perforations which would occur in long sticks.

It is assumed that the flow resistance for stacked granular propellant is similar to that of stick propellant when the propellant is initially loaded into a configuration which creates well organized axial flow channels. However, as the propellant burns and moves it is expected that the original well ordered configuration will be lost. The grains will tumble and eventually the aggregate will develop the random structure associated with ordinary granular propellant. To capture the variation of the flow resistance with the changing structure of the aggregate, we consider the ratio of the volume per grain to the volume of a sphere in which the grain may freely rotate. The dynamics of the rearrangement of the structure of the aggregate are not modeled explicitly. It is assumed that when the ratio has the initial value one or less, the aggregate is well organized due to the confinement imposed on each grain by its neighbors and that the flow resistance is therefore essentially that of a geometrically equivalent stick charge. For generality, as we see below, we admit the possibility that some fraction of the randomly packed bed flow resistance is experienced even when the bed is well ordered. When the volume ratio exceeds one, each grain is free to rotate and we assume that the aggregate becomes randomly structured so that the flow resistance is that of an ordinary granular bed. For intermediate values of the ratio, we simply interpolate between the resistance of the stick charge and that of the granular charge. In practice, the bed is fully ignited prior to any significant expansion. Since the flow resistance of a stick charge is taken to be zero in the XKTC Code, its contribution is neglected in the intermediate regime where interpolation is involved.

The volume per grain is $V_{p_e}/(1 - \varepsilon_e)$ where V_{p_e} is the superficial or exterior volume of the grain and ε_e is the exterior porosity computed by neglecting the presence of the perforations. We take the volume for free rotation to be $4/3\pi L^3$ where L is the length of the grain, presumably its

largest dimension. The volume for free rotation is evidently that of a sphere with radius equal to L. This is thought to be a conservative estimate of the volume. One could make a case for the use of L as the diameter of the sphere which would lead to an earlier occurrence of the prediction of randomization of the aggregate. However, the use of the smaller estimate implies a level of retained structure in the sense that the grains would be required to be centered within their respective cells.

The ratio of the volume per grain to the volume for free rotation is evidently

$$\eta = \frac{3}{4\pi L^3} \frac{V_{p_e}}{(1 - \varepsilon_e)} \tag{2.1.1}$$

We take the initial value of η to be η_o. Until the bed is ignited at a given location the flow resistance is assumed to be that of stick propellant. Following ignition, the flow resistance of a stick charge is assumed to be zero. We admit an input datum t_r such that for values of the time less than t_r the flow resistance of stacked granular propellant is likewise zero. The flow resistance of the stacked granular charge for $t > t_r$ is evaluated on the basis of η according to

$$\frac{f_s}{f_{s,NOM}} = \begin{cases} 1 & \text{if } \eta \geq 1 \\ C_{\eta_o} + (1 - C_{\eta_o}) \left[\dfrac{(\eta - \eta_o)}{(1 - \eta_o)} \right]^{n_r} & \text{if } \eta_o < \eta < 1 \\ C_{\eta_o} & \text{if } \eta \leq \eta_o \end{cases} \tag{2.1.2}$$

Here C_{η_o} is a dimensionless coefficient whose value is less than one and n_r is a relaxation exponent. The form of (2.1.2) is speculative and the user of the code is required to provide values of C_{η_o} and n_r. It is suggested that values be determined by matching the code to detailed observations of the pressure distributions in instrumented gun firings.

It is emphasized that the analysis of flow resistance is performed locally. Thus the flow resistance can vary strongly from point to point as a consequence of local bed randomization.

The foregoing analysis is only implemented if $\eta_o < 1$. If the stacked granular charge is defined so that η_o is greater than one then it is supposed that special means of regulating the bed geometry have been included and the flow resistance is always evaluated as that of stick propellant.

We conclude this section with a comment on numerical stability. When a stacked granular charge is dispersed there are no intergranular stresses. If in addition, the interphase drag is zero due to the choice of t_r, the only force acting on the grains will be the gas-phase pressure gradient, the buoyancy force. In such a situation instability can occur due to fundamental physical mechanisms. Consider the situation of steady flow and choose a reference frame in which the propellant is at rest. Let there be a local minimum of porosity and let the gas velocity be subsonic. Then the flow contraction will be associated with a pressure minimum which implies that the pressure gradient will be such as to move the propellant into the compacted region from both sides, further reducing the porosity. Such problems are ill-posed and cannot be simulated without the use of artificial dissipative terms or fictitious forces. It may be possible to complete solutions, but mesh indifference will not be demonstrable. Accordingly, the use of large values of t_r is not recommended and non-zero values of C_{n_o} may be desirable in some cases when instability is noted in the distribution of porosity.

2.2 Analysis of Grain Fracture

The analysis of grain fracture is predicated on the maximum value of intergranular stress experienced by each local element of the propelling charge. During the calculation we monitor the stress in the bed and update the maximum values as these are established. The effect of fracture is assumed to be embedded in experimentally determined tables of multipliers to the nominal surface area and flow resistance predicated on the values of the maximum stress.

An important aspect of this approach relates to the numerical accuracy with which the stress field is determined. In particular, we are concerned here with the stress levels achieved as a result of impact of the propellant bed against the projectile base. For the sake of numerical fidelity it is desirable to represent the resulting granular shock wave as an explicit surface of discontinuity. The arguments in support of this approach may be found in Gough (1980b). We also include herewith a review of the analysis presented therein and which was encoded into an earlier version of the NOVA Code. That analysis was recoded and made compatible with the current solution algorithm of XKTC.

In keeping with the numerical formulation of XKTC we require a lumped parameter analysis of a two-phase region to model the compacted region shortly after formation when its resolution as a one-dimensional continuum would impose a restrictively low time step. This topic is covered in Section 2.2.1. In Section 2.2.2 we summarize the constitutive relations including boundary

conditions to be used at the internal boundary. Section 2.2.3 notes some aspects of the implementation of the analysis which may help in the interpretation of the solution.

2.2.1 Balance Equations for a Two-Phase Lumped Parameter Region

Consider a lumped parameter region as depicted in the sketch. It is bounded by surfaces located at x_L and x_R whose functional dependence on time will be furnished from independent considerations. The region is assumed to have an instantaneous volume V which is available to the two-phase flow and the cross sectional areas of the bounding surfaces available to the flow are taken to be A_L and A_R. We identify x_R with the external boundary, which is at most gas-permeable and x_L with the granular compaction wave. Accordingly, we consider the flux of both phases across x_L and only the gas across x_R. We note also that the flux of gas may correspond either to mass addition or mass loss but that only mass addition is expected in regard to the solid-phase.

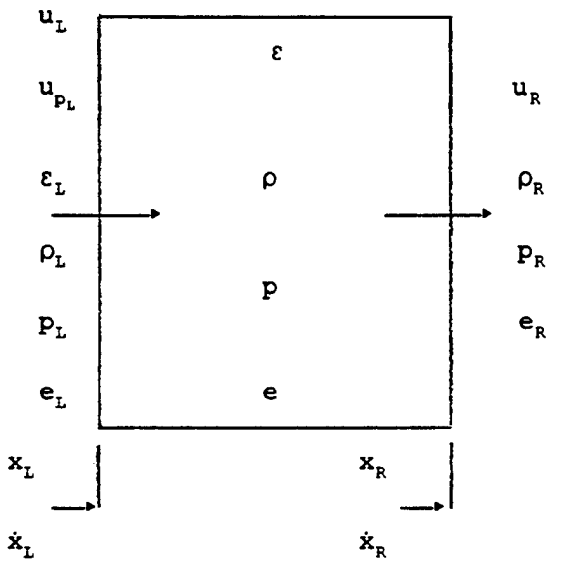

We assume that the igniter or primer condensed phase may have a finite density ρ_{IG} and be characterized by a rate of gasification ψ per unit volume. With this in mind it is easy to see that the volume of the lumped parameter region is governed by the ordinary differential equation.

$$\dot{V} = A_R\dot{x}_R - A_L\dot{x}_L + \dot{V}_{IG} \qquad (2.2.1.1)$$

where

$$\dot{V}_{IG} = \frac{1}{\rho_{IG}} \int_{x_L}^{x_R} A(x)\psi(x)\,dx \qquad (2.2.1.2)$$

represents the rate of increase in volume due to consumption of the igniter.

The porosity or void fraction is predicated on the available volume V. Hence the balance of mass of the solid-phase may be expressed as

$$\frac{d}{dt}[(1-\varepsilon)V] = A_L(1-\varepsilon_L)(u_{p_L} - \dot{x}_L) - \frac{\dot{m}}{\rho_p}V \qquad (2.2.1.3)$$

where

$$\dot{m} = (1-\varepsilon)\rho_p \frac{S_p}{V_p}\dot{d} \qquad (2.2.1.4)$$

describes the rate of gasification of the solid propellant. We have ρ_p, propellant density; S_p, the surface area of a grain; V_p, the volume of a grain; and $\dot{d}$, the rate of surface regression. We have, moreover, used the familiar nomenclature for the state variables: ε, porosity; , u_p solid-phase velocity. The subscript L refers to values on the boundary of the contiguous continuum region.

In view of (2.2.1.1), we may expand the differential on the left hand side of (2.2.1.3) to get the result

$$\dot{\varepsilon} = \frac{1}{V}\left\{(1-\varepsilon)(A_R\dot{x}_R - A_L\dot{x}_L) - (1-\varepsilon_L)A_L(u_{p_L} - \dot{x}_L)\right\} + (1-\varepsilon)\frac{\dot{V}_{IG}}{V} + \frac{\dot{m}}{\rho_p} \qquad (2.2.1.5)$$

The balance of mass of the gas-phase may be stated in the form

$$\frac{d}{dt}[\varepsilon\rho V] = \varepsilon_L\rho_L A_L(u_L - \dot{x}_L) - \varepsilon_R\rho_R A_R(u_R - \dot{x}_R) + \dot{m}V + \rho_{IG}\dot{V}_{IG} \qquad (2.2.1.6)$$

where we have ρ, the gas-density and u its velocity. As in the preceding section, the subscripts refer to values on the boundaries of the contiguous regions.

By expanding the left hand side and making use of (2.2.1.1) and (2.2.1.5) we may put (2.2.1.6) into the computational form

$$\dot{\rho} = \frac{1}{\varepsilon V}\left\{\varepsilon_L\rho_L A_L(u_L - \dot{x}_L) - \varepsilon_R\rho_R A_R(u_R - \dot{x}_R) - \rho(A_R\dot{x}_R - A_L\dot{x}_L)\right. \qquad (2.2.1.7)$$

$$\left. + \rho(1-\varepsilon_L)A_L(u_{p_L} - \dot{x}_L)\right\} + \frac{\dot{m}}{\varepsilon}\left(1 - \frac{\rho}{\rho_p}\right) + \frac{\rho_{IG}\dot{V}_{IG}}{\varepsilon V}\left(1 - \frac{\rho}{\rho_{IG}}\right)$$

Using e to denote internal energy and $h = e + p/\rho + u_{rel}^2/2$ to denote the total enthalpy, we may express the balance of energy of the gas-phase in a frame of reference whose instantaneous velocity is equal to that of the gas in the lumped parameter region in the following form.

$$\frac{d}{dt}[\varepsilon\rho eV] = A_L\varepsilon_L\rho_L h_L(u_L - \dot{x}_L) - A_R\varepsilon_R\rho_R h_R(u_R - \dot{x}_R)$$

$$+ h_p\dot{m}V + h_{IG}\rho_{IG}\dot{V}_{IG} - p\frac{d}{dt}[\varepsilon V] - q_p \qquad (2.2.1.8)$$

This equation may be interpreted as the statement: rate of change of energy within the control volume occupied by the gas-phase equals total enthalpy flux into the volume less work to expand the control volume and heat lost to the propellant. The terms h_p and h_{IG} refer to the propellant and igniter products respectively and are assumed to embed the chemical energy. As we discuss further, the mass transfer is assumed to be adiabatic and to be governed by a quasi-steady law in the frame of reference of the gas within the lumped parameter region.

Using Equations (2.2.1.1) and (2.2.1.5) and (2.2.1.6) to simplify (2.2.1.8) we have the result

$$\dot{e} = \frac{1}{\varepsilon\rho V}\Big\{A_L\varepsilon_L\rho_L(u_L - \dot{x}_L)(h_L - e) - A_R\varepsilon_R\rho_R(u_R - \dot{x}_R)(h_R - e)$$

$$- p(A_R\dot{x}_R - A_L\dot{x}_L) + p(1 - e_L)A_L(u_{p_L} - \dot{x}_L) \qquad (2.2.1.9)$$

$$+ \dot{m}V(e_p - e) + \rho_{IG}\dot{V}_{IG}(e_{IG} - e) - q_p\Big\}$$

2.2.2 Constitutive Relations

We first state the conditions which apply in general at a discontinuity in macroscopic two-phase flow (Gough, 1979). Next we note the conditions which apply at a solid-phase contact discontinuity. Then we turn to the case of the compaction wave.

We note that we have given no provision yet for the determination of the intergranular stress in the compacted region. The intergranular stress will be assumed to be equal to the value deduced from an analysis of the jump conditions. Accordingly, the stress is not taken to be a function of the porosity of the compacted region as a whole.

In addition, we note that the preceding equations have referred to such quantities as the interphase heat transfer q_p and the rate of surface regression. A separate accounting of these quantities is not maintained. The values in a lumped parameter region are assumed to be equal to those on the boundary of the neighboring continuum region.

General Results

Let the speed of the surface of discontinuity be u_s. Denote the properties of the phases on each side of discontinuity by the subscripts 1 and 2. The principles of conservation of mass, momentum and energy lead to the following four jump conditions or conditions of finite compatibility.

$$\varepsilon_1 \rho_1 (u_1 - u_s) = \varepsilon_2 \rho_2 (u_2 - u_s) \tag{2.2.2.1}$$

$$(1 - \varepsilon_1) \rho_p (u_{p_1} - u_s) = (1 - \varepsilon_2) \rho_p (u_{p_2} - u_s) \tag{2.2.2.2}$$

$$p_1 + \sigma_1 + \frac{\rho_1 \varepsilon_1}{g_o} (u_1 - u_s)^2 + \frac{\rho_p}{g_o} (1 - \varepsilon_1)(u_{p_1} - u_s)^2$$

$$= p_2 + \sigma_2 + \frac{\rho_2 \varepsilon_2}{g_o} (u_2 - u_s)^2 + \frac{\rho_p}{g_o} (1 - \varepsilon_2)(u_{p_2} - u_s)^2 \tag{2.2.2.3}$$

$$e_1 + \frac{p_1}{\rho_1} + \frac{(u_1 - u_s)^2}{2 g_o} = e_2 + \frac{p_2}{\rho_2} + \frac{(u_2 - u_s)^2}{2 g_o} \tag{2.2.2.4}$$

Equations (2.2.2.1) and (2.2.2.2) state the principles of conservation of mass for each of the phases. Equation (2.2.2.3) expresses the conservation of momentum of the mixture and introduces σ, the intergranular stress (Gough, 1979). Equation (2.2.2.4) expresses conservation of energy for the gas-phase. No energy equation is stated for the solid-phase as it is assumed to be microscopically incompressible.

The fact that the principle of conservation of momentum can only be stated, in general, for the mixture implies that an element of indeterminacy has been introduced which can only be resolved by making some sort of constitutive assumption regarding the exchange of momentum between the phases. Analytically, our inability to state separate, generally valid, relationships to describe the momentum jump for each of the phases stems from the nature of

the mechanical interaction between the phases. The mechanical interaction involves a term of the form $p\nabla\varepsilon$ which clearly cannot be assumed a priori to be bounded everywhere within a control volume which envelopes the discontinuity. Only by recognizing the possibility of momentum exchange between the phases can (2.2.2.3) be split.

Solid-Phase Contact Discontinuity

If the discontinuity is such as to admit a jump in porosity as we pass from one mixture region to another then, provided the discontinuity is physically stable, we may assume

$$u_{p_1} = u_{p_2} = u_s \qquad (2.2.2.5)$$

as is usual in a contact discontinuity.

Moreover, we may postulate, by analogy with the single phase case that the intergranular stress will also be continuous.

$$\sigma_1 = \sigma_2 \qquad (2.2.2.6)$$

With the assumption (2.2.2.6), Equations (2.2.2,1), (2.2.2.3) and (2.2.2.4) may be restated as follows

$$\varepsilon_1\rho_1(u_1 - u_s) = \varepsilon_2\rho_2(u_2 - u_s) \qquad (2.2.2.7)$$

$$p_1 + \frac{\varepsilon_1\rho_1}{g_o}(u_1 - u_s)^2 = p_2 + \frac{\varepsilon_2\rho_2}{g_o}(u_2 - u_s)^2 \qquad (2.2.2.8)$$

$$e_1 + \frac{p_1}{\rho_1} + \frac{(u_1 - u_s)^2}{2g_o} = e_2 + \frac{p_2}{\rho_2} + \frac{(u_2 - u_s)^2}{2g_o} \qquad (2.2.2.9)$$

and are analogous to the Rankine-Hugoniot jump conditions which constrain the state variables on either side of a single phase discontinuity, as for example, a shock.

Granular Compaction Wave

We postulate that (2.2.2.7), (2.2.2.8) and (2.2.2.9) continue to govern the jumps in the properties of the gas-phase. The properties of the solid-phase are therefore governed by the jump condition (2.2.2.2), which is independent of our assumption, and by the following

$$\sigma_1 + (1 - \varepsilon_1)\frac{\rho_p}{g_o}(u_{p_1} - u_s)^2 = \sigma_2 + (1 - \varepsilon_2)\frac{\rho_p}{g_o}(u_{p_2} - u_s)^2 \qquad (2.2.2.10)$$

which, of course, reduces to (2.2.2.6) as $u_{p_1}, u_{p_2} \to u_s$.

In XKTC we have the following nominal relationship between σ and ε under monotonic loading from the settling porosity ε_o at which $\sigma = 0$ by definition

$$\sigma_*(\varepsilon) = \begin{cases} \rho_p \dfrac{a_1^2}{g_o}\varepsilon_o^2\left(\dfrac{1}{\varepsilon} - \dfrac{1}{\varepsilon_o}\right) & , \quad \varepsilon \le \varepsilon_o \\ \\ 0 \text{ if } \varepsilon > \varepsilon_o \end{cases} \qquad (2.2.2.11)$$

and we assume that this applies under the condition of shock loading.

In addition we note the following relationship which describes reloading to the nominal curve $\sigma_*(\varepsilon)$ from a state $(\varepsilon_1, \sigma_1)$ lying below the curve

$$\sigma'(\varepsilon) = \sigma_1 + \frac{\rho_p a_2^2}{g_o}(\varepsilon_1 - \varepsilon) \qquad (2.2.2.12)$$

and we note that a_2^2 is expected to be an order of magnitude greater than a_1^2. Then if $(\varepsilon_1, \sigma_1)$ are identified as the porosity and stress on the uncompacted side of the granular shock we take

$$\sigma_2(\varepsilon_2) = \min(\sigma'(\varepsilon_2), \sigma_*(\varepsilon_2)) \qquad (2.2.2.13)$$

In most cases of interest, the granular bed is dispersed prior to impact. Accordingly, $\sigma_1 = 0$ and $\varepsilon_1 > \varepsilon_o$. It then follows that $\sigma_2(\varepsilon_2) = \sigma_*(\varepsilon_2)$ and, of course, $\varepsilon_2 \le \varepsilon_o$.

Concerning the method of solution, consider first the case when a lumped parameter representation has been made of the compacted region. We therefore assume, from the uniformity of the compacted region, that u_{p_2} is given as equal to the velocity of the external boundary. Moreover, the values ε_1, σ_1 and u_{p_1} are known on the uncompacted side from the usual computational procedure, although we shall have to comment a little further on the case when $\sigma_1 \neq 0$. Taking ε_1, σ_1 and u_{p_1} as given for the moment we recast (2.2.2.2) and (2.2.2.10) to yield

$$\sigma_2 = \sigma_1 + \frac{\rho_p}{g_o} \frac{(1 - \varepsilon_1)(1 - \varepsilon_2)}{\varepsilon_1 - \varepsilon_2} (u_{p_2} - u_{p_1})^2 \qquad (2.2.2.14)$$

and

$$u_s = \frac{(1 - \varepsilon_2) u_{p_2} - (1 - \varepsilon_1) u_{p_1}}{\varepsilon_1 - \varepsilon_2} \qquad (2.2.2.15)$$

Equations (2.2.2.13) and (2.2.2.14) may be solved simultaneously, using a midpoint search, to yield the values of ε_2 and σ_2. Then u_s follows from (2.2.2.15) and the gas-phase properties follow from the usual NOVA Code methodology for a solid-phase contact discontinuity.

2.2.3 Coding Considerations

The user specifies the value of the switch NXCW. If this is non-zero, an explicit representation will be made of the granular compaction wave. Because several collisions may occur between the bed and the external boundary, an additional datum is supplied so as to preclude the explicit representation of weak waves. The user supplies a value XIMPV which is the minimum velocity of impact for which the explicit analysis will be conducted. As presently encoded, the explicit analysis can be performed just once per interior ballistic cycle.

To incorporate the explicit analysis, the input program initializes NRG = 2n + 4 regions where n is the number of regions of propellant. We note that this value of NRG is greater by 2 than the normal value. The two additional regions are placed at the leading edge of the forward propellant segment. They are, of course, initially collapsed.

On impact region NRG-3 is given a value of NDTACH = 1 signifying that boundary motion must be computed, but the compacted region is not modeled until it is large enough to be treated as lumped parameter. Eventually, the boundary motion may be sufficient to warrant a continuum representation in accordance with the user-specified value of RZOLV.

At that point, subroutine REG21A is called to transfer the solution to region NRG-2. Region NRG-3 is closed and, except that the boundary motion is that of a shock, the solution technique is now very close to the standard NOVA condition. When the velocity jump across the moving boundary is less than 0.01 times XIMPV or when the compacted region expands and the rate of propagation of intergranular disturbances becomes zero, the shock is considered to have degenerated. The boundary is then frozen as a contact discontinuity.

If the wave degenerates while the compacted region is still lumped parameter, the region representation is maintained until sufficient expansion occurs for it to treated as a continuum. If, on the other hand, the wave is so persistent as to approach the far boundary of the propellant bed, it is transformed to a contact discontinuity at the point at which the uncompacted section would have to be treated as a lumped parameter region according to the value of RZOLV.

Appendix A may be consulted for further details concerning the input data NXCW, RZOLV and XIMPV.

3.0 PRESSURE GRADIENT IN GUN PROPELLING CHARGES

In lumped parameter models of gun interior ballistics it is generally assumed that the modeled value of pressure must represent a spacemean value, $\overline{p}$. On the other hand, the equation of motion of the projectile requires a knowledge of the value of the base pressure, p_B. Closure of the lumped parameter model therefore requires a specification of the relation between p_B and $\overline{p}$. Moreover, the charge designer needs to know the maximum local pressure in order to assure integrity of the gun tube. This maximum is assumed to occur at the breech and we denote the value by the symbol p_{BR}. A traditional approach has been to use the results of Lagrange (Corner, 1950). If the tube is assumed to have uniform area and the mixture of propellant and combustion products is assumed to constitute a homogeneous mixture whose density is independent of position, the continuity equation shows the velocity distribution to be linear and this, in turn, enables one to deduce from the momentum equation that the pressure distribution is quadratic. If C is the charge mass and M is the projectile mass, it emerges that

$$\frac{\overline{p}}{p_B} = 1 + \frac{C}{3M} \quad , \tag{3.1}$$

and

$$\frac{p_{BR}}{p_B} = 1 + \frac{C}{2M} \quad , \tag{3.2}$$

at all times. These formulae seem to give satisfactory results in simulations of artillery charges in which C/M is typically of the order of 0.2 and the difference between $\overline{p}$ and p_B is therefore only a few percent. In tank gun charges for which C/M is of the order of one and the difference between $\overline{p}$ and p_B is therefore appreciable, the results are not as satisfactory.

In seeking improvements to Equations (3.1) and (3.2) we may identify the following processes which are omitted from the theory of Lagrange:

(1) The theory is inherently incapable of representing the occurrence of pressure waves due to the interplay between the ignition train and the packaging of the charge.

(2) Even for smoothly ignited charges, there is no representation of the propagation of rarefaction waves due to the acceleration of the projectile.

(3) Gun chambers are generally tapered and the difference between chamber area and tube area can be significant in tank guns. Moreover, the projectile afterbody may intrude significantly into the chamber.

(4) An examination of two-phase flow simulations shows that the assumption of uniform mixture density is not unreasonable for granular propellant. Although the propellant lags behind the gas with the result that a small region of ullage is created behind the moving projectile, the distributions of each of the two phases are fairly uniform over the length of the tube. However, the velocity lag of the solid-propellant should not be neglected in the momentum equation for the mixture which is used to construct the pressure profile from the velocity distributions.

Of course, all the foregoing processes may be accommodated in a natural way through the use of a fully two-phase analysis such as that embedded in the NOVA Code (Gough, 1980a). However, we may still enquire whether improvements can be made to Equations (3.1) and (3.2) to reflect some of the foregoing processes while at the same time retaining the computational economy and general utility of a lumped parameter approach.

We conclude these introductory remarks with some additional discussion of each of the foregoing processes. In Section 3.1 we show how the Lagrange hypothesis can be extended to account for tubes whose cross-sectional area varies with position. In Section 3.2 we address the effects of the slip velocity between the propellant and the products of combustion. Analytical results are obtained. In Section 3.3 we consider the effects of time dependence of the cross-sectional area. In contrast to the two preceding topics, complete analytical results are not pursued. In Section 3.4 we consider the combined effects of propellant slip velocity and cross-sectional area as a function of position. Again, full analytical results are obtained to describe extended Lagrange relationships between $\overline{p}$, p_B and p_{BR}.

Ignition Transients

The representation of pressure waves due to ignition transients seems the most difficult process to embed in a lumped parameter model. Possibly, an ensemble of NOVA solutions could be obtained with the objective of expressing the ratios $\overline{p}/p_B$ and p_{BR}/p_B, as functions of time, parametrically with respect to the charge attributes. However, it is not clear that the number of runs required to establish the functional relations would be significantly less than the number of runs required to address specific charge configurations of actual interest. As far as the present study is concerned, we implicitly exclude from consideration those charges for which strong ignition-induced pressure waves are present. We note, however, that the occurrence of such waves may have little ballistic consequence provided that they are not so severe as to be accompanied by grain fractures. For example, NOVA simulations of the 5-inch/54

caliber Navy case charge exhibit strong pressure waves, in accord with experiments. Nevertheless, good agreement between predicted values of maximum pressure and muzzle velocity is found when consistent data are used to run NOVA and a lumped parameter code. This suggests that the ballistic event occurs sufficiently slowly for the effects of the ignition transient to be averaged out.

Rarefaction Waves

Rarefaction due to motion of the projectile is embedded in the Lagrange representation in a manner which assumes all elements of the mixture to be expanding at the same rate, a rate which is determined by the instantaneous velocity of the projectile. In reality, of course, it takes time for the state of motion of the projectile to be impressed throughout the propulsion gas and the pressure gradient may be expected to undulate as the unloading waves travel back and forth between the breech and the base of the projectile.

An analytical solution was obtained by Love and Pidduck (Corner, 1950) for the special case in which the propellant is all burnt and quiescent prior to projectile motion. Their results show the ratio $\bar{p}/p_B$ to undergo a damped oscillation about an asymptotic value which is presumably achieved with infinite projectile displacement. The value of $\bar{p}/p_B$, initially equal to one, increases as the rarefaction due to projectile motion propagates rearward. When the rarefaction is reflected from the breech, the ratio undergoes a maximum and returns to the value one when the reflected wave reaches the projectile base, after which it begins to rise again.

Pidduck and Kent (Corner, 1950), noting that the initial rarefaction tended to damp rather quickly, sought a similarity solution which would agree asymptotically with the solution of Love and Pidduck although it would differ in the early stages. From their analysis emerges an alternative to Equation (3.1) in the form

$$\frac{\bar{p}}{p_B} = 1 + \frac{C}{\delta M} \quad , \tag{3.3}$$

where δ is the Pidduck-Kent constant, a function of C/M and the ratio of specific heats. Their observation that the oscillations due to the system of rarefaction waves tend to damp out is consistent with our previous comment concerning the averaging out of the ignition transients. The fact that the Pidduck-Kent solution does not accord with the earlier stages of the exact solution is not really of importance, since the initial stages of the exact solution are quite remote from actual propelling charge behavior. Typically, in real charges, the propellant is fifty percent consumed and the projectile has achieved fifty percent of the muzzle velocity at the time when maximum

pressure occurs. On the other hand, the asymptotic agreement between the similarity solution and the exact solution may or may not be of importance. One has to assume that in spite of the highly idealized initial conditions, the exact solution nevertheless tends towards the behavior of a real charge.

An alternative approach is contained in a R.A.R.D.E. paper (Anon, 1964). It is assumed that the tube is straight and attention is focussed on the balance equations for the gas-phase alone. In place of the linear velocity distribution which emerges from the standard Lagrange assumption, it is supposed that the velocity distribution is a quadratic whose coefficients are functions of time. At the same time, it is also assumed that the pressure distribution remains quadratic, as in the standard Lagrange formulation. The balance equations are converted to ordinary differential equations at one point, arbitrarily selected to be the breech. Limiting arguments are used, together with the boundary conditions, to determine governing equations for the coefficients in the velocity distribution. A global energy balance is also invoked. The propellant is supposed to be uniformly distributed, although a method of relaxing this assumption is discussed. The propellant is assumed to burn at a finite rate. However, we note that the balance equations for the gas-phase implicitly assume the propellant to be at rest and no consideration is given to interphase drag. Neglect of interphase drag is appropriate only for stick propellant; however, the assumption of uniform distribution is only appropriate for granular charges.

Non-Uniform Flow Area

Non-uniformity can be due not only to variations in the tube cross-sectional area, but also to the intrusion of the projectile afterbody. Variations in tube area are presumably confined to the chamber region and are a function of position only. This problem has been previously addressed by Vinti (1942) who presented results corresponding to a cylindrical chamber connected to a cylindrical tube of smaller diameter. Vinti also considered the effects of gun recoil and wall friction on the pressure gradient. These latter effects, which are omitted from the NOVA Code, are not considered here. Analytical results to express the influence of flow area on the pressure gradient have been obtained more recently by Morrison and Wren (1987). Variations in flow area due to the intrusion of the afterbody are a function of both position and time. We will show that the spacewise variations in flow area can be accommodated in an extended Lagrange formulation.

When the flow area decreases with distance downbore, as is the case in normal situations, and the spacemean pressure is understood to be an area-weighted quantity, one may deduce that the ratio $\overline{p}/p_B$ is reduced relative to the ideal Lagrange value, Equation (3.1). The Lagrange value will be attained asymptotically with infinite projectile displacement, provided that the non-uniformity of area is localized to the chamber and the projectile afterbody.

However, an additional complication to be considered in the case of a projectile afterbody is that the motion of the projectile depends on a spacewise integral of pressure rather than a local value. This consideration is not pursued in the present study.

Propellant Velocity Lag

The analysis of Lagrange implicitly assumes that either the propellant is all burnt at the initial instant, or that the burning propellant moves with the same velocity as the gas-phase. The degree to which the propellant velocity remains in equilibrium with that of the gas-phase is determined primarily by the interphase drag. If there were no drag, or flow resistance, one might expect that Equation (3.1) would apply provided that C were replaced by the total mass of the gas-phase at any time. In such a situation one would expect that the ratio $\bar{p}/p_B$ would initially be nearly equal to one and would gradually increase to the limiting Lagrange value as the propellant was consumed. In reality, flow resistance will be present and the pressure gradient will therefore be expected to exceed that which would arise with no flow resistance. Depending on the magnitude of the velocity lag, the contribution of the flow resistance, which is quadratically dependent on the difference between the velocity of the gas and that of the propellant, might be such as to produce instantaneous values of $\bar{p}/p_B$ in excess of the Lagrange value given by Equation (3.1). The influence of the propellant velocity lag may therefore be such as to introduce complex structure into the time dependence of the ratio $\bar{p}/p_B$.

3.1 Non-Uniform Bore Area

We consider the continuity and momentum equations for unsteady flow of a homogeneous inviscid substance through a tube with variable area $A = A(z)$.

$$\frac{\partial \rho}{\partial t} + \frac{1}{A}\frac{\partial \rho A u}{\partial z} = 0 \quad , \tag{3.1.1}$$

$$\rho \frac{\partial u}{\partial t} + \rho u \frac{\partial u}{\partial z} + g_0 \frac{\partial p}{\partial z} = 0 \quad . \tag{3.1.2}$$

Here we have t, time; z, axial position; ρ, density; u, velocity; p, pressure; and g_0 is a constant used to reconcile dimensions.

We make the Lagrange assumption:

$$\frac{\partial \rho}{\partial z} = 0 \quad . \tag{3.1.3}$$

Equation (3.1.1) becomes

$$\frac{\partial Au}{\partial z} = - \frac{A}{\rho} \frac{\partial \rho}{\partial t} \quad . \tag{3.1.4}$$

From global conservation:

$$\rho = \frac{C}{\int_0^{z_p} A(z)dz} \quad , \tag{3.1.5}$$

where z_p is the projectile position and C is the total charge mass. Using V(z) to represent the volume between the breech face and station z this may be written as

$$\rho = \frac{C}{V(z_p)} \quad . \tag{3.1.6}$$

We assume that the variations in A(z) are due only to the shape of the combustion chamber and, possibly, the afterbody of the projectile. The projectile is assumed to have velocity V_p and to move through a tube whose area is fixed and equal to A_B. Differentiating (3.1.6) with respect to time we see that

$$\frac{\partial \rho}{\partial t} = - \frac{A_B C V_p}{V^2(z_p)} = - \frac{\rho A_B V_p}{V(z_p)} \quad , \tag{3.1.7}$$

which is a function of time alone. Substituting into (3.1.4) and using the boundary condition u = 0 at z = 0, we have

$$A(z)u(z) = \frac{A_B V_p}{V(z_p)} \int_0^z A(z)dz = \frac{A_B V(z) V_p}{V(z_p)} \quad . \tag{3.1.8}$$

If $A(z) = A_B$, a constant, this becomes

$$u(z) = V_p \frac{z}{z_p} \quad , \tag{3.1.9}$$

which is the usual Lagrange result. Note that since

$$\frac{\partial u}{\partial z} = f(t) - \frac{u}{A} \frac{\partial A}{\partial z} \quad ,$$

it follows that for $\partial A/\partial z < 0$, as is expected to be the case, $\partial u/\partial z$ is not constant but increases with z. The distribution of velocity is therefore superlinear or sublinear according as $\partial A/\partial z \gtrless 0$.

The pressure distribution follows from the momentum equation (3.1.2)

$$g_0 \frac{\partial p}{\partial z} = - \frac{C}{V(z_p)} \left[\frac{A_B V(z)}{A(z) V(z_p)} \left[\dot{V}_p - \frac{A_B V_p^2}{V(z_p)} \right] + \frac{V_p^2 A_B^2}{A(z)} \frac{V(z)}{V^2(z)_p} \left[1 - \frac{V(z)}{A^2(z)} \frac{\partial A}{\partial z} \right] \right] \quad , \tag{3.1.10}$$

Combining terms, and noting that $\int \frac{V^2}{A^3} \frac{\partial A}{\partial z} dz = \int \frac{V}{A} dz - \frac{V^2}{2A^2}$,

it follows that

$$g_0 [p(z) - p(0)] = J_1(z) \frac{C A_B}{V^2(z_p)} \left[\frac{A_B V_p^2}{V(z_p)} - \dot{V}_p \right] - \frac{C V_p^2}{2} \frac{A_B^2 V^2(z)}{A^2(z) V^3(z_p)} \quad , \tag{3.1.11}$$

where

$$J_1(z) = \int_0^z \frac{V(z)}{A(z)} dz \quad .$$

Note that $p(z)$ depends on both V_p and $\dot{V}_p$. It should also be noted that (3.1.11) remains unchanged even if $\partial A/\partial z = 0$ for part of the flow, as would be expected in a normal gun tube.

In order to define the spacemean pressure, it seems appropriate to use

$$\bar{p} = \frac{\int_0^{z_p} p(x)\,A(x)\,dx}{\int_0^{z_p} A(x)\,dx} \quad . \tag{3.1.12}$$

While we cannot establish quantitative results at this point, we can draw conclusions concerning the qualitative behavior of the pressure ratio $\bar{p}/p_B$. We expect actual gun tubes to have a tapered chamber with area reduction (chambrage) at the entrance to the bore. Consider the limiting case when the bore area is infinitesimal compared with that of the chamber. A condition of stagnation will occur in the chamber and the pressure drop will occur only in the tube. At low projectile velocities (low Mach number) we will have

$$p_B \sim p_{BR} - \frac{\rho_{BR}}{2g_0} V_p^2 \quad , \tag{3.1.13}$$

where p_{BR} and ρ_{BR} are respectively the pressure and density in the breech and where we assume that the amount of gas in the tube is small compared with the projectile mass. This also follows from (3.1.11) if we note that $J(z) \sim \frac{V(z_p)}{A_B}(z_p - z_{p_o})$ under the stated conditions; only the last term of (3.1.11) remains.

It is easy to see that, if $M << 1$, then $\bar{p}/p_B \sim 1$ and is much less than the Lagrange value $L = 1 + C/3M$. We expect the Lagrange number to be established as $z_p \to \infty$ and $V(z_p) >> V(z_{p_o})$. Thus, with chambrage, we expect a gradual increase of $\bar{p}/p_B$ as shown in the following sketch.

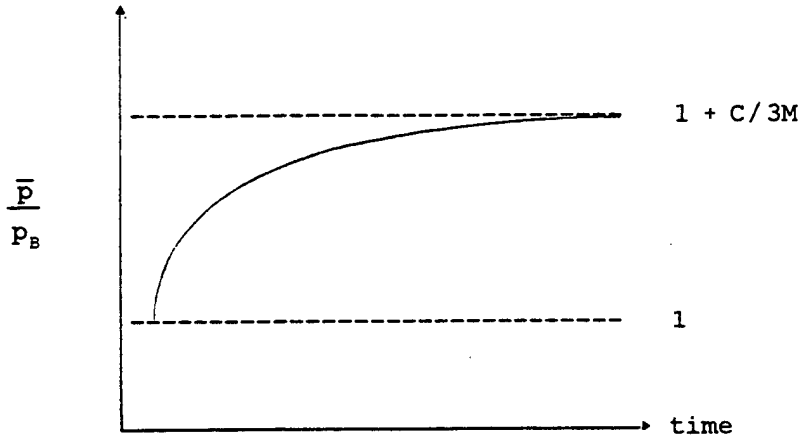

We conclude this section by considering the computational implications of the foregoing analysis. We may write Equation (3.1.11) in the form

$$p(z) = p(0) + a(t)J_1(z) + b(t)J_2(z) \quad , \tag{3.1.14}$$

where

$$a(t) = \frac{CA_B}{g_0 V^2(z_p)} \left[\frac{A_B V_p^2}{V(z_p)} - \dot{V}_p \right] \quad , \tag{3.1.15}$$

$$b(t) = - \frac{CV_p^2}{2g_0} \frac{A_B^2}{V^3(z_p)} \quad , \tag{3.1.16}$$

$$J_1(z) = \int_0^z \frac{V(z)}{A(z)} dz \quad , \tag{3.1.17}$$

$$J_2(z) = \frac{V^2(z)}{A^2(z)} \quad . \tag{3.1.18}$$

The spacemean pressure, as defined by Equation (3.1.12), becomes

$$\bar{p} = p(0) + \frac{a(t)}{V(z_p)} J_3(z_p) + \frac{b(t)}{V(z_p)} J_4(z_p) \quad , \tag{3.1.19}$$

where

$$J_3(z_p) = \int_0^{z_p} A(z)J_1(z)dz \quad , \tag{3.1.20}$$

$$J_4(z_p) = \int_0^{z_p} A(z)J_2(z)dz \quad . \tag{3.1.21}$$

We assume that $\overline{p}$ is the value of pressure determined from the lumped parameter model using the equation of state. Then the breech pressure, p_{BR}, and the base pressure, p_B, are evidently given as

$$p_{BR} = \overline{p} - \frac{a(t)}{V(z_p)} J_3(z_p) - \frac{b(t)}{V(z_p)} J_4(z_p) \quad , \tag{3.1.22}$$

and

$$p_B = p_{BR} + a(t) J_1(z_p) + b(t) J_2(z_p) \quad . \tag{3.1.23}$$

Some simplification follows when the variation in area is confined to the chamber. Such a situation is expected when the tube is not tapered and when the projectile has no afterbody. If the initial position of the projectile base is z_{p_o} and if $A(z) = A_B$ for $z \geq z_{p_o}$ it follows that

$$V(z_p) = V(z_{p_o}) + A_B(z_p - z_{p_o}) \quad , \tag{3.1.24}$$

$$J_1(z_p) = J_1(z_{p_o}) + \frac{1}{A_B}\left[V(z_{p_o})(z_p - z_{p_o}) + \frac{A_B}{2}(z_p - z_{p_o})^2 \right] \quad , \tag{3.1.25}$$

$$J_2(z) = \frac{1}{A_B^2}\left[V(z_{p_o}) + A_B(z_p - z_{p_o}) \right]^2 \quad , \tag{3.1.26}$$

$$J_3(z_p) = J_3(z_{p_o}) + A_B J_1(z_{p_o})(z_p - z_{p_o}) + \frac{V(z_{p_o})}{2}(z_p - z_{p_o})^2 + \frac{A_B}{6}(z_p - z_{p_o})^3 \quad , \tag{3.1.27}$$

$$J_4(z_p) = J_4(z_{p_o}) + \frac{1}{3A_B^2}\left[\left[V(z_{p_o}) + A_B(z_p - z_{p_o}) \right]^3 - V^3(z_{p_o}) \right] \quad . \tag{3.1.28}$$

Hence the geometric terms $V(z_{p_o})$, $J_1(z_{p_o})$, $J_2(z_{p_o})$, $J_3(z_{p_o})$ and $J_4(z_{p_o})$ need be computed just once at the start of the calculation and the values may then be saved for subsequent use.

In principle, the global energy balance should be revised to a form consistent with the assumptions of the pressure gradient analysis. The kinetic energy of the propellant is found to be $CV_p^2/6g_0$ when the conventional Lagrange hypothesis is used. From Equation (3.1.8) we see that an expression consistent with the present analysis is

$$KE = \frac{CV_p^2}{2g_0} \frac{A_B^2}{V^3(z_p)} J_4(z_p) \quad . \tag{3.1.29}$$

Finally, we eliminate the implicit dependence of Equations (3.1.22) and (3.1.23) on p_B through $a(t)$ as defined by (3.1.15). The equation of motion of the projectile may be written as

$$\dot{V}_p = \frac{g_0 A_B}{M_p} \left[p_B - p_{RES} \right] \quad , \tag{3.1.30}$$

where M_p is the mass of the projectile and p_{RES} is the bore resistance. Evidently,

$$a(t) = a_1(t) + a_2(t) p_B \quad , \tag{3.1.31}$$

where

$$a_1(t) = \frac{CA_B}{g_0 V^2(z_p)} \left[\frac{A_B V_p^2}{V(z_p)} + \frac{g_0 A_B}{M_p} p_{RES} \right] \quad , \tag{3.1.32}$$

$$a_2(t) = - \frac{C}{M_p} \frac{A_B^2}{V^2(z_p)} \quad . \tag{3.1.33}$$

Substituting (3.1.31) into Equations (3.1.22) and (3.1.23) we find

$$p_{BR} = \alpha p_B + \beta \quad , \tag{3.1.34}$$

$$\bar{p} = \gamma p_B + \delta \quad , \tag{3.1.35}$$

where

$$\alpha = 1 - a_2(t)\, J_1(z_p) \quad , \tag{3.1.36}$$

$$\beta = - a_1(t)\, J_1(z_p) - b(t)\, J_2(z_p) \quad , \tag{3.1.37}$$

$$\gamma = \alpha + \frac{J_3(z_p)\, a_2(t)}{V(z_p)} \quad , \tag{3.1.38}$$

$$\delta = \beta + \frac{J_3(z_p)\, a_1(t)}{V(z_p)} + \frac{b(t)\, J_4(z_p)}{V(z_p)} \quad . \tag{3.1.39}$$

3.2 Propellant Velocity Lag

In this section we explore the consequences of the inhomogeneity of the mixture. We note that the velocity of the solid-phase differs from that of the gas-phase. We seek to determine the effect on the pressure gradient of the propellant velocity lag as an isolated effect. Thus, in the present section we assume the cross-sectional area of the tube to be uniform, $\partial A/\partial z = 0$. Moreover, we retain the basic Lagrange assumption that the density of the gas is uniform throughout the tube. However, since the propellant velocity lags that of the gas, we explicitly consider the consequences of the formation of a region of ullage between the propellant bed and the base of the projectile. The propellant is assumed to be distributed uniformly only over the region between the breech and the leading edge of the bed. Our formulation is intended to be applicable not only to granular propellant, for which the region of ullage is relatively small, but also, with the help of certain additional assumptions, to stick propellant which remains highly localized and for which the region of ullage becomes very large.

The assumed structure of the flow is illustrated in the following sketch which also introduces some nomenclature.

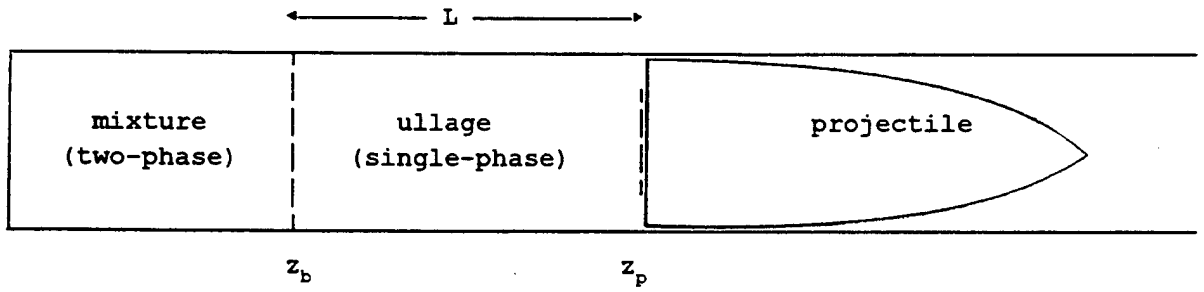

The position of the leading edge of the propellant bed is taken to be at z_b while the base of the projectile is at z_p, both positions relative to the breech face. The length of the ullage is $L = z_p - z_b$.

We may write the continuity equations for each of the phases in the mixture region in the form

$$\frac{\partial \varepsilon \rho}{\partial t} + \frac{\partial \varepsilon \rho u}{\partial z} = \dot{m}(t) \quad , \tag{3.2.1}$$

$$\rho_p \frac{\partial \varepsilon}{\partial t} - \frac{\partial}{\partial z} (1 - \varepsilon) \rho_p u_p = \dot{m}(t) \quad , \tag{3.2.2}$$

where we have ε, porosity; ρ_p, propellant density; u_p, propellant velocity; and $\dot{m}$, the rate of combustion of propellant. With respect to the gas-phase we have the traditional Lagrange assumption, which we will assume to apply throughout the tube, namely

$$\frac{\partial \rho}{\partial z} = 0 \quad . \tag{3.2.3}$$

With respect to the solid phase we make the analogous assumption but we restrict it to the region occupied by the mixture, namely

$$\frac{\partial \varepsilon}{\partial z} = 0 \quad . \tag{3.2.4}$$

In addition we assume that, within the mixture region, $\dot{m}$ is a function only of time even though, due to the pressure gradient, it must vary with position, too.

Evidently,

$$(1 - \varepsilon)\rho_p \frac{\partial u_p}{\partial z} = \frac{\partial \varepsilon}{\partial t} - \dot{m}(t) \quad . \tag{3.2.5}$$

It therefore follows that u_p is a linear function of position and evidently

$$u_p = U_p\left[\frac{z}{z_b}\right] \quad , \tag{3.2.6}$$

when the breech boundary condition $u_p(0) = 0$ is taken into account, and where $U_p = u_p(z_p)$ is the solid-phase velocity at the leading edge of the propellant bed.

Moreover:

$$\varepsilon\rho \frac{\partial u}{\partial z} = - \frac{\partial \varepsilon \rho}{\partial t} + \dot{m}(t) \tag{3.2.7}$$

shows that within the mixture region $u(z,t)$ continues to obey the Lagrange distribution

$$u = U_g(t)\left[\frac{z}{z_b}\right] \quad , \tag{3.2.8}$$

where $U_g = u(z_b)$ is the gas-phase velocity at the leading edge of the bed. The symbol U_g refers to the mixture side of the interface. Due to the discontinuity in porosity the gas velocity jumps discontinuously at the interface, at least from a macroscopic perspective.

The discontinuity in gas velocity is retained in the present formulation. However, we will ignore the concomitant jumps in the thermodynamic properties. The finite mass balance at the interface yields

$$\varepsilon(U_g - U_p) = U_{g+} - U_p \quad , \tag{3.2.9}$$

where U_{g_*} is the gas velocity on the ullage side of the interface. The continuity equation for the region of ullage may be written in the form

$$\frac{\partial u}{\partial z} = - \frac{1}{\rho} \frac{D\rho}{Dt} \quad . \tag{3.2.10}$$

Since we retain the basic assumption of Lagrange, namely uniform density at all times, it follows that $D\rho/Dt$ is a function of time alone and we may write

$$U_{g+} = V_p + L \frac{D}{Dt} ln\rho \quad . \tag{3.2.11}$$

where V_p is the projectile velocity and L is the length of the ullage. Combining (3.2.9) and (3.2.11) we have

$$U_g = U_p + \frac{1}{\varepsilon} \left[V_p + L \frac{D}{Dt} ln\rho - U_p \right] \quad . \tag{3.2.12}$$

We will also require $\dot{U}_g$ which we have as

$$\dot{U}_g = \frac{\dot{V}_p}{\varepsilon} - \frac{1 - \varepsilon}{\varepsilon} \dot{U}_p - \frac{\dot{\varepsilon}}{\varepsilon^2} \left[V_p + L \frac{D}{Dt} ln\rho - U_p \right] + \frac{L}{\varepsilon} \frac{D^2}{Dt^2} ln\rho + \frac{\dot{L}}{\varepsilon} \frac{D}{Dt} ln\rho \quad . \tag{3.2.13}$$

Equations (3.2.12) and (3.2.13) introduce the first and second time derivatives of the density. It is possible to express these derivatives algebraically and thereby to identify more precisely the dependence of the pressure gradient on the state variables. However, the formulation is made more complicated. For the present, therefore, we will simply assume that these derivatives can be furnished from the lumped parameter solution by means of numerical differentiation. This approximate treatment is expected to be adequate for granular propellant in which the region of ullage is expected to remain small at all times. The more complete analytical approach may prove necessary in the case of stick propellant for which the region of ullage becomes increasingly large as the projectile moves down the bore.

We now consider the momentum equations for the mixture region which we may express as

$$\frac{\partial u}{\partial t} + u \frac{\partial u}{\partial t} + \frac{g_0}{\rho} \frac{\partial p}{\partial z} = - \frac{f_s}{\varepsilon \rho} + \frac{\dot{m}}{\varepsilon \rho} (u_p - u) \quad , \tag{3.2.14}$$

$$\frac{\partial u_p}{\partial t} + u_p \frac{\partial u_p}{\partial z} + \frac{g_0}{\rho_p} \frac{\partial p}{\partial z} = \frac{f_s}{(1 - \varepsilon)\rho_p} \quad , \tag{3.2.15}$$

where f_s is the interphase drag and we assume the granular aggregate to be dispersed so that the intergranular stress $\sigma_p = 0$. To get the pressure gradient we need to specify f_s. We assume

$$f_s = \frac{1 - \varepsilon}{D_p} \rho (u - u_p)^2 \hat{f}_s \quad , \tag{3.2.16}$$

where D_p is the effective grain diameter and $\hat{f}_s$ is a dimensionless friction factor. In general, $\hat{f}_s$ is a function of Reynolds number and particle shape and therefore of both z and t.

Equations (3.2.14) and (3.2.15) are better posed in divergence form as

$$\frac{\partial \varepsilon \rho u}{\partial t} + \frac{\partial \varepsilon \rho u^2}{\partial z} + \varepsilon g_0 \frac{\partial p}{\partial z} = - f_s + \dot{m} u_p \quad , \tag{3.2.17}$$

$$\frac{\partial}{\partial t} (1 - \varepsilon) \rho_p u_p + \frac{\partial}{\partial z} (1 - \varepsilon) \rho_p u_p^2 + (1 - \varepsilon) g_0 \frac{\partial p}{\partial z} = f_s - \dot{m} u_p \quad , \tag{3.2.18}$$

which can be obtained through the use of the continuity equations.

Adding (3.1.17) and (3.1.18) we see that

$$g_0 \frac{\partial p}{\partial z} = - \frac{\partial \varepsilon \rho u}{\partial t} - \frac{\partial}{\partial t} (1 - \varepsilon) \rho_p u_p - \frac{\partial \varepsilon \rho u^2}{\partial z} - \frac{\partial}{\partial z} (1 - \varepsilon) \rho_p u_p^2 \quad . \tag{3.2.19}$$

We introduce the mass fraction burned, ϕ, so that

$$\varepsilon \rho = \frac{\phi C - \rho A_B L}{V(z_b)} = \frac{\phi_* C}{V(z_b)} \quad , \tag{3.2.20}$$

where

$$\phi_* = \phi(1 - \rho A_B L/C) \quad . \tag{3.2.21}$$

Also,

$$(1 - \varepsilon)\rho_p = \frac{(1 - \phi)C}{V(z_b)} \quad , \tag{3.2.22}$$

where C is total charge mass and $V(z_b)$ is the instantaneous volume of the region occupied by the mixture. We also note that

$$\dot{\phi}_* = \dot{\phi}\left[1 - \frac{\rho A_B L}{C}\right] - \frac{\rho A_B \phi}{C}\left[\dot{L} + L\frac{D}{Dt}\ln\rho\right] \quad , \tag{3.2.23}$$

$$\dot{\varepsilon} = \frac{\dot{\phi}C}{\rho_p V(z_b)} + \frac{(1 - \phi)CA_B U_p}{\rho_p V^2(z_p)} \quad . \tag{3.2.24}$$

In view of Equations (3.2.6), (3.2.8), (3.2.20) and (3.2.21), Equation (3.2.19) becomes

$$g_0 \frac{\partial p}{\partial z} = -\frac{\partial}{\partial t}\left[\frac{z}{z_b}\frac{C}{V(z_b)}\left[\phi_* U_g + (1 - \phi)U_p\right]\right]$$

$$-\frac{\partial}{\partial z}\left[\frac{z^2}{z_b^2}\frac{C}{V(z_b)}\left[\phi_* U_g^2 + (1 - \phi)U_p^2\right]\right] \quad . \tag{3.2.25}$$

Following expansion of the derivatives and simplification this becomes

$$g_0 \frac{\partial p}{\partial z} = -\frac{z}{z_b}\frac{C}{V(z_b)}\left[\phi_*\dot{U}_g + (1 - \phi)\dot{U}_p + \dot{\phi}_* U_g - \dot{\phi}U_p + \frac{2\phi_* U_g}{z_b}(U_g - U_p)\right] \quad . \tag{3.2.26}$$

We may eliminate $\dot{U}_g$ by means of Equation (3.2.13). Also, we may express the solid-phase momentum equation in the form

$$\dot{U}_p = \frac{1}{D_p}\frac{\rho}{\rho_p}\left[U_g - U_p\right]^2 \hat{f}_s - \frac{g_0}{\rho_p}\left[\frac{\partial p}{\partial z}\right]_{z_b} \quad , \tag{3.2.27}$$

which then allows us to eliminate $\dot{U}_p$ from (3.2.26). We get

$$g_0 \frac{\partial p}{\partial z} = -\frac{z}{z_b}\frac{C}{V(z_b)}\left[\psi_1 - \psi_2 \frac{g_0}{\rho_p}\left[\frac{\partial p}{\partial z}\right]_{z_b}\right] \quad , \tag{3.2.28}$$

where

$$\psi_1 = \psi_1' + \frac{\Phi_*}{\varepsilon}\dot{V}_p \quad , \tag{3.2.29}$$

$$\begin{aligned}\psi_1' = {} & \dot{\Phi}_* U_g - \dot{\Phi} U_p - \Phi_* \frac{\dot{\varepsilon}}{\varepsilon^2}\left[V_p + L\frac{D}{Dt}ln\rho - U_p\right] \\ & + \frac{\Phi_*}{\varepsilon}\left[L\frac{D^2}{Dt^2}ln\rho + \dot{L}\frac{D}{Dt}ln\rho\right] + \frac{2\Phi_* U_g}{z_b}\left[U_g - U_p\right] \\ & + \frac{\psi_2}{D_p}\frac{\rho}{\rho_p}\left[U_g - U_p\right]^2 \hat{f}_s \quad ,\end{aligned} \tag{3.2.30}$$

$$\psi_2 = 1 - \Phi - \Phi_* \frac{(1-\varepsilon)}{\varepsilon} \quad . \tag{3.2.31}$$

Evidently,

$$\left[\frac{\partial p}{\partial z}\right]_{z_b} = -\frac{C}{g_0 V(z_b)}\frac{\psi_1}{1 - \frac{\psi_2 C}{\rho_p V(z_b)}} \quad . \tag{3.2.32}$$

Substituting back into (3.2.28) we have the following expression for the pressure gradient in the mixture region

$$\frac{\partial p}{\partial z} = - k_1(t) z \quad , \tag{3.2.33}$$

where

$$k_1 = \frac{C}{g_0 z_b V(z_b)} \frac{\psi_1}{1 - \frac{\psi_2 C}{\rho_p V(z_b)}} \quad . \tag{3.2.34}$$

We note that k_1 depends on the base pressure $p_B = p(z_p)$ through the term $\dot{V}_p$. We take the equation of motion of the projectile to be

$$\dot{V}_p = \frac{g_0 A_B}{M_p} \left[p_B - p_{RES} \right] \quad . \tag{3.2.35}$$

Evidently, from Equations (3.2.29) and (3.2.35),

$$k_1 = k_{11} p_B + k_{12} \quad , \tag{3.2.36}$$

where

$$k_{11} = \frac{C \Phi_* A_B}{V(z_b) M_p z_b} \frac{k_2}{\varepsilon} \quad , \tag{3.2.37}$$

$$k_2 = \frac{1}{1 - \frac{\psi_2 C}{\rho_p V(z_b)}} \quad , \tag{3.2.38}$$

$$k_{12} = \frac{C}{g_0 V(z_b)} \frac{k_2}{z_b} \psi_1' - k_{11} p_{RES} \quad . \tag{3.2.39}$$

Then by integrating (3.2.33) we see that the pressure distribution within the mixture can be expressed in terms of p_{BR} and p_B as follows

$$p(z) = p_{BR} - \frac{z^2}{2} \left[k_{11} p_B + k_{12} \right] \quad . \tag{3.2.40}$$

To complete the analysis we must now turn our attention to the pressure distribution in the region of ullage. The momentum equation for the gas in the ullage is

$$\frac{\partial p}{\partial z} = - \frac{\rho}{g_0} \left[\frac{\partial u}{\partial t} + u \frac{\partial u}{\partial z} \right] \quad . \tag{3.2.41}$$

We note that the velocity distribution in the ullage varies linearly with distance between the value U_{g_*} at the mixture boundary and the value V_p at the projectile base. Evidently, from Equation (3.2.10),

$$u = V_p + (z_p - z) \frac{D}{Dt} ln\rho \quad . \tag{3.2.42}$$

Substitution into (3.2.41) and integrating yields the pressure distribution in the ullage in the form

$$p(z) = p(z_b) - \frac{\rho}{g_0} \left[\left[\dot{V}_p + z_p \Delta \right] \left[z - z_b \right] - \left[z^2 - z_b^2 \right] \frac{\Delta}{2} \right] \quad , \tag{3.2.43}$$

where

$$\Delta = \frac{D^2}{Dt^2} ln\rho - \left[\frac{D}{Dt} ln\rho \right]^2 \quad . \tag{3.2.44}$$

We note the implicit dependence on p_B through the term $\dot{V}_p$ in (3.2.43).

From (3.2.40) and (3.2.43) we can now determine the spacemean pressure $\bar{p}$ as

$$\bar{p} = p_{BR} \frac{z_b}{z_p} - k_1 \frac{z_b^3}{6 z_p} + p(z_b) \frac{L}{z_p} - \frac{\rho}{g_0} \left[\dot{V}_p + \frac{2L\Delta}{3} \right] \frac{L^2}{2 z_p} \quad . \tag{3.2.45}$$

We may eliminate $p(z_p)$ by means of (3.2.40). Also, $\dot{V}_p$ may be eliminated from (3.2.43) and (3.2.45) by means of (3.2.35). We note the tacit neglect of the pressure jump at the mixture boundary.

Following some straightforward manipulations we find the following relationships between $\bar{p}$, p_{BR} and p_B.

$$p_{BR} = \alpha p_B + \beta \quad , \tag{3.2.46}$$

$$\bar{p} = \gamma p_B + \delta \quad , \tag{3.2.47}$$

$$\alpha = 1 + \frac{z_b^2}{2} k_{11} + \frac{\rho L A_B}{M_p} \quad , \tag{3.2.48}$$

$$\beta = k_{12} \frac{z_b^2}{2} - \frac{\rho L A_B}{M_p} p_{RES} + \frac{\rho L^2 \Delta}{2 g_0} \quad , \tag{3.2.49}$$

$$\gamma = \alpha - \frac{k_{11} z_b^2}{2 z_p} \left[\frac{z_b}{3} + L \right] - \frac{\rho A_B L^2}{2 z_p M_p} \quad , \tag{3.2.50}$$

$$\delta = \beta - \frac{k_{12} z_b^2}{2 z_p} \left[\frac{z_b}{3} + L \right] - \frac{\rho L^2}{2 g_0 z_p} \left[\frac{2 L \Delta}{3} - g_0 \frac{A_B}{M_p} p_{RES} \right] \quad . \tag{3.2.51}$$

We also note the total kinetic energy of the propellant and the combustion products. From Equations (3.2.6), (3.2.8) and (3.2.42) it follows that the kinetic energy is given by

$$KE = \frac{A_B z_b}{6 g_0} \left[\varepsilon \rho U_g^2 + (1 - \varepsilon) \rho_p U_p^2 \right] + \frac{A_B \rho L}{6 g_0} \left[3 V_p^2 + 3 V_p L \frac{D}{Dt} ln\rho + L^2 \left[\frac{D}{Dt} ln\rho \right]^2 \right] \quad . \tag{3.2.52}$$

The foregoing may be used to make the lumped parameter energy equation consistent with the present two-phase analysis.

As we noted previously, the explicit recognition of the presence of the region of ullage allows the present two-phase analysis to be extended to the case of stick propellant. Two additional considerations are necessary. First, we must recognize that Equation (3.2.27) does not apply to stick charges because it neglects the important influence of the stress transmitted through the stick charge. Because stick propellant normally retains its mechanical

integrity, its length does not change appreciably during combustion. To apply the present analysis to stick charges we retain all the foregoing results with the exception of (3.2.27) as a means of determining the mixture boundary. Equation (3.2.27) is replaced by the assumption that $U_p = 0$ at all times and that the stick charge remains uniformly distributed between the breechface and the mouth of the tube throughout the interior ballistic cycle. NOVA Code simulations show this assumption to be reasonably good for single increment slotted stick charges, the type most commonly used. Since Equation (3.2.27) is equivalent to (3.2.15) it follows that some approximation must also be involved in the use of Equation (3.2.33) which is derived from (3.2.15). It is not difficult to see that (3.2.33) remains valid provided that p is viewed as the total stress, a sum of contributions due to the gas-phase pressure and the intergranular stress. The validating assumption in connection with the use of (3.2.33) for stick propellant is that the partial stress due to the intergranular forces is small by comparison with the pressure of the gas. Again, NOVA solutions show this assumption to be reasonable in cases of practical interest.

The second consideration relates to the burnout of the stick charge. NOVA solutions exhibit a pronounced wave propagation effect in relation to the influence of burnout on the pressure at the base of the projectile. This wave effect stems from two causes. First, the slotted stick has a rather neutral burning characteristic so that the rate of gasification is nearly constant right up to the instant of burnout. The flowfield is therefore required to adjust itself to a nearly instantaneous loss of a strong local source of combustion products. The adjustment is transient in nature and takes some time to propagate from the combustion chamber to the base of the projectile. Until the burnout wave reaches the base of the projectile the base pressure is relatively elevated and some performance enhancement can result if muzzle exit occurs prior to arrival of the wave.

We address this topic in an approximate manner. We assume that after burnout occurs for a stick charge the velocity distribution becomes bilinear. A hingepoint propagates from the mouth of the tube towards the base of the projectile at the local acoustic wavespeed. At the hingepoint the velocity distribution suffers a discontinuity of slope. We assume that this bilinear distribution can capture the effects of the primary burnout wave. We do not consider the implications of reflection of the wave from the base of the projectile. After the wave overtakes the projectile the velocity distribution is assumed to remain linear in accordance with the basic Lagrange assumption. Thus the approach taken here is intended to address stick charges for which overtaking of the projectile by the burnout wave either does not occur or else occurs shortly before muzzle exit.

Let t_b be the time at which burnout occurs and let $\dot{\phi}_b$ be the fractional rate of consumption of the propellant at burnout. Let z_* and u_* respectively denote the position of the hingepoint and the local gas velocity. Evidently we will have to integrate the ordinary differential equation

$$\frac{dz_*}{dt} = u_* + c \quad , \tag{3.2.53}$$

where c is the isentropic sound speed which we may approximate in terms of spacemean properties as

$$c = \sqrt{\frac{g_0 \bar{\gamma} \bar{p}}{(1 - b\rho)}} \quad . \tag{3.2.54}$$

Here we have used $\bar{\gamma}$ as the ratio of specific heats, the overbar being used to avoid confusion with the term defined by Equation (3.2.50). We have used b to denote the covolume.

The initial condition for Equation (3.2.53) is taken to be

$$z_*(t_b) = z_{p_o} \quad . \tag{3.2.55}$$

Then the bilinear velocity distribution is given by

$$u(z) = \begin{cases} u_* z / z_* & , \quad 0 \le z \le z_* \quad , \\ u_* + \dfrac{(V_p - u_*)(z - z_*)}{(z_p - z_*)} & , \quad z_* \le z \le z_p \quad . \end{cases} \tag{3.2.56}$$

Following burnout, Equations (3.2.10) and (3.2.41) apply throughout the chamber and tube and may be used to construct the velocity and pressure distributions. However, we note a fundamental inconsistency between the Lagrange assumption of uniform density and the assumption of a bilinear velocity distribution after burnout. The bilinear distribution implies different values of $\partial u/\partial x$ and hence of $D/Dt \ln\rho$ on each side of the hingepoint. After burnout the global mass balance, expressed in terms of the spacemean density, is

$$\frac{1}{\rho} \frac{D\rho}{Dt} = - \frac{A_B V_p}{V(z_p)} \quad . \tag{3.2.57}$$

While we will use this equation to resolve values of density and rate of change of density in the subsequent analysis, we assume implicitly that the densities on each side of the hingepoint may differ from the spacemean value.

In front of the hingepoint the flow is adapting to the motion of the projectile but is still under the impression that the propellant is burning. Thus we have

$$\frac{1}{\rho}\frac{D\rho}{Dt} = -\frac{A_B V_p}{V(z_p)} + \dot{\phi}_b C\left[\frac{1}{\rho} - \frac{1}{\rho_p}\right] \quad , \quad z_* \le z \le z_p \quad . \tag{3.2.58}$$

From Equation (3.2.10) we may now identify the gas velocity at the hingepoint as

$$u_* = V_p - (z_p - z_*)\left[\frac{A_B V_p}{V(z_p)} - \dot{\phi}_b C\left[\frac{1}{\rho} - \frac{1}{\rho_p}\right]\right] \quad . \tag{3.2.59}$$

We may now construct the pressure distribution from the momentum equation, (3.2.41). We use (3.2.56), (3.2.59) and (3.2.35). We find

$$p(z) = \begin{cases} p_{BR} - z^2(k_{34}p_B + k_{35}) \quad , & 0 \le z \le z_* \\ \\ p_* - (k_{51} + k_{52}p_B)(z - z_*) - k_{53}(z^2 - z_*^2) \quad , & z_* \le z \le z_p \end{cases} \tag{3.2.60}$$

where p_* is the pressure at the hingepoint. We also have introduced the following terms

$$k_{31} = 1 - (z_p - z_*)\frac{A_B}{V(z_p)} \quad , \tag{3.2.61}$$

$$k_{32} = \frac{A_B V_p}{V^2(z_p)}\left[A_B V_p + \frac{\dot{\phi}_b C}{\rho_p}\right] \quad , \tag{3.2.62}$$

$$k_{33} = -\frac{(V_p - \dot{z}_*)}{V(z_p)}\left[A_B V_p - \dot{\phi}_b C\left[\frac{1}{\rho} - \frac{1}{\rho_p}\right]\right] \quad , \tag{3.2.63}$$

$$k_{34} = \frac{\rho A_B}{2M_p} \frac{k_{31}}{z_*} \quad , \tag{3.2.64}$$

$$k_{35} = \frac{\rho}{2g_0 z_*^2} \left[\left[k_{32}(z_p - z_*) + k_{33} \right] z_* - u_* \dot{z}_* + u_*^2 \right] - k_{34} p_{RES} \quad , \tag{3.2.65}$$

$$k_{41} = 1 - \frac{(z_p - z) A_B}{V(z_p)} \quad , \tag{3.2.66}$$

$$k_{42} = k_{32} \quad , \tag{3.2.67}$$

$$k_{43} = - \frac{V_p}{V(z_p)} \left[A_B V_p - \dot{\phi}_b C \left[\frac{1}{\rho} - \frac{1}{\rho_p} \right] \right] \quad , \tag{3.2.68}$$

$$\lambda = (V_p - u_*) / (z_p - z_*) \quad , \tag{3.2.69}$$

$$k_{51} = \frac{\rho}{g_0} \left[k_{42} z_p + k_{43} + \lambda (u_* - \lambda z_*) \right] - k_{52} p_{RES} \quad , \tag{3.2.70}$$

$$k_{52} = \frac{\rho A_B}{M_p} k_{41} \quad , \tag{3.2.71}$$

$$k_{53} = \frac{\rho}{2 g_0} (\lambda^2 - k_{42}) \quad . \tag{3.2.72}$$

From Equation (3.2.60) we may eliminate p_* and deduce

$$p_{BR} = \alpha p_B + \beta \quad , \tag{3.2.73}$$

where

$$\alpha = 1 + z_*^2 k_{34} + k_{52}(z_p - z_*) \quad , \tag{3.2.74}$$

$$\beta = z_*^2 k_{35} + k_{51}(z_p - z_*) + k_{53}(z_p^2 - z_*^2) \quad . \tag{3.2.75}$$

Furthermore, integration of (3.2.60) and elimination of p_* and p_{BR} yields

$$\bar{p} = \gamma p_B + \delta \quad , \tag{3.2.76}$$

where

$$\gamma = \alpha - \frac{z_*^3}{3z_p} k_{34} - (z_p - z_*) \frac{z_*^2}{z_p} k_{34} - \frac{(z_p - z_*)^2}{2z_p} k_{52} \quad , \tag{3.2.77}$$

$$\delta = \beta - \frac{z_*^3}{3z_p} k_{35} - \frac{(z_p - z_*)}{z_p} (k_{35} - k_{53}) z_*^2 - \frac{k_{51}}{2z_p} (z_p - z_*)^2 - \frac{k_{53}}{3z_p} (z_p^3 - z_*^3) \quad . \tag{3.2.78}$$

A similar approach has been used by Morrison and Coffee (1990) in an application to Regenerative Liquid Propellant Guns.

3.3 Area a Function of Position and Time

We now consider the continuity and momentum equations for unsteady flow of a homogeneous inviscid fluid through a tube with variable area $A = A(z,t)$

$$\frac{\partial A\rho}{\partial t} + \frac{\partial \rho A u}{\partial z} = 0 \quad , \tag{3.3.1}$$

$$\rho \frac{\partial u}{\partial t} + \rho u \frac{\partial u}{\partial z} + g_0 \frac{\partial p}{\partial z} = 0 \quad . \tag{3.3.2}$$

We assume that

$$A = A_e - A_i \quad , \tag{3.3.3}$$

where A_e is the area of the tube, a function of z only, and A_i is the area defined by the local intrusion of the afterbody, a function of both z and t. We note that

$$\frac{\partial A}{\partial t} = - \frac{\partial A_i}{\partial t} \quad , \tag{3.3.4}$$

and since A_i is constant in a frame moving with the projectile velocity V_p

$$\frac{\partial A}{\partial t} = V_p \frac{\partial A_i}{\partial z} \quad . \tag{3.3.5}$$

We make the Lagrange assumption

$$\frac{\partial \rho}{\partial z} = 0 \quad , \tag{3.3.6}$$

so that (3.3.1) becomes

$$\frac{\partial Au}{\partial z} = - \frac{A}{\rho} \frac{\partial \rho}{\partial t} - \frac{\partial A}{\partial t} \quad . \tag{3.3.7}$$

As before, we note that

$$\rho V(z_p) = C \quad ,$$

so that

$$\frac{1}{\rho} \frac{\partial \rho}{\partial t} = - \frac{1}{V(z_p)} \frac{\partial}{\partial t} V(z_p) \quad .$$

Also, we have

$$\frac{\partial}{\partial t} V(z_p) = \frac{\partial}{\partial t} \int_0^{z_p} A(z,t)\,dz \quad ,$$

or,

$$\frac{\partial}{\partial t} V(z_p) = \int_0^{z_p} \frac{\partial A}{\partial t}\,dz + V_p A_B \quad ,$$

where A_B is understood to be $A(z_p,t)$ and will not, in general, be the area of the tube. Equation (3.3.7) may be integrated with respect to z. Using the boundary condition $u(0,t) = 0$ it follows that

$$A(z,t)u(z,t) = \frac{V(z,t)}{V(z_p,t)} \left[V_p A_B + \int_0^{z_p} \frac{\partial A}{\partial t}\,dz \right] - \int_0^{z} \frac{\partial A}{\partial t}\,\partial z \quad . \tag{3.3.8}$$

Equation (3.3.8) may be compared with Equation (3.1.8). We note that (3.3.8) satisfies the boundary condition $u(z_p,t) = V_p$, as it must for consistency, independently of the form of $\partial A/\partial t$. No further progress or simplification can be made unless $\partial A/\partial t$ is specified. For the particular case of interest here we may make use of Equation (3.3.5) to deduce the result

$$\begin{aligned} A(z,t)u(z,t) = \frac{V(z,t)}{V(z_p,t)} \left[A_B + A_i(z_p,t) - A_i(0,t) \right] V_p \\ - \left[A_i(z,t) - A_i(0,t) \right] V_p \quad . \end{aligned} \tag{3.3.9}$$

If, moreover, $A_i(0,t) = 0$, as might be expected for this case, then

$$u(z,t) = \frac{V_p}{A(z,t)V(z_p,t)} \left[V(z,t) A_e(z_p,t) - V(z_p,t) A_i(z,t) \right] \quad . \tag{3.3.10}$$

As in Section 3.1 we could now proceed to determine the pressure distribution from the momentum equation. The formulism will, however, be complicated by the presence of the integrals of $A_i(z,t)$. Moreover, the equation of motion (3.1.32) will be complicated by the introduction of an integral of pressure over the intruding afterbody. Accordingly, further analytical results are not pursued.

3.4 Combined Effects of Area and Propellant Lag

We now attempt to combine the influence of variable area with that of propellant velocity lag. We assume that the variation in area is confined to the propellant chamber and that the propellant initially fills the chamber. Subsequently, a region of ullage may develop between the mixture and the base of the projectile. However, the cross-sectional area within the ullage is assumed to be constant and equal to A_B at all points. Attention is focussed principally on granular propellant although we comment on the applicability of the results to stick propellant at the end of the section. Nomenclature is as in the previous sections.

We have the continuity equations for each of the phases within the mixture region in the forms

$$\frac{\partial \varepsilon \rho}{\partial t} + \frac{1}{A} \frac{\partial \varepsilon \rho u A}{\partial z} = \dot{m}(t) \quad , \tag{3.4.1}$$

$$\rho_p \frac{\partial \varepsilon}{\partial t} - \frac{1}{A} \frac{\partial}{\partial z} (1 - \varepsilon) \rho_p u_p A = \dot{m}(t) \quad . \tag{3.4.2}$$

As in Section 3.2 we assume that within the mixture region

$$\frac{\partial \rho}{\partial z} = \frac{\partial \varepsilon}{\partial z} = 0 \quad . \tag{3.4.3}$$

Moreover, the uniformity of the gas-phase density is assumed to extend throughout the tube and to apply in the region of ullage as well as in the mixture. Let the mixture boundary be at z_b and let the boundary values of the gas- and solid-phases be U_g and U_p respectively. Moreover, since $A(z_b) = A_B$ it follows from (3.4.1) and (3.4.2) that

$$u_p(z) = U_p \left[\frac{A_B}{A(z)} \right] \left[\frac{V(z)}{V(z_b)} \right] \quad , \tag{3.4.4}$$

$$u(z) = U_g \left[\frac{A_B}{A(z)} \right] \left[\frac{V(z)}{V(z_b)} \right] \quad , \tag{3.4.5}$$

The conditions in the region of ullage are unchanged from Section 3.2. Accordingly, Equations (3.2.9) through (3.2.13) are applicable here. To construct the pressure gradient in the mixture region we require the momentum equations which we may express in divergence form as

$$\frac{1}{A}\left[\frac{\partial}{\partial t} A\varepsilon\rho u + \frac{\partial}{\partial z} A\varepsilon\rho u^2\right] + \varepsilon g_0 \frac{\partial p}{\partial z} = - f_s + \dot{m} u_p \quad , \tag{3.4.6}$$

$$\frac{1}{A}\left[\frac{\partial}{\partial t} A(1-\varepsilon)\rho_p u_p + \frac{\partial}{\partial z} A(1-\varepsilon)\rho_p u_p^2\right] + (1-\varepsilon) g_0 \frac{\partial p}{\partial z} = f_s - \dot{m} u_p \quad . \tag{3.4.7}$$

As in Section 3.2 we assume that intergranular stresses can be neglected. By adding (3.4.6) and (3.4.7) we get

$$\begin{aligned} g_0 \frac{\partial p}{\partial z} = & - \frac{1}{A(z)} \frac{\partial}{\partial t}\left[A(z)\varepsilon\rho u + A(z)(1-\varepsilon)\rho_p u_p\right] \\ & - \frac{1}{A(z)} \frac{\partial}{\partial z}\left[A(z)\varepsilon\rho u^2 + A(z)(1-\varepsilon)\rho_p u_p^2\right] \quad . \end{aligned} \tag{3.4.8}$$

If we now introduce ϕ, the mass fraction burned, we see that the previous relations (3.2.20) through (3.2.24) are applicable here. Thus we may substitute (3.2.20) and (3.2.22) together with (3.4.4) and (3.4.5) into (3.4.8) to get the result

$$\begin{aligned} g_0 \frac{\partial p}{\partial z} = & - \frac{CA_B V(z)}{A(z)} \frac{\partial}{\partial t}\left[\frac{\phi_* U_g}{V^2(z_b)} + \frac{(1-\phi)U_p}{V^2(z_b)}\right] \\ & - \frac{CA_B^2}{A(z)V^3(z_b)}\left[\phi_* U_g^2 + (1-\phi)U_p^2\right] \frac{\partial}{\partial z} \frac{V^2(z)}{A(z)} \quad . \end{aligned} \tag{3.4.9}$$

Following expansion of the derivatives and simplification we get

$$g_0 \frac{\partial p}{\partial z} = - \frac{CA_B V(z)}{A(z)V^2(z_b)} \left[\phi_* \dot{U}_g + (1 - \phi)\dot{U}_p + \dot{\phi}_* U_g - \dot{\phi} U_p + \frac{2A_B}{V(z_b)} \phi_* U_g \left[U_g - U_p \right] \right.$$

$$\left. - \frac{A_B V(z)}{V(z_b)A^2(z)} \frac{\partial A}{\partial z} \left[\phi_* U_g^2 + (1 - \phi) U_p^2 \right] \right] \quad . \tag{3.4.10}$$

It is easy to verify that when $A(z) = A_B$ so that $V(z) = A_B z$, then (3.4.10) reduces to (3.2.26) as it should. On the other hand, when $\phi = \phi_* = 1$, $z_b = z_p$, $L = 0$, $U_g = U_p = V_p$, then (3.4.10) reduces to (3.1.10).

As in Section 3.2 we proceed to eliminate $\dot{U}_g$ from (3.4.10) using (3.2.13). Similarly, we use (3.2.27) to eliminate $\dot{U}_p$. We find

$$g_0 \frac{\partial p}{\partial z} = - \frac{V(z)}{A(z)} \frac{CA_B}{V^2(z_b)} \left[\psi_1 - \psi_2 \frac{g_0}{\rho_p} \left[\frac{\partial p}{\partial z} \right]_{z_b} - \psi_3 \frac{A_B}{V(z_b)} \frac{V(z)}{A^2(z)} \frac{\partial A}{\partial z} \right] \quad , \tag{3.4.11}$$

where

$$\psi_1 = \psi_1' + \frac{\phi_*}{\varepsilon} \dot{V}_p \quad , \tag{3.4.12}$$

$$\psi_1' = \dot{\phi}_* U_g - \dot{\phi} U_p - \phi_* \frac{\dot{\varepsilon}}{\varepsilon^2} \left[V_p + L \frac{D}{Dt} ln\rho - U_p \right] + \frac{\phi_*}{\varepsilon} \left[L \frac{D^2}{Dt^2} ln\rho + \dot{L} \frac{D}{Dt} ln\rho \right]$$

$$+ 2\phi_* U_g \frac{A_B}{V(z_b)} \left[U_g - U_p \right] + \frac{\psi_2}{D_p} \frac{\rho}{\rho_p} \left[U_g - U_p \right]^2 \hat{f}_s \quad , \tag{3.4.13}$$

$$\psi_2 = 1 - \phi - \phi_* \frac{(1 - \varepsilon)}{\varepsilon} \quad , \tag{3.4.14}$$

$$\Psi_3 = \phi_* U_g^2 + (1 - \phi) U_p^2 \quad . \tag{3.4.15}$$

It should be noted that (3.4.12) through (3.4.14) are identical with (3.2.29) through (3.2.31) except for the penultimate term of (3.4.13). By setting $z = z_b$ in (3.4.11) we may solve for $(\partial p/\partial z)_{z_b}$. Recalling that $(\partial A/\partial z)_{z_b} = 0$ we find

$$\left[\frac{\partial p}{\partial z}\right]_{z_b} = - \frac{C}{g_0 V(z_b)} \frac{\Psi_1}{1 - \dfrac{\Psi_2 C}{\rho_p V(z_b)}} \quad , \tag{3.4.16}$$

which is identical to (3.2.32). We may substitute (3.4.16) into (3.4.11), integrate with respect to z, and use (3.2.25) to eliminate $\dot{V}_p$ from Ψ_1 to get the following relation for the pressure in the mixture

$$p(z) = p_{BR} + \left[a_1(t) + a_2(t) p_B \right] J_1(z) + b(t) J_2(z) \quad , \tag{3.4.17}$$

where $J_1(z)$ and $J_2(z)$ are defined by Equations (3.1.17) and (3.1.18) and we have

$$a_1(t) = \frac{C A_B}{g_0 V^2(z_b)} \left[\frac{\Psi_3 A_B}{V(z_b)} - \frac{\Psi_1' - \dfrac{g_0 A_B}{M_p} \dfrac{\phi_*}{\varepsilon} p_{RES}}{1 - \dfrac{\Psi_2 C}{\rho_p V(z_b)}} \right] \quad , \tag{3.4.18}$$

$$a_2(t) = - \frac{C A_B^2}{M_p V^2(z_b)} \frac{\phi_*}{\varepsilon} \left[1 - \frac{\Psi_2 C}{p_p V(z_b)} \right]^{-1} \quad , \tag{3.4.19}$$

$$b(t) = - \frac{C \Psi_3}{2 g_0} \frac{A_B^2}{V^3(z_b)} \quad . \tag{3.4.20}$$

In the ullage the pressure distribution is unchanged from the form deduced in Section 3.2; thus Equation (3.2.43) applies. The procedure outlined in Sections 3.1 and 3.2 may be followed here. The spacemean pressure is assumed to be area-weighted as in Section 3.1 We deduce

$$p_{BR} = \alpha p_B + \beta \quad , \tag{3.4.21}$$

where

$$\alpha = 1 - a_2(t)\, J_1(z_b) + \frac{\rho A_B L}{M_p} \quad , \tag{3.4.22}$$

$$\beta = - a_1(t)\, J_1(z_b) - b(t)\, J_2(z_b) - \frac{\rho A_B L}{M_p} p_{RES} + \frac{\rho L^2 \Delta}{2 g_0} \quad , \tag{3.4.23}$$

and,

$$\bar{p} = \gamma p_B + \delta \quad , \tag{3.4.24}$$

where

$$\gamma = \alpha + \frac{a_2(t)}{V(z_p)} \left[J_3(z_b) + A_B L J_1(z_b) \right] - \frac{\rho A_B^2 L^2}{2 M_p V(z_p)} \quad , \tag{3.4.25}$$

$$\delta = \beta + \frac{a_1(t)}{V(z_p)} \left[J_3(z_b) + A_B L J_1(z_b) \right] + \frac{b(t)}{V(z_p)} \left[J_4(z_b) + A_B L J_2(z_b) \right]$$

$$- \frac{\rho A_B L^2}{2 g_0 V(z_p)} \left[\frac{2 L \Delta}{3} - \frac{g_0 A_B p_{RES}}{M_p} \right] \quad , \tag{3.4.26}$$

We have introduced $J_3(z)$ and $J_4(z)$ as defined by Equations (3.1.20) and (3.1.21). Under the stated assumptions of the present section it follows that $V(z_p)$ and $J_1(z_p)$, $J_2(z_p)$, $J_3(z_p)$, $J_4(z_p)$ may be evaluated according to Equations (3.1.24) through (3.1.28) with z_b replacing z_p in the evaluation of the J_i terms, $i = 1, \ldots\ldots, 4$.

We have tacitly assumed that we were dealing with granular propellant. As in Section 3.2, however, the present analysis is applicable to stick charges provided that the same approximations can be made. Moreover, the analysis of the pressure gradient subsequent to burnout of the stick charge can be treated as in Section 3.2. The only modification is the replacement of a linear velocity distribution behind the hingepoint by the form expressed in Equation (3.4.5). Further results may be found in a report by Robbins et al (1990).

INTENTIONALLY LEFT BLANK.

REFERENCES

Anon. "An Extended Form of the Lagrange Hypothesis in Interior Ballistics" Document P2K/1 R.A.R.D.E. Woolwich 1964

Corner, J. "Theory of the Interior Ballistics of Guns" Wiley, New York 1950

Gough, P.S. "Discontinuities in Two-Phase Flow" Final Report, Contract N00174-78-M-8024 1979

Gough, P.S. "The NOVA Code: A User's Manual" Indian Head Contract Report IHCR 80-8 1980a

Gough, P.S. "Explicit Analysis of Granular Compaction Wave in NOVA Code" Final Report, Task II, Contract N00174-79-C-0082 PGA-TR-80-2 1980b

Gough, P.S. "XNOVA -- An Express Version of the NOVA Code" Final Report, Contract N00174-82-M-8048 1983

Gough, P.S. "Theoretical Modeling of Navy Propelling Charges" Final Report, Contract N00174-83-C-0241 PGA-TR-84-1 1984

Gough, P.S. "XNOVAT -- A Two-Phase Model of Tank Gun Interior Ballistics" Final Report, Task Order I, Contract DAAK11-85-D-0002 1985

Gough, P.S. "Theoretical Modeling of Interior Ballistic Phenomena in Navy Guns" Final Report, Contract N00174-84-C-0242 PGA-TR-86-2 1988a

Gough, P.S. "Continuum Modeling of Regenerative Liquid Propellant Guns and Hybrid Travelling Charge Systems" Final Report, Contract DAAK11-84-C-0080 PGA-TR-88-1 1988b

Gough, P.S. "The XNOVAKTC Code" Ballistic Research Laboratory Contract Report BRL-CR-627 1990

Gough, P.S. "Modification to XKTC in Support of Thermal Management" Final Report, Task Order 8, Contract DAAA15-88-D-0013 PGA-TR-91-1 1991

Gough, P.S. "One-Dimensional Two-Phase Model of Plasma Guided Endburning Propellant Charge" Contract DAAA+L03-91-C-0034 TCN 92046 1992

Gough, P.S. "Theoretical Modeling of the Interior Ballistics of the Electrothermal Gun" ARL-CR-47 1993

Gough, P.S. "Improvements to the XKTC and TDNOVA Codes"
ARL-CR-233 1995

Morrison, W.F. and Wren, G.P. "A Model of Liquid Injection
in a Regenerative Liquid Propellant Gun"
Technical Report BRL-TR-2851 1987

Morrison, W.F. and Coffee, T.P. "A Modified Lagrange Pressure
Gradient for the Regenerative Liquid Propellant Gun"
Technical Report BRL-TR-3073 1990

Robbins, F.W., Anderson, R.D. and Gough, P.S.
"New Pressure Gradient Equations for Lumped Parameter Interior
Ballistic Codes"
Technical Report BRL-TR-3097 1990

Vinti, John, P. "The Equations of Interior Ballistics"
Ballistic Research Laboratory Report No. 307 October 1942

Appendix A:

XNOVAKTC (XKTC)—Structure and Use

INTENTIONALLY LEFT BLANK.

Appendix A
Table of Contents

Page

Introduction 55

Structure and Linkages 56

Routines Added in Preparation of XNOVAK 56
Routines Added in Preparation of XNOVAT 56
Structure of NOVATC 57
Routines Added in Preparation of Previous Version of XKTC 57
Routines Added in Preparation of Present Version of XKTC 58

Description of Input Files 58

References Cited in Appendix A 67

Figure A.1 Nomenclature for Definition of Charge Configuration in XKTC With MODET = 0 59
Figure A.2 Nomenclature for Definition of Charge Configuration in XNOVAT With MODET = 1 60
Figure A.3 Example of a Hybrid Charge Consisting of Conventional and Traveling Charge Increments 61
Figure A.4 Example of Hybrid Charge Consisting of Traveling Liquid Propellant and Solid Propellant Booster 62
Table A.1 Summary of Routines and Linkages 68
Table A.2 Summary of XKTC "Mandatory" Input Files 86
Table A.3 Summary of XKTC Contingent Input Files 87
Table A.4 Summary of XKTC Traveling Charge Input Files 91
Table A.5 Summary of XKTC Traveling Liquid Charge Input Files 92
Table A.6 Description of Input Files 93

INTENTIONALLY LEFT BLANK.

INTRODUCTION

Our intention in this Appendix is to provide the user of the code with some understanding of its macrostructure and full details of the specification of input data. We do not attempt to document the code in such detail as to permit revisions by the user. XKTC is an extension of NOVATC, XNOVAT and XNOVAK which are, in turn, extensions of the express version of the NOVA Code known as XNOVA. XNOVA is a subset of the NOVA Code and certain of the details of the original versions of the NOVA Code which were deleted in the preparation of XNOVA are also absent from its successors XNOVAK and XNOVAT. Discussions of the structure of NOVA, NOVATC, XNOVA, XNOVAK and XNOVAT may be found in earlier reports (Gough, 1980a,1981,1983a,1983b,1984,1985). Although we provide a complete tabulation of the present set of code subroutines and functions, our general discussion is confined to the differences between the current version of XKTC and its predecessors, including the previous version (Gough, 1986a).

The discussion of structure and of input is contained in the two following Sections. Before proceeding, however, we wish to draw the user's attention to certain general restrictions on the use of the code.

First, it should be noted that existing NOVA, XNOVA and NOVATC data bases cannot always be read by XNOVAK, XNOVAT or XKTC. Although we always attempt to maintain data base compatibility between the various code versions, XNOVAK, XNOVAT and XKTC do require a minor change to pre-existing data bases. File [M4], described in Table A.6, always consists of two cards in XNOVAK/XNOVAT/XKTC data sets. Pre-existing NOVA, XNOVA and NOVATC data sets in which File [M4] consisted of just one card may be made compatible with XNOVAK/XNOVAT/XKTC by the incorporation of a single blank card following the pre-existing File [M4]. No change is required to pre-existing data bases for which [M4] already consisted of two cards. A corresponding revision to XNOVAK/XNOVAT/XKTC data bases is required if they are to be run on NOVATC, XNOVA or NOVA. However, all XNOVAK data bases can be read by XNOVAT and XKTC.

Second, in regard to the summarized solution histories given at the conclusion of each run, it should be noted that the energy defect calculation does not presently support the full chemistry option. If intermediate combustion products are present, the tabulated energy defect may become quite large. Only the mass defect can be depended upon to gage the accuracy of the numerical solution in such cases. The single exception to this statement is that of the traveling charge with a finite flame thickness. In this special case, where there is just one intermediate species, the energy defect calculation reflects the chemical energy stored in the intermediates. Moreover, in this special case, the mass fraction calculation for propellant type three in the summary table is used to tabulate the ratio of the mass of the unburned intermediates to that of the original traveling charge increment.

STRUCTURE AND LINKAGES

A complete summary of the routines and their linkages is given in Table A.1. The overall macrostructure is unchanged from that of XNOVA as documented by Gough (1983b). The following brief comments provide a summary of the routines which were added to XNOVA to produce XNOVAK, the revisions which subsequently transformed XNOVAK into XNOVAT, the amalgam of XNOVAT and BRLTC (Gough, 1980b) to produce the previous version of XKTC, and the amalgam of XKTC and RLPTC (Gough, 1988) to produce the current version. We note that the current version is intended for use on 32-bit word machines and is therefore written in double precision.

Routines Added in Preparation of XNOVAK

XNOVAK was developed as an extension of XNOVA. Accordingly, XNOVA is a subset of both XNOVAK and NOVA. Moreover, in developing XNOVAK it was found necesary to restore certain capabilities which had been removed from NOVA during the preparation of XNOVA. Specifically, we restored the invariant embedding solution for the thermal response of the solid propellant. Thus, in addition to the capabilities of XNOVA, XNOVAK and NOVA also share a transient combustion modeling capability.

The NOVA routines restored to XNOVAK were CMBUST, FBAK, IMBED and ROOT together with necessary I/O linkages. The routines were then modified to support the XNOVAK features of subsurface reactivity and the evaporative boundary condition. New routines added to support the kinetics option included CHEMR, CHEMRS, CONLOS, COVC and GAMMOL. The new routine FILLBR implements the analysis of the rear filler elements and was created by making appropriate editing changes to the pre-existing routine FILLER. One additional routine, AVN, was included for the purpose of documenting Code revisions and printing the version number on each run.

Routines Added in Preparation of XNOVAT

Several routines were required to produce XNOVAT. Subroutine INTRPC determines the rate of combustion of the reactive layers ascribed to the tube wall, the centerline, and the projectile afterbody. To support the new form functions we have added the routines BLSL, HEX19, and SLIVER. To treat the reactivity and flow resistance of the endwalls of the bundles of propellant we added the routines CALFLO, CALPRM, FLUX, FLUXDR and TDBCAL, all of which were adapted from the TDNOVA Code (Gough, 1983c). The routine TDBUF acts as a link between the existing boundary value solver BCAL and the routine TDBCAL. In addition we added the routines JCON, SETSUB and RCASE which perform various utility functions.

Structure of NOVATC

XKTC was essentially formed by substituting XNOVAT in place of XNOVA in the previously developed NOVATC Code (Gough, 1983a). As we have previously discussed,[3] NOVATC is an amalgam of XNOVA and BRLTC (Gough, 1980b, 1983b).

In forming the amalgam care was taken to minimize cross-contamination of the coding. The approach was to take BRLTC and delete all references to the flow behind the base of the traveling charge while retaining the storage, data reads and processing pertinent to the regression of the surface, the traveling charge and the projectile. This stripped down code was linked to a complete version of XNOVA (Gough, 1983b) in which a minimal number of linking subroutine calls were placed. Although a more tightly written code could have been developed it would have been more difficult to maintain such a code in a form compatible with future versions of XNOVA and BRLTC. Also, it is the case that XNOVA and BRLTC have many variables whose Fortran names are identical, but whose meanings differ and, conversely, some variables with different names but identical meanings.

It will be noted in Table A.1 that all routines pertinent to the traveling charge have the prefix TC. A single routine, TCLINK, has the function of reconciling the storage conventions of the two codes and of passing data between them. Processing follows the usual NOVA conventions with the traveling charge logic activated at a number of places. NOVSUB calls TCDATA and TCLINK to read and initialize data. INTEG calls TCLINK, TCOUT to print the solutions and TCBR4 to determine the traveling charge time step constraint. INTAL calls TCLINK and TCXC, the main integration executive for the traveling charge. TABLES calls TCLINK. It was also necessary to restructure slightly the routines BCAL and BDMOV.

Routines Added in Preparation of Previous Version of XKTC

The approach followed in the development of NOVATC made the replacement of XNOVA by XNOVAT fairly straightforward. It should be noted, however, that the present effort involved substantial exercising of the algorithm and several revisions were made to the analysis of the boundary values at the base of the burning traveling charge. Accordingly, the versions of TCLINK and TCBASE used here differ from those in earlier versions of NOVATC.

Apart from linking the kinetics, tank gun and traveling charge options in a physically complete fashion, it was necessary to add several new routines in the development of XKTC. Subroutine GETLS computes the values of L^* for the intermediate products of combustion of the traveling charge. ATACH enforces the attachment of a propellant type to the tube or to the projectile.

Routines Added in Preparation of Present Version of XKTC

The revisions described in the main body of the present report have not entailed the addition of many new subroutines. Subroutines EXCW, FRACT and REG21A have been added to support the explicit analysis of an intergranular shock wave and the effects of grain fracture. The bulk of the new routines have been required in order to effect the amalgam with the RLPTC Code to support the modeling of charges with a traveling liquid propellant component. The approach to the amalgam with RLPTC was perfectly analogous to that described above in connection with BRLTC. The RLPTC routines added to XKTC are all prefaced with the letters TLC. Gough (1988) may be consulted for a table indicating the precise correspondence between the TLC - routines and their RLPTC counterparts. A new routine TLCLNK performs the task of linking the TLC storage with that of XKTC.

Finally, we note that the present version of XKTC includes those revisions made for the Navy to permit the modeling of inbore rockets (Gough, 1986b) and a linkage to the plasma model of Powell and Zielinsky (1992).

DESCRIPTION OF INPUT FILES

We preface the detailed description of the input file structure with some general observations. We note, in particular, the nomenclature for the definition of the geometry of the propelling charge.

Figure A.1 illustrates a charge configuration with does not make use of the tank gun option (MODET = 0). We illustrate the base of the projectile, an arbitrary number of filler elements -- some at the rear and some at the front of the charge -- and two types of propellant, the first of which is in two increments, the latter increment overlapping that of the second propellant. The figure also illustrates the significance of the input data ZGR, XEL, XBL and ZBPR.

Figure A.2 illustrates a charge configuration which does make use of the tank gun option (MODET = 1). We illustrate the intrusion of the projectile afterbody into the combustion chamber, the reactive layers on the tube wall, the centerline and the projectile afterbody, and three types of propellant, the first of which is present as two increments. To the rear of the afterbody we represent the three types of propellant as being parallel packaged and we illustrate the significance of the input data RGRI and RGRO.

Figures A.1 and A.2 both assume that the propellant is of the conventional type. Figure A.3 illustrates a charge configuration in which a solid propellant traveling charge is present. We note that the traveling charge may consist of several increments, each having distinct mechanical and thermochemical properties. The simulation of the traveling charge may be performed

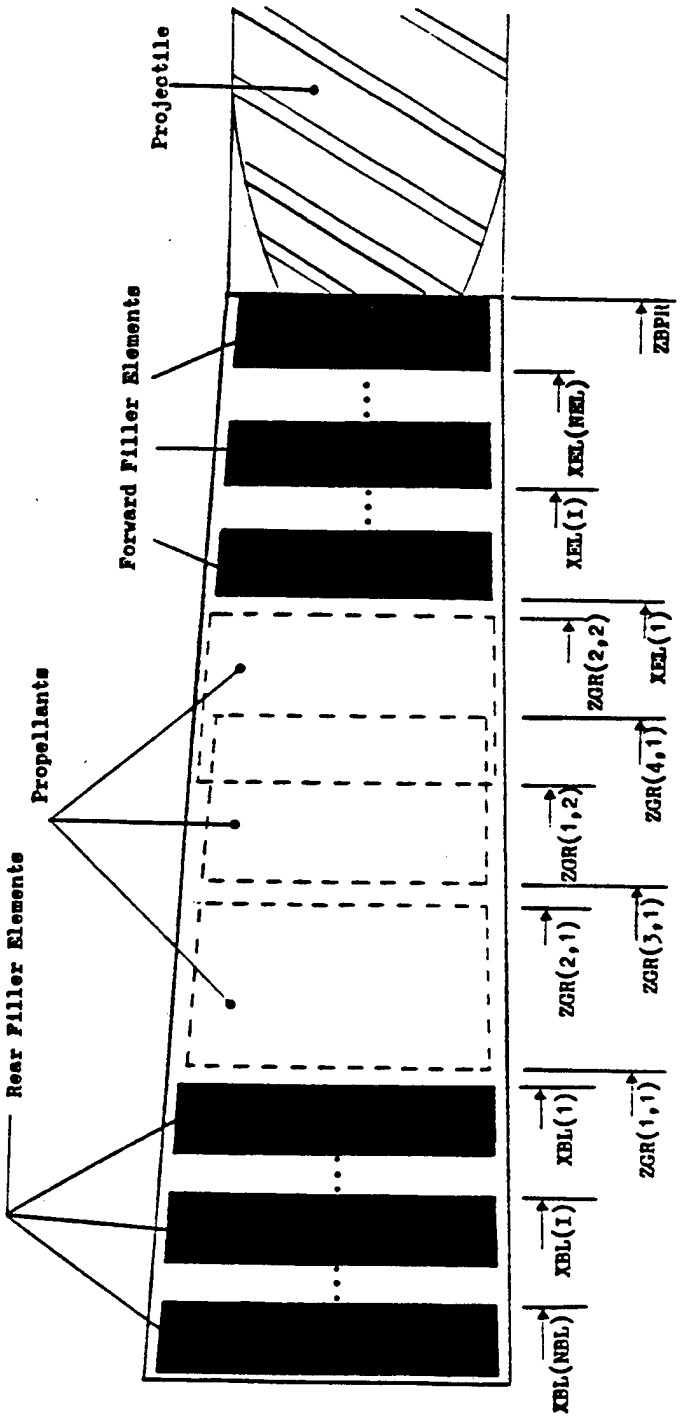

Figure A.1 Nomenclature for Definition of Charge Configuration in XKTC with MODET = 0.

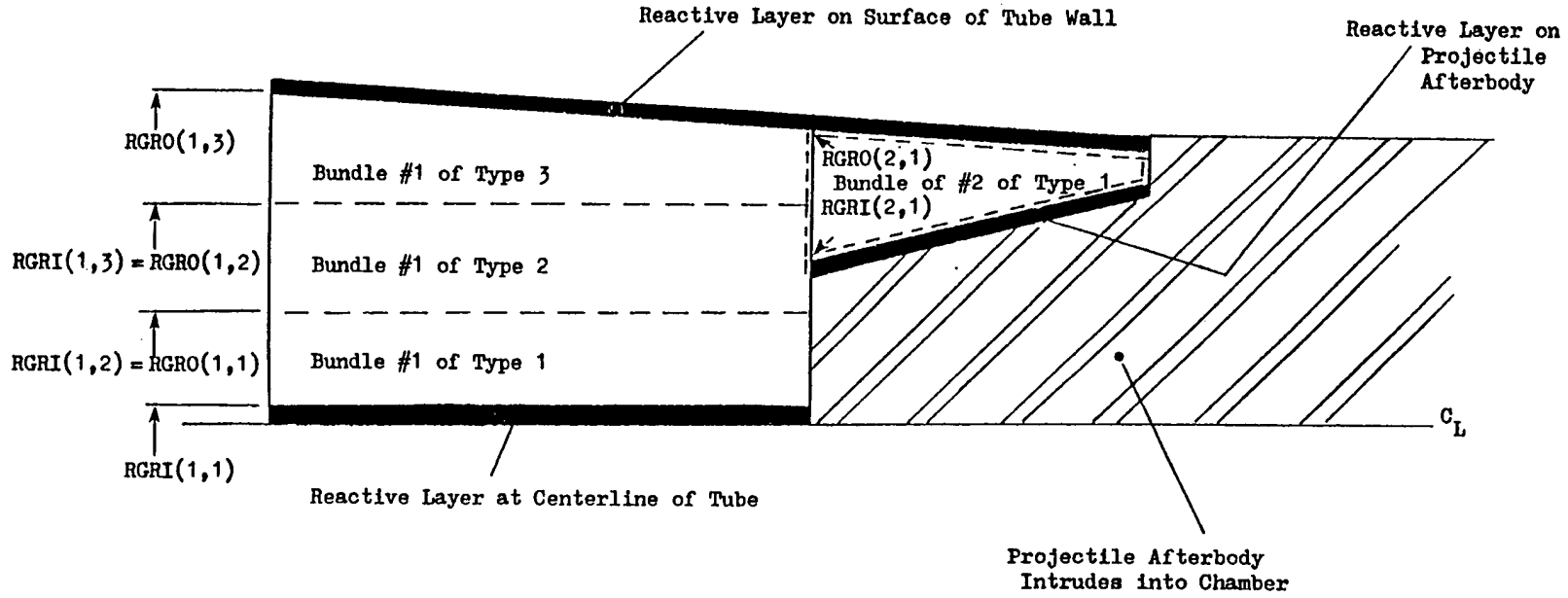

Figure A.2 Nomenclature for Definition of Charge Configuration in XNOVAT with MODET = 1.

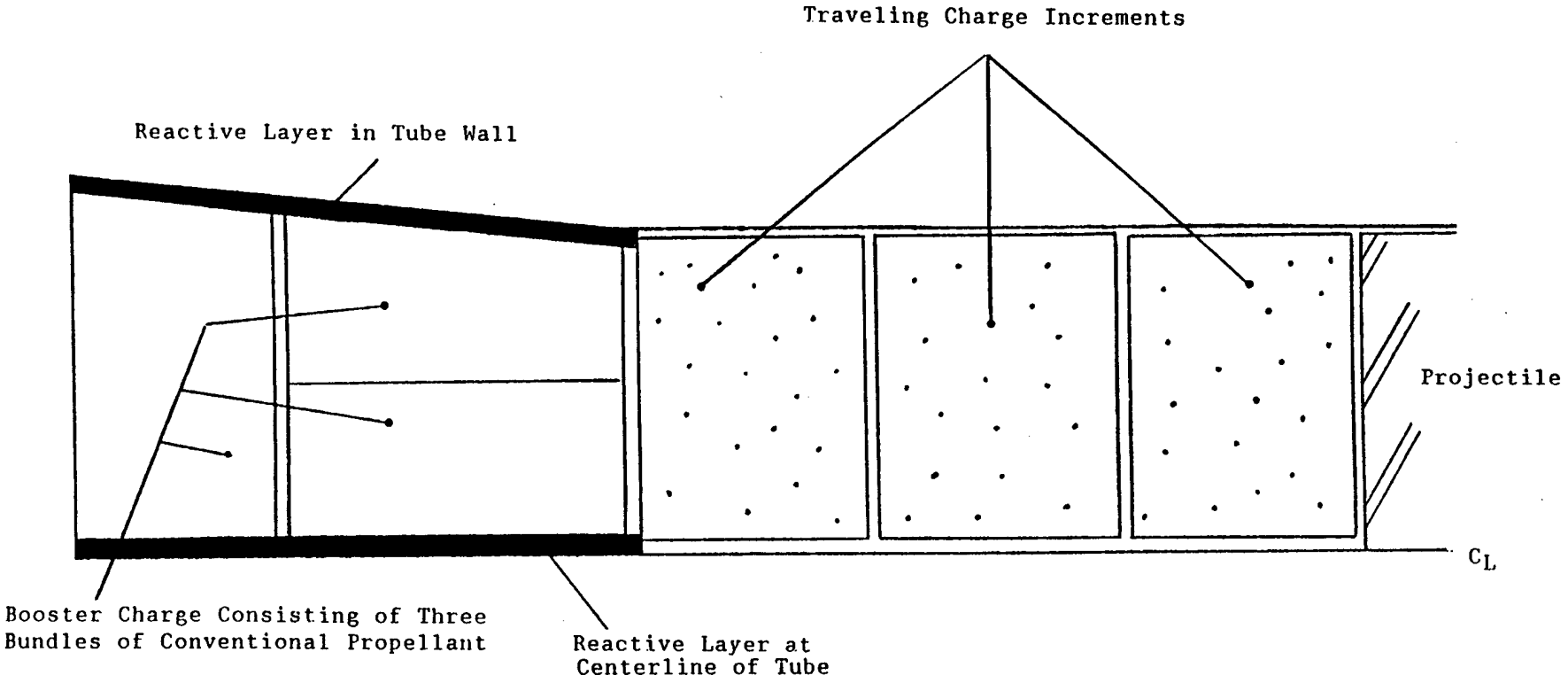

Figure A.3 Example of a Hybrid Charge Consisting of Conventional and Traveling Charge Increments.

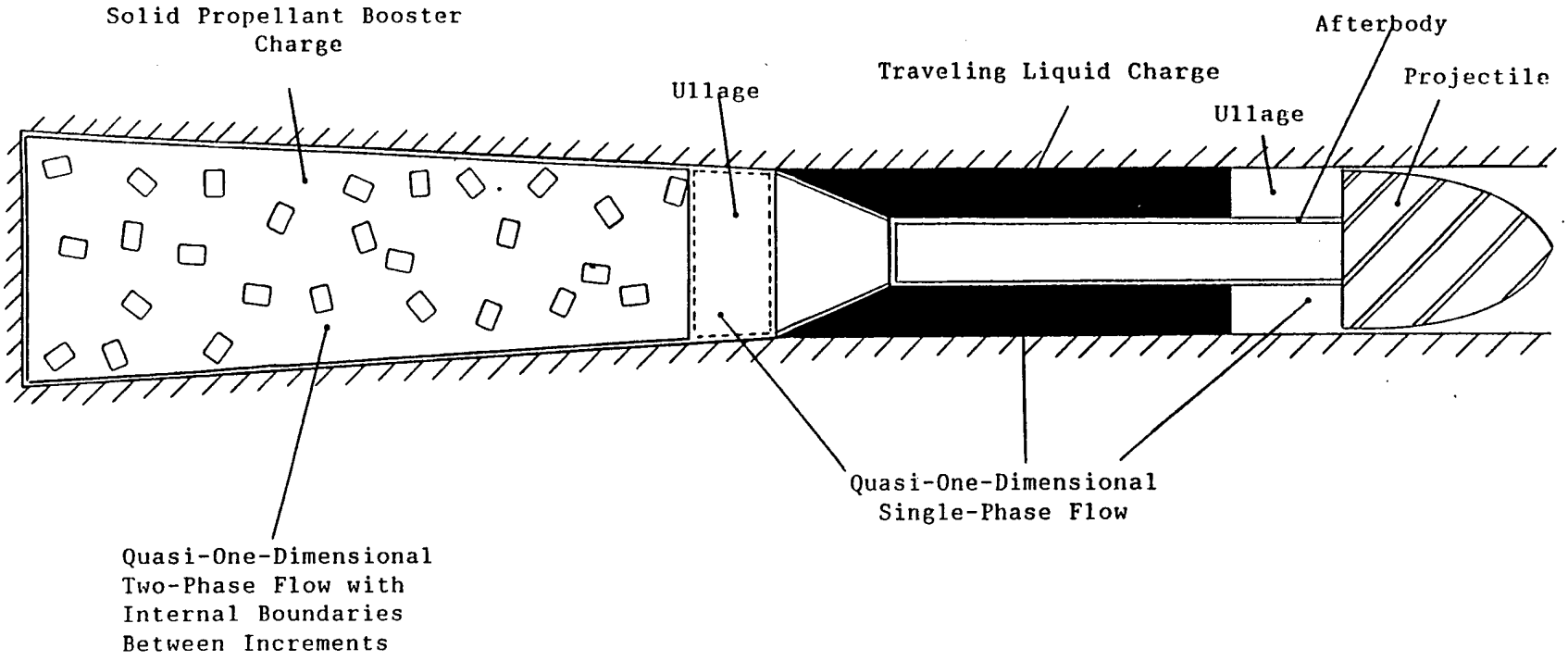

Figure A.4 Example of Hybrid Charge Consisting of Traveling Liquid Propellant and Solid Propellant Booster.

in conjunction with an arbitrarily configured conventional charge. It is assumed, however, that when the traveling charge is present there are no compactible filler materials at the front of the chamber, as in Figure A.1, and that the projectile does not have an afterbody as in Figure A.2. Reactive sidewalls may nevertheless be present, as shown in Figure A.3.

Figure A.4 illustrates a charge configuration in which a liquid propellant traveling charge is present. The solid propellant booster is permitted to take any of the configurations compatible with the solid propellant traveling charge. Figure A.4 shows a projectile with an afterbody which stabilizes the traveling liquid charge and allows the propellant to vent at the rear face. In the representation of Figure A.4 it is tacitly assumed that the discharged liquid propellant is fully burned within a negligibly short time so that the mass transferred to the booster region consists of final products of combustion. Gough (1988) may be consulted for further details.

Input to XKTC consists of XNOVAT data followed by a subset of the BRLTC data base when the solid propellant traveling charge option is selected in the control data field of XKTC and by a subset of the RLPTC data base when the liquid propellant traveling charge option is exercised. Tables A.2, A.3, A.4 and A.5 enumerate the "Mandatory", Contingent, Traveling Charge and Traveling Liquid Charge data files. The files prefixed with an M are always mandatory in XNOVAT. Here, File [M13] is optional. We have retained the file labels of XNOVAT, in spite of this minor inconsistency, to promote commonality among the various codes.

The enumeration of the M and C files follows that for the NOVA Code. We have attempted to maximize the compatibility of XKTC, XNOVAT, XNOVAK, XNOVATC, XNOVA and NOVA data bases. As noted in the introduction to this appendix, compatibility is complete with the possible exception of File [M4]. In XKTC, XNOVAT and XNOVAK, File [M4] always consists of two cards. In XNOVATC, XNOVA and NOVA it may consist of either one or two cards. Existing NOVATC, XNOVA and NOVA data sets for which File [M4] consists of only one card may be made compatible with XKTC, XNOVAT and XNOVAK by the insertion of a single blank card after the existing [M4] data card. NOVA files not supported by XKTC, XNOVAT and XNOVAK are read and subsequently ignored. The tabulation of data by XKTC only includes those elements which are supported.

All mandatory files, Table A.2, are common to all codes. However, not all the members of every file are supported by XKTC, XNOVAT and XNOVAK. The detailed definition of the input files given in Table A.6 describes all the elements which are supported and simply denotes the others as "Inactive." Those contingent files, Table A.3, which are supported are defined while the others are denoted as "not supported." Only those contingent files which are supported by XKTC appear in the detailed discussion of Table A.6.

The program input files are structured to permit the running of only one problem at a time. A problem may be restarted from disc, provided suitable options have been selected in a prior run. Each problem may be terminated according to a criterion of number of integration steps, projectile displacement or problem time. Termination occurs at whichever of the three criteria is first satisfied. However, if the blowdown option is exercised the projectile displacement criterion does not serve to terminate the calculation. The muzzle is assumed to be open when the specified displacement is reached and termination is subsequently based on number of integration steps, problem time, or breech pressure, whichever is satisfied first.

It should be noted that file counters are edited by subroutine NOVSUB to establish their conformality with internal storage dimensions. However, other data are not edited, and it is recommended that the program user perform a first run on a new problem with termination set to follow initial set-up, so that all data may be validated.

The following notes (1) - (10) apply whether or not the traveling charge option is exercised. Subsequent notes (11) - (16) pertain to the traveling charge option. Note (17) applies to the inbore rocket motor option. Notes 18 and 19 apply to the traveling liquid charge option.

(1) For problems involving only granular propellant, the representations of the grain distributions are arbitrary. The granular propellants may doubly or triply overlap. However, a region occupied by stick propellant may not be shared by any other type unless MODET = 1. If MODET = 1, it is permissible to have an increment of stick propellant parallel packaged with another increment of stick or granular propellant. The monolithic charge is not permitted to share a cross-section of the tube with any other type. If a given type is specified as bonded to the tube or projectile, the bonding will be presumed to apply to any other propellant which shares a region with the given type.

(2) The mode of representation of one type of propellant is independent of the mode of representation of any other. If tables of volume fractions are used, it should be recalled that the volume fraction is the complement of the porosity, being zero when no propellant is present and increasing to unity as the pore volume vanishes. The volume fraction defaults to zero outside the range of positions defined by the tables.

(3) An internal boundary is identified at any location in which any volume fraction is discontinuous. Thus an internal boundary may be established at a point at which the porosity is continuous.

(4) Absolutely no restrictions, other than that on note (1), are placed on the relative positions of the bags of propellant. After the data are read, they are all converted internally to volume fraction tables. These are all then scanned to create a list of internal boundary positions. This list is then sorted to put them into order and to define the computational regions.

(5) The right-hand boundary is always set equal to XEL(1). If NEL = 0, XEL(1) defaults to ZBPR. Similarly, the left-hand boundary is always set equal to XBL(1). If NBL = 0, XBL(1) defaults to zero. It should be noted that the configuration of the forward elements is specified by reference to the position of the left-hand or rear boundary of each element. Conversely, the configuration of the rear elements is specified by reference to the position of the right-hand or forward boundary of each element. In both cases the elements are ordered so that the first is closest to the propelling charge.

(6) Although filler elements may be included if MODET = 1, the coding does not consider the influence of the afterbody on the behavior of the filler elements.

(7) It is emphasized that every case closure element must be accounted for, including spaces. Any element, other than the first, may be entered as a space by setting its mass equal to zero.

(8) It is noted that one may use a single element to represent more than one physical component and that conversely, one may use several elements to characterize a single component.

(9) The present storage allocation in the code imposes certain restrictions on the modeling of subsurface reactions in the propellant. It is assumed that only one type of propellant is present if an invariant embedding solution of the thermal response is desired (KMODE = 2 in File [M2]). At most 21 stations are permitted for the analysis of the thermal response. At most two chemical species can be associated with the subsurface chemistry. While these limits are thought to be adequate for present needs, they may readily be relaxed by means of changes in certain dimension statements.

(10) It will be noted that the data required when KMODE ≠ 0 Files [C23.1] - [C23.6] are to some extent already provided by the data of Files [M7] -[C7]. The latter data are superseded in such a case and consistency between the two sets of data is not essential. However, inconsistencies may yield an apparent energy defect in the summarized interior ballistics table.

(11) Unit 9 is reserved for storage of the traveling charge data if disk logout is specified.

(12) The code does not support the traveling charge option simultaneously with the compactible case closure option. It is also assumed that the projectile has no afterbody if the traveling charge option is exercised.

(13) The code termination data are always specified according to the NOVA format. The projectile data follow the NOVA format only if the traveling charge option is not in effect.

(14) Due to the cross-linking of the codes, no more than KQ-2 mesh points and no more than 9 increments can be specified for the booster region when the traveling charge option is in effect. Here KQ is the dimension of the XKTC storage arrays, currently set equal to 999 by a PARAMETER statement.

(15) A composition dependent covolume is not considered. The covolume for the calculation is presently based on the booster charge data according to the NOVA convention.

(16) The gun tube is assumed to have a constant area in the region occupied by the unreacted traveling charge.

(17) If an inbore rocket motor is present it is assumed that there are no forward filler elements, that the projectile has no afterbody and that no booster increments are attached to the projectile.

(18) The base of the traveling liquid charge is assumed to be permeable to the gas-phase if a cavity is present, but impermeable to the solid propellant booster charge.

(19) A region of ullage is assumed to exist at all times between the booster charge and the base of the traveling liquid charge. It is therefore recommended that the input datum RZOLV be less than or equal to 0.01. See the discussion of File [M3] in Table A.6.

REFERENCES CITED IN APPENDIX A

Gough, P.S. "The NOVA Code: A User's Manual"
Indian Head Contract Report IHCR-80-8 1980a

Gough, P.S. "A Model of the Traveling Charge"
Ballistic Research Laboratory Contract Report ARBRL-CR-00432 1980b

Gough, P.S. "Extensions to NOVA Flamespread Modeling
Capacity" PGA-TR-81-2 1981

Gough, P.S. "A Two-Phase Model of the Interior Ballistics
of Hybrid Solid-Propellant Traveling Charges"
Final Report, Task I, Contract DAAK11-82-C-0154 1983a

Gough, P.S. "XNOVA - An Express Version of the NOVA Code"
Final Report, Contract N00174-82-M-8048 1983b

Gough, P.S. "Modeling of Rigidized Gun Propelling Charges"
Contract Report ARBRL-CR-00518 1983c

Gough, P.S. "Theoretical Modeling of Navy Propelling
Charges" Final Report, Contract N00174-83-C-0241, PGA-TR-84-1 1984

Gough, P.S. "XNOVAT - A Two-Phase Flow Model of Tank Gun
Interior Ballistics"
Final Report, Task Order I, Contract DAAK11-85-D-0002 1985

Gough, P.S. "The XNOVAKTC Code" Final Report, Task Order II,
Contract DAAK11-85-D-0002, PGA-TR-86-1 1986a

Gough, P.S. "Theoretical Modeling of Interior Ballistic
Phenomena in Navy Guns"
Final Report, Contract N00174-84-C-0242, PGA-TR-86-2 1986b

Gough, P.S. "Continuum Modeling of Regenerative Liquid
Propellant Guns and Hybrid Traveling Charge Systems"
Final Report, Contract DAAK11-84-C-0080, PGA-TR-88-1 1988

Powell, J.D. and Zielinsky, A.E. "Theory and Experiment for
an Ablating - Capillary Discharge and Application to
Electrothermal -Chemical Guns"
Ballistic Research Laboratory Technical Report BRL-TR-3355 1992

TABLE A.1 SUMMARY OF ROUTINES AND LINKAGES

XKTC	Purpose	XKTC is a dummy main routine which immediately transfers control to NOVSUB.
	Calls:	NOVSUB.
	Called by:	None.
AFTSET	Purpose:	Subroutine AFTSET performs region management in the case when the base of the afterbody of the projectile is represented as an explicit discontinuity.
	Calls:	OUTPUT.
	Called by:	MESH, NOVSET.
ATACH	Purpose:	Subroutine ATACH enforces the attachment of a charge increment to either the tube or the projectile.
	Calls:	None.
	Called by:	INTAL.
AVN	Purpose:	Subroutine AVN is used to document code revisions and print the version number.
	Calls:	None.
	Called by:	NOVSUB.
BCAL	Purpose:	Subroutine BCAL accepts trial boundary values for the gas- and solid-phases and adjusts them so as to satisfy simultaneously the physical and characteristic boundary conditions.
	Calls:	COVC, EPTOR, EXCW, GAMMOL, GRLOAD, LUMPS, OUTPUT, PRTOC, PRTOE, RHEO, TABLES, TDBUF.
	Called by:	INTAL.
BDMOV	Purpose:	Subroutine BDMOV updates the position of the region boundaries. It also updates the projectile displacement and velocity, making use of FILLER and/or FILLBR when case closure elements are present.
	Calls:	EXCW, FILLBR, FILLER, FRATE, GMOVE, RCASE, RESFUN, RHEO.
	Called by:	INTAL, OUTPUT, TABLES.
BLKDAT	Purpose:	BLKDAT performs block data initialization.
	Calls:	None.
	Called by:	None.

BLSL	Purpose:	Subroutine BLSL computes the volume and surface area for the blind slit form function during the slivering phase.
	Calls:	None.
	Called by:	FORM.
BRNOUT	Purpose:	Subroutine BRNOUT detects the instant when all the propellant has been consumed and then consolidates all the computational regions into a single region with uniform mesh spacing.
	Calls:	FITSP, REG21.
	Called by:	None.
CALEOS	Purpose:	Subroutine CALEOS calculates specific heats and enthalpy according to formulation of NASA SP-273.
	Calls:	None.
	Called by:	EPTOR, ERTOP, FRICT, HEATP, HEATW, INTAL, INTRPC, LUMPS, NOVSET, NOVSUB, PRTOE.
CALFLO	Purpose:	Subroutine CALFLO computes the rate of reaction of the surface fluxes associated with the endwalls of the charge increments.
	Calls:	None.
	Called by:	TDBUF.
CALPRM	Purpose:	Subroutine CALPRM computes the flow resistance coefficient for the endwalls of the charge increments.
	Calls:	None.
	Called by:	TDBUF.
CHEMR	Purpose:	Subroutine CHEMR computes the effects of chemical reactions on the species mass fractions in the combustion product mixture and returns the value of the heat liberated by chemical reaction.
	Calls:	None.
	Called by:	INTAL, LUMPS.
CHEMRS	Purpose:	Subroutine CHEMRS performs a function similar to that of CHEMR; however it addresses the reactions within the solid propellant.
	Calls:	None.
	Called by:	IMBED.

CMBUST	Purpose:	Subroutine CMBUST interfaces the invariant embedding solution of the solid propellant thermal response with the macroscopic two-phase flow.
	Calls:	FBAK, IMBED.
	Called by:	INTEG, NOVSET.
CONLOS	Purpose:	Subroutine CONLOS computes the rate of transfer of condensed species from the combustion product mixture to the surface of the solid propellant.
	Calls:	None.
	Called by:	HEATP.
COVC	Purpose:	Function COVC computes the covolume of the combustion product mixture.
	Calls:	None.
	Called by:	BCAL, FRICT, HEATP, HEATW, INTAL, INTEG, INTRPC, LUMPS, REG12, REG32, STATES, TCLINK, TDBCAL, TDBUF.
DPDER	Purpose:	Function DPDER computes the partial derivative $(\partial p/\partial e)_\rho$ for the covolume equation of state.
	Calls:	None.
	Called by:	LUMPS.
DPDRE	Purpose:	Function DPDRE computes the partial derivative $(\partial p/\partial \rho)_e$ for the covolume equation of state.
	Calls:	None.
	Called by:	LUMPS.
EPTOR	Purpose:	Function EPTOR evaluates the density as a function of internal energy and pressure for the covolume equation of state.
	Calls:	CALEOS.
	Called by:	BCAL, FRICT, HEATP, HEATW, INTRPC, NOVSET, TDBCAL, TLCBCL, TLCBCX, TLCINT, TLCLPV.
ERTOP	Purpose:	Function ERTOP evaluates the pressure as a function of internal energy and density for the covolume equation of state.
	Calls:	CALEOS.
	Called by:	INTAL, LPVB, LUMPS, NOVSET, REG12, REG32, TLCLPV.
EXCW	Purpose:	Subroutine EXCW computes the state of the solid-phase after passing through a granular shock wave.
	Calls:	GRLOAD.
	Called by:	BCAL, BDMOV.

FBAK	Purpose:	Function FBAK computes the temperature gradient at the surface of the solid propellant taking into account heat transfer from the igniter and heat feedback from the flame.
	Calls:	None.
	Called by:	CMBUST, NOVSET.
FILLBR	Purpose:	Subroutine FILLBR updates the motion of the rear case closure elements.
	Calls:	OUTPUT, TABLES.
	Called by:	BDMOV, NOVSET.
FILLER	Purpose:	Subroutine FILLER updates the motion of the forward case closure elements and the projectile.
	Calls:	OUTPUT, TABLES.
	Called by:	BDMOV, NOVSET.
FITSP	Purpose:	Subroutine FITSP sets values of the state variables, following re-allocation of the mesh, by means of a cubic spline interpolation scheme.
	Calls:	None.
	Called by:	BRNOUT, MESH, NOVSET.
FLUX	Purpose:	Subroutine FLUX computes the state of gas at the boundaries of the reactive endwalls.
	Calls:	None.
	Called by:	FLUXDR, TDBCAL.
FLUXDR	Purpose:	Subroutine FLUXDR computes the derivatives of the state variables in a lumped parameter region with respect to the fluxes to that region from the contiguous continuum regions.
	Calls:	FLUX.
	Called by:	TDBUF.
FORM	Purpose:	Subroutine FORM computes the surface area and volume of the propellant grains. It is supported by PERF19 which treats the slivering phase of nineteen perforation propellant.
	Calls:	BLSL, HEX19, PERF19.
	Called by:	INTEG, NOVSET.

FORMCR	Purpose:	Subroutine FORMCR is effectively a subset of FORM and is used to support subroutine LPVB as a modular package.
	Calls:	None.
	Called by:	LPVB, TLCLPV.
FRACT	Purpose:	Subroutine FRACT determines the effects of grain fracture.
	Calls:	None.
	Called by:	INTEG, NOVSET.
FRATE	Purpose:	Function FRATE computes the steady flow through a nozzle using the covolume equation of state.
	Calls:	None.
	Called by:	BDMOV, LPVB.
FRICT	Purpose:	Subroutine FRICT computes the interphase drag for granular propellant.
	Calls:	CALEOS, COVC, EPTOR, VIS.
	Called by:	INTEG.
GAMMOL	Purpose:	Subroutine GAMMOL computes the ratio of specific heats and the molecular weight of the combustion product mixture.
	Calls:	None.
	Called by:	BCAL, LUMPS, STATES, TCLINK, TDBCAL, TDBUF.
GETLS	Purpose:	Subroutine GETLS computes L^* values for the intermediate combustion products of the traveling charge.
	Calls:	None.
	Called by:	INTAL, INTEG.
GMOVE	Purpose:	Subroutine GMOVE updates the motion of the gun tube when the recoil option is exercised.
	Calls:	None.
	Called by:	BDMOV.
GRLOAD	Purpose:	Subroutine GRLOAD computes the nominal loading curve for granular propellant.
	Calls:	None
	Called by:	BCAL, EXCW, INTAL, RHEO.

HEATP	Purpose:	Subroutine HEATP determines the interphase heat transfer, updates the surface temperature of the solid-phase prior to ignition, and also determines the interphase drag in stick propellant.
	Calls:	CALEOS, CONLOS, COVC, EPTOR, VIS.
	Called by:	INTEG.
HEATW	Purpose:	Subroutine HEATW determines the rate of heat transfer to the tube wall and updates the tube surface temperature.
	Calls:	CALEOS, COVC, EPTOR, VIS.
	Called by:	INTEG, NOVSET.
HEX19	Purpose:	Subroutine HEX19 computes the volume and surface area of nineteen-perforation hexagonal grains.
	Calls:	SLIVER.
	Called by:	FORM.
IGNITE	Purpose:	Subroutine IGNITE determines the time of ignition of the propellant.
	Calls:	None.
	Called by:	INTEG.
IMBED	Purpose:	Subroutine IMBED integrates the thermal profile in the solid propellant by means of the method of invariant embedding.
	Calls:	CHEMRS, FBAK, ROOT, ROOTR.
	Called by:	CMBUST, NOVSET.
INTAL	Purpose:	Subroutine INTAL updates the principal state variables, p, ρ, u, ε, u_p, σ at all interior mesh points. It also determines trial update boundary values together with characteristic coefficients which are transmitted to BCAL for imposition of the physical boundary conditions.
	Calls:	ATACH, BCAL, BDMOV, CALEOS, CHEMR, COVC, ERTOP, GETLS, GRLOAD, INTRP1, LPVB, PRTOC, PRTOE, RCASE, RDEDPR, RHEO, TCLINK, TCXC, TLCLNK, TLCXC.
	Called by:	INTEG.

INTEG	Purpose:	Subroutine INTEG is the principal integration executive. It is cycled twice per time step, once for the predictor level and once for the corrector level. It establishes the constitutive data by calls to individual subroutines and effects the update of the principal state variables by a call to INTAL. INTEG itself updates the surface regression and thermal parameter H for the solid-phase and, if KMODE = 0 (File [M2] of Table A.4), it also updates the molecular weight and ratio of specific heats for the gas phase.
	Calls:	CMBUST, COVC, FORM, FRACT, FRICT, GETLS, HEATP, HEATW, IGNITE, INTAL, INTRP1, INTRP2, INTRPC, JCON, MESH, OUTPUT, PRTOC, REGRES, STATES, TABLES, TCBR4, TCLINK, TCOUT, TERMIN, TLCGDT, TLCLNK, TLCMSH, TLCOUT, VOIDS, WALTEM.
	Called by:	NOVSET.
INTRP1	Purpose:	Subroutine INTRP1 determines the cross-sectional area of the tube at each mesh point, including an allowance for the unburned portion of the primer.
	Calls:	JCON.
	Called by:	INTAL, INTEG, MESH, NOVSET, TABLES.
INTRP2	Purpose:	Subroutine INTRP2 computes the rate of discharge of the igniter at each mesh point.
	Calls:	PLASMA.
	Called by:	INTEG, MESH, NOVSET.
INTRPC	Purpose:	Subroutine INTRPC computes the local mass addition due to combustion of the reactive sidewalls.
	Calls:	CALEOS, COVC, EPTOR, JCON, RCASE, VIS.
	Called by:	INTEG, MESH, NOVSET.
JCON	Purpose:	Function JCON locates the nearest continuum mesh point.
	Calls:	None.
	Called by:	INTEG, INTRP1, INTRPC, LUMPS.
LPDATA	Purpose:	Subroutine LPDATA converts the XNOVA data base into an equivalent data base for a lumped parameter interior ballistic model.
	Calls:	None.
	Called by:	NOVSET.

LPVB	Purpose:	Subroutine LPVB provides a lumped parameter analysis of a control volume which undergoes mass transfer with some external ambient.
	Calls:	ERTOP, FORMCR, FRATE.
	Called by:	INTAL, NOVSET.
LUMPS	Purpose:	Subroutine LUMPS provides a trial update of the state of all lumped parameter regions. It also computes derivatives of the state variables with respect to the mass fluxes to the lumped parameter region. These are used by BCAL to enforce the physical boundary conditions.
	Calls:	CALEOS, CHEMR, COVC, DPDER, DPDRE, ERTOP, GAMMOL, JCON, RCASE.
	Called by:	BCAL, TDBUF.
MESH	Purpose:	Subroutine MESH determines the level of modeling of each region and assigns mesh points to the continuum regions on the basis of their relative sizes.
	Calls:	AFTSET, FITSP, INTRP1, INTRP2, INTRPC, OUTPUT, REG12, REG21, REG21A, REG32, SETSUB, STATES.
	Called by:	INTEG, NOVSET.
NOVSET	Purpose:	Subroutine NOVSET performs the initialization of variables which are not set by BLKDAT.
	Calls:	AFTSET, CALEOS, CMBUST, EPTOR, ERTOP, FBAK, FILLBR, FILLER, FITSP, FORM, FRACT, HEATW, IMBED, INTEG, INTRP1, INTRP2, INTRPC, LPDATA, LPVB, MESH, REGRES, SETSUB, TABLES, TCDATA, TCINIT, TCLINK, TLCINP, TLCINT, TLCLNK.
	Called by:	NOVSUB.
NOVSUB	Purpose:	Subroutine NOVSUB reads and prints the input data used to define the problem.
	Calls:	AVN, CALEOS, NOVSET.
	Called by:	XKTC.
OUTPUT	Purpose:	Subroutine OUTPUT is responsible for logout of the solution to the printer and/or direct access device unit 8.
	Calls:	BDMOV, REGRES, TABLES, VIS.
	Called by:	AFTSET, BCAL, FILLBR, FILLER, INTEG, MESH.

PERF19

Purpose: Subroutine PERF19 computes the surface area and covolume of nineteen-perforation propellant during the slivering phase.

Calls: None.

Called by: FORM.

PGINT

Purpose: Function PGINT performs truncation of a floating point variable to a fixed point variable.

Calls: None.

Called by: TABLES.

PLASMA

Purpose: Subroutine PLASMA computes the fluxes from a capillary given the history of current. It is supported by block data "atomic" and two subroutines "mixture" and "zjawja" which are not described here. See Powell and Zielinsky (1992).

Calls: mixture, zjawja

Called by: INTRP2

PRTOC

Purpose: Function PRTOC computes the square of the speed of sound according to the covolume equation of state.

Calls: None.

Called by: BCAL, INTAL, INTEG, TDBUF.

PRTOE

Purpose: Function PRTOE computes the internal energy from the pressure and density according to the covolume equation of state.

Calls: None.

Called by: BCAL, CALEOS, INTAL, STATES, TCLINK, TDBCAL, TDBUF, TLCBCL, TCLMSH, TLCXC.

RCASE

Purpose: Subroutine RCASE determines the density of the case as a function of pressure.

Calls: None.

Called by: BDMOV, INTAL, INTRPC, LUMPS.

RDEDPR

Purpose: Function RDEDPR computes the quantity $\rho(\partial e/\partial p)_\rho$ according to the covolume equation of state.

Calls: None.

Called by: INTAL, TLCFDR.

REG12

Purpose: Subroutine REG12 transforms data for a region of continuum ullage into data for a region of lumped parameter ullage.

Calls: COVC, ERTOP.

Called by: MESH.

REG21	Purpose:	Subroutine REG21 transforms data for a region of lumped parameter ullage into data for a region of continuum ullage.
	Calls:	None.
	Called by:	BRNOUT, MESH.
REG21A	Purpose:	Subroutine REG21A transforms data for a region of lumped parameter two-phase flow into data for a region of continuous two-phase flow.
	Calls:	None.
	Called by:	MESH.
REG32	Purpose:	Subroutine REG32 sets initial data for a lumped parameter region of ullage which is newly opened.
	Calls:	COVC, ERTOP.
	Called by:	MESH.
REGRES	Purpose:	Subroutine REGRES computes the rate of regression of the surface of the propellant.
	Calls:	VIS.
	Called by:	INTEG, NOVSET, OUTPUT.
RESFUN	Purpose:	Function RESFUN computes the resistance to projectile motion due to interference of the rotating band with the gun tube.
	Calls:	None.
	Called by:	BDMOV.
RHEO	Purpose:	Subroutine RHEO computes the rate of propagation of intergranular disturbances.
	Calls:	GRLOAD.
	Called by:	BCAL, BDMOV, INTAL.
ROOT	Purpose:	Subroutine ROOT selects a new value for the solution of an arbitrary equation by the method of regula falsi.
	Calls:	None.
	Called by:	IMBED.
ROOTR	Purpose:	Subroutine ROOTR is similar to ROOT, but contains additional logic for the situation in which the slope of the test function vanishes.
	Calls:	None.
	Called by:	IMBED.

SETSUB	Purpose:	Subroutine SETSUB sets the reactivity and permeability pointers.
	Calls:	None.
	Called by:	MESH, NOVSET.
SLIVER	Purpose:	Subroutine SLIVER computes the volume and surface area of nineteen-perforation hexagonal grains during the slivering process.
	Calls:	None.
	Called by:	HEX19.
STATES	Purpose:	Subroutine STATES computes certain of the dependent state variables from the principal storage arrays for the gas-phase.
	Calls:	COVC, GAMMOL, PRTOE.
	Called by:	INTEG, MESH, TERMIN.
TABLES	Purpose:	Subroutine TABLES compiles the summary data which describe the conventional interior ballistic quantities such as histories of breech and base pressure and of the projectile trajectory.
	Calls:	BDMOV, INTRP1, PGINT, TCLINK, TLCLNK.
	Called by:	BCAL, FILLBR, FILLER, INTEG, NOVSET, OUTPUT.
TCARAC	Purpose:	Subroutine TCARAC defines characteristic data in conjunction with the determination of boundary values for the traveling charge when modeled as a continuum.
	Calls:	TCBR2, TCDSDR.
	Called by:	TCBASE, TCBPR, TCONTC.
TCBASE	Purpose:	Subroutine TCBASE determines the regression rate of the traveling charge and provides trial boundary values for the unreacted side.
	Calls:	TCARAC, TCBURN, TCDSDR, TCIG, TCLINK, TCPROP, TCRESP, TCRNOM.
	Called by:	TCXC.
TCBMDC	Purpose:	Subroutine TCBMDC computes mechanical properties of the traveling charge when its rheology is specified in tabular format.
	Calls:	ISCICU (An IMSL routine).
	Called by:	TCDATA, TCDSDR, TCRNOM, TCSNOM.

TCBPR	Purpose:	Subroutine TCBPR updates the boundary values of the traveling charge at the base of the projectile.
	Calls:	TCARAC, TCDSDR, TCRNOM.
	Called by:	TCXC.
TCBR1	Purpose:	Subroutine TCBR1 initializes the computational arrays associated with the traveling charge.
	Calls:	TCRFIT, TCRNOM.
	Called by:	TCINIT.
TCBR2	Purpose:	Subroutine TCBR2 moves the traveling charge computational arrays into working arrays. This routine performs a trivial function in the present code but it is retained in order to maintain structural commonality with BRLTC where its function is non-trivial.
	Calls:	None.
	Called by:	TCARAC, TCBR3, TCBR4, TCOUT.
TCBR3	Purpose:	Subroutine TCBR3 updates the state variables for the traveling charge at all internal mesh points.
	Calls:	TCBR2, TCDSDR, TCWFR.
	Called by:	TCXC.
TCBR4	Purpose:	Subroutine TCBR4 determines the CFL time step restriction for the traveling charge.
	Calls:	TCBR2, TCDSDR, TCLINK.
	Called by:	INTEG.
TCBURN	Purpose:	Subroutine TCBURN calculates the regression rate of the traveling charge when specified as an empirical function of pressure (on the reacted side) or stress (on the unreacted side).
	Calls:	TCDVDI.
	Called by:	TCBASE.
TCDATA	Purpose:	Subroutine TCDATA reads and prints the input data associated with the traveling charge.
	Calls:	TCBMDC, TCINIT.
	Called by:	NOVSET.
TCDSDR	Purpose:	Function TCDSDR calculates the speed of sound in the traveling charge.
	Calls:	TCBMDC, TCSNOM.
	Called by:	TCARAC, TCBASE, TCBPR, TCBR3, TCBR4, TCONTC.

TCDVDI	Purpose:	Subroutine TCDVDI performs interpolation by the method of divided differences.
	Calls:	None.
	Called by:	TCBURN.
TCGETK	Purpose:	Subroutine TCGETK updates the ordinary differential equations associated with the traveling charge.
	Calls:	TCRESP.
	Called by:	TCXC.
TCIG	Purpose:	Subroutine TCIG determines the time at which ignition occurs for the traveling charge.
	Calls:	None.
	Called by:	TCBASE.
TCINIT	Purpose:	Subroutine TCINIT performs the initialization of constants and pointers for the traveling charge.
	Calls:	TCBR1, TCRFIT, TCVUPD.
	Called by:	NOVSET, TCDATA.
TCLINK	Purpose:	Subroutine TCLINK transfers data between the NOVA routines and the BRLTC routines.
	Calls:	COVC, GAMMOL, PRTOE, TCPROP.
	Called by:	INTAL, INTEG, NOVSET, TABLES, TCBASE, TCBR4, TCOUT, TCXC.
TCONTC	Purpose:	Subroutine TCONTC updates the boundary values for the traveling charge at the interfaces between increments.
	Calls:	TCARAC, TCDSDR, TCRNOM.
	Called by:	TCXC.
TCOUT	Purpose:	Subroutine TCOUT performs the logout of the traveling charge state variables.
	Calls:	TCBR2, TCLINK.
	Called by:	INTEG.
TCPROP	Purpose:	Subroutine TCPROP moves the traveling charge property data from vector into scalar storage.
	Calls:	None.
	Called by:	TCBASE, TCLINK.

TCRESP	Purpose:	Subroutine TCRESP computes the resistance on the projectile when the traveling charge option is in effect.
	Calls:	None.
	Called by:	TCBASE, TCGETK.
TCRFIT	Purpose:	Subroutine TCRFIT performs the mesh allocation for the traveling charge and the interpolation of data associated with revisions to the number of points.
	Calls:	None.
	Called by:	TCBR1, TCINIT, TCXC.
TCRNOM	Purpose:	Function TCRNOM computes the density of the traveling charge as a function of pressure on the nominal loading curve.
	Calls:	TCBMDC.
	Called by:	TCBASE, TCBPR, TCBR1, TCONTC.
TCSCHK	Purpose:	Subroutine TCSCHK enforces the requirement that the pressure in the traveling charge not exceed the nominal loading value for the current value of density.
	Calls:	TCSNOM.
	Called by:	TCXC.
TCSNOM	Purpose:	Function TCSNOM computes the pressure in the traveling charge as a function of density on the nominal loading curve.
	Calls:	TCBMDC.
	Called by:	TCDSDR, TCSCHK.
TCVCHK	Purpose:	Subroutine TCVCHK checks that the velocity in the traveling charge has not been reversed as a consequence of the friction term.
	Calls:	None.
	Called by:	TCXC.
TCVUPD	Purpose:	Subroutine TCVUPD updates the continuum boundary velocities for the traveling charge.
	Calls:	None.
	Called by:	TCINIT, TCXC.
TCWFR	Purpose:	Subroutine TCWFR computes the friction between the traveling charge and the tube wall.
	Calls:	None.
	Called by:	TCBR3.

TCXC	Purpose:	Subroutine TCXC is the integration executive for the traveling charge state variables.
	Calls:	TCBASE, TCBPR, TCBR3, TCGETK, TCLINK, TCONTC, TCRFIT, TCSCHK, TCVCHK, TCVUPD, TCZUPD.
	Called by:	INTAL.
TCZUPD	Purpose:	Subroutine TCZUPD updates the positions of the continuum boundaries associated with the traveling charge.
	Calls:	None.
	Called by:	TCXC.
TDBCAL	Purpose:	Subroutine TDBCAL uses the physical boundary conditions and the characteristic forms to determine the boundary values at each time step.
	Calls:	COVC, EPTOR, FLUX, GAMMOL, PRTOE.
	Called by:	TDBUF.
TDBUF	Purpose:	Subroutine TDBUF acts as an interface from the NOVA storage conventions to those of the solver TDBCAL.
	Calls:	CALFLO, CALPRM, COVC, FLUXDR, GAMMOL, LUMPS, PRTOC, PRTOE, TDBCAL.
	Called by:	BCAL.
TERMIN	Purpose:	Subroutine TERMIN tests for the termination of the calculation.
	Calls:	STATES.
	Called by:	INTEG.
TLCBCL	Purpose:	Subroutine TLCBCL enforces the physical boundary conditions associated with the traveling liquid charge.
	Calls:	EPTOR, PRTOE, TLCOUT, TLCPTR, TLCSMQ.
	Called by:	TLCBCX.
TLCBCX	Purpose:	Subroutine TLCBCX organizes data for TLCBCL.
	Calls:	EPTOR, TLCBCL, TLCFDR, TLCMIX, TLCPTR.
	Called by:	TLCXC.
TLCFDR	Purpose:	Subroutine TLCFDR evaluates the effect of a mass flux on a lumped parameter region for the traveling liquid charge.
	Calls:	RDEDPR, TLCMIX, TLCPTR.
	Called by:	TLCBCX.

TLCGAC	Purpose:	Subroutine TLCGAC computes flow areas associated with the traveling liquid charge.
	Calls:	None.
	Called by:	TLCINT, TLCMSH, TLCXC.
TLCGAS	Purpose:	Function TLCGAS computes the speed of sound in the gas-phase for the traveling liquid charge.
	Calls:	None.
	Called by:	TLCMIX.
TLCGBL	Purpose:	Subroutine TLCGBL computes the total mass and energy in the regions defined by the traveling liquid charge.
	Calls:	TLCPTR.
	Called by:	TLCINT, TLCLNK.
TLCGDT	Purpose:	Subroutine TLCGDT computes the time step constraint associated with the traveling liquid charge.
	Calls:	TLCMIX.
	Called by:	INTEG.
TLCINP	Purpose:	Subroutine TLCINP reads the input data for the traveling liquid charge.
	Calls:	None.
	Called by:	NOVSET.
TLCINT	Purpose:	Subroutine TLCINT performs initialization associated with the traveling liquid charge.
	Calls:	EPTOR, TLCGAC, TLCGBL, TLCLPV, TLCMSH, TLCPTR.
	Called by:	NOVSET.
TLCLIQ	Purpose:	Function TLCLIQ computes the speed of sound in the liquid phase for the traveling liquid charge.
	Calls:	TLCPTR.
	Called by:	TLCMIX.
TLCLNK	Purpose:	Subroutine TLCLNK interfaces the traveling liquid charge data storage with the conventional XKTC storage arrays.
	Calls:	TLCGBL.
	Called by:	INTAL, INTEG, NOVSET, TABLES, TLCUPD.

TLCLPV	Purpose:	Subroutine TLCLPV models a two-phase lumped parameter region for the traveling liquid charge.
	Calls:	EPTOR, ERTOP, FORMCR.
	Called by:	TLCINT, TLCXC.
TLCLUB	Purpose:	Subroutine TLCLUB is used to perform matrix inversion for the traveling liquid charge.
	Calls:	None.
	Called by:	TLCSMQ.
TLCLUD	Purpose:	Subroutine TLCLUD is used to perform matrix inversion for the traveling liquid charge.
	Calls:	None.
	Called by:	TLCSMQ.
TLCMIX	Purpose:	Function TLCMIX computes the speed of sound in the two-phase mixture for the traveling liquid charge.
	Calls:	TLCGAS, TLCLIQ, TLCPTR.
	Called by:	TLCBCX, TLCFDR, TLCGDT, TLCUPD.
TLCMSH	Purpose:	Subroutine TLCMSH allocates mesh storage for the traveling liquid charge.
	Calls:	PRTOE, TLCGAC.
	Called by:	INTEG, TLCINT.
TLCOUT	Purpose:	Subroutine TLCOUT prints the solution in regions occupied by the traveling liquid charge.
	Calls:	TLCSTR.
	Called by:	INTEG, TLCBCL.
TLCPTR	Purpose:	Function TLCPTR computes the density of the liquid phase as a function of pressure in the traveling liquid charge.
	Calls:	None.
	Called by:	TLCBCL, TLCBCX, TLCFDR, TLCGBL, TLCINT, TLCLIQ, TLCMIX, TLCUPD.
TLCRSP	Purpose:	Function TLCRSP computes the resistive pressure acting on the projectile when a traveling liquid charge is modeled.
	Calls:	None.
	Called by:	TLCUPD.

TLCRTP	Purpose:	Function TLCRTP computes the pressure of the liquid phase as a function of density in the traveling charge.
	Calls:	None.
	Called by:	None.
TLCSMQ	Purpose:	Subroutine TLCSMQ determines the solution of a system of linear equations.
	Calls:	TLCLUB, TLCLUD.
	Called by:	TLCBCL.
TLCSTR	Purpose:	Subroutine TLCSTR computes the stresses in the afterbody of a projectile carrying a traveling liquid charge.
	Calls:	None.
	Called by:	TLCOUT, TLCUPD.
TLCUPD	Purpose:	Subroutine TLCUPD performs the integration of the governing equations associated with the traveling liquid charge.
	Calls:	TLCLNK, TLCMIX, TLCPTR, TLCRSP, TLCSTR.
	Called by:	TLCXC.
TLCXC	Purpose:	Subroutine TLCXC is the executive routine for the data associated with the traveling liquid charge.
	Calls:	PRTOE, TLCBCX, TLCGAC, TLCLPV, TLCUPD.
	Called by:	INTAL.
VIS	Purpose:	Function VIS computes the viscosity of the gas-phase as a function of temperature.
	Calls:	None.
	Called by:	FRICT, HEATP, HEATW, INTRPC, OUTPUT, REGRES.
VOIDS	Purpose:	Subroutine VOIDS updates the volume fractions of each of the constituent solid-phase species from the history of the porosity.
	Calls:	None.
	Called by:	INTEG.
WALTEM	Purpose:	Subroutine WALTEM updates the thermal equation for the tube wall temperature determined according to a cubic profile approximation.
	Calls:	None.
	Called by:	INTEG.

TABLE A.2 SUMMARY OF XKTC "MANDATORY" INPUT FILES

FILE NUMBER	FILE NAME
M1	Problem Name
M2	Control Data
M3	Integration Parameters
M4	File Counters
M5	Properties of Ambient Gas
M6	General Properties of Propellant Bed
M7	I-th Propellant Type, Location and Mass
M8	I-th Propellant Form Function Data
M9	I-th Propellant Rheology
M10	I-th Propellant Solid-Phase Thermochemistry
M11	I-th Propellant Gas-Phase Thermochemistry
M12	Tube Geometry
*M13	Projectile and Rifling Characteristics

* File M13 is not mandatory in XKTC. It is required only if neither the traveling charge option nor the liquid traveling charge option is exercised.

TABLE A.3 SUMMARY OF XRTC CONTINGENT INPUT FILES

FILE NUMBER	FILE NAME
C1	Logout Counters
C2	Erosive Burn Rate Parameters
C3	Not Supported.
C4	Position and Mass of Additional Bags of I-th Propellant
C5	Distribution of Volume Fraction of I-th Propellant
C5.05	I-th Propellant Drag Relaxation Data
C5.1	I-th Propellant Port Diameter File Counter
C5.2	I-th Propellant Port Diameter
C5.3	I-th Arbitrary Form Function File Counter
C5.4	I-th Arbitrary Form Function Description
C5.5	I-th Propellant Fracture Data Counter
C5.6	I-th Propellant Fracture Characteristics
C6	Not Supported.
C7	I-th Propellant Deterred Layer Properties
C8	Igniter Thermochemistry
C9	Igniter Discharge Times
C10	Igniter Discharge Positions
C11	Igniter Rate of Discharge
C12	Bore Resistance
C12.1	Air Shock Data
C12.2	Projectile Setback Resistance Data
C13	Tube Thermal Properties
C14	Tube Initial Temperature Profile
C15	Not Supported.
C16	Not Supported.
C17	Not Supported.
C17.5	Blowdown Parameters
C18	I-th Forward Compactible Filler Element Properties
C19	Constitutive Data for I-th Forward Element

TABLE A.3 continued

FILE NUMBER	FILE NAME
C19.1	I-th Rear Compactible Filler Element Properties
C19.2	Constitutive Data for I-th Rear Element
C20	Not Supported.
C21	Not Supported.
C22	Not Supported.
C23	Positions for Pressure Table Storage
C23.01	Projectile Afterbody Pressure History Option
C23.1	Kinetics Option Counters
C23.2	Properties of Species
C23.21	Properties of Species in NASA SP-273 Formulation
C23.3	Composition of Propellant Near Field Combustion Products
C23.31	Pressure Dependent Composition of Propellant Near Field Combustion Products
C23.4	Composition of Igniter Discharge Combustion Products
C23.41	Pressure Dependent Composition of Igniter Discharge Combustion Products
C23.5	Composition of Initial Ambient Gas
C23.6	Initial Composition of Solid Propellant
C23.61	Composition of Traveling Charge Near Field Combustion Products
C23.62	Types of Reactions in Mixture of Combustion Products
C23.63	Species Thermal Equilibration Switches
C23.7	Description of Arrhenius Reactions in Mixture of Combustion Products
C23.71	Description of Pressure-Dependent Reactions in Mixture of Combustion Products
C23.8	Description of Reactions in Solid Propellant
C23.9	Solid Propellant Thermal Response Parameters
C24	Parameters to Define Mesh in Invariant Embedding Analysis
C25	Tank Gun Option Control Data
C25.1	Geometry of Projectile Afterbody
C25.11	Spatial Resolution Factor for Analysis of Base of Afterbody as Surface of Area Discontinuity
C25.2	Thickness and Density Counters for Reactive Layer I

TABLE A.3 continued

FILE NUMBER	FILE NAME
C25.3	Thickness of Reactive Layer I
C25.31	Segment Pointers for Reactive Layer I
C25.4	Density of Reactive Layer I
C25.5	Counter to Describe Discharge of Reactive Layer I
C25.6	Times to Describe Discharge of Reactive Layer I
C25.7	Positions to Describe Discharge of Reactive Layer I
C25.8	Rate of Discharge of Reactive Layer I
C25.9	Burn Rate Counters for Reactive Layer I
C26	Burn Rate Data for Reactive Layer I
C26.1	Ignition Data for Reactive Layer I
C26.2	Thermochemical Data for Reactive Layer I
C26.21	Composition of Reactive Layer Near Field Combustion Products
C26.3	Properties of Deterred Layer of Reactive Layer I
C26.31	Surface Area Multiplier for Reactive Layer I
C26.4	Endwall Property Pointers
C26.5	Permeability Model Data
C26.6	File Counters for I-th Reactivity Model
C26.7	Thermochemical Data for I-th Reactivity Model
C26.71	Composition of Near Field Combustion Products of I-th Reactivity Model
C26.8	Ignition Value for I-th Reactivity Model
C26.9	Burn Rate Data for I-th Reactivity Model
C27	Tabular Description of I-th Reactivity Model
C28	Internal Properties of Control Charge Combustion Chamber
C28.1	External Properties of Control Charge Combustion Chamber
C28.2	Control Charge Type
C28.3	Control Charge Form Function

TABLE A.3 continued

FILE NUMBER	FILE NAME
C28.4	Control Charge Burn Rate Counter
C28.5	Control Charge Burn Rate Description
C28.6	Control Charge Thermochemistry
C28.7	Properties of Deterred Layer
C29	Forward Boundary Discharge Data
C30	Inbore Rocket Motor Data
C30.1	Composition of Rocket Motor Combustion Products
C31	ETG Control Switches
C31.1	I-th Propellant Helmholtz Wiping Coefficient
C31.2	I-th Propellant Tabular Regression Rate Counter
C31.3	I-th Propellant Tabular Regression Rate Data
C31.4	I-th Plasma Jet File Counters
C31.5	Global Properties of I-th Plasma Jet
C31.6	Composition of I-th Plasma Jet
C31.7	I-th Plasma Jet Mixing Length Parameters in Integrated Format
C31.71	Plasma Capillary Data
C31.72	Stoichiometry Coefficients for Plasma Model
C31.73	Current History
C31.8	I-th Plasma Jet Integrated Data
C31.9	I-th Plasma Jet Mixing Length Parameters in Detailed Format
C32	I-th Plasma Jet Detailed Data

TABLE A.4 SUMMARY OF XKTC TRAVELING CHARGE INPUT FILES

FILE NUMBER	FILE NAME
TC1	Traveling Charge Control Data
TC2	Mesh Parameters
TC3	General Properties
TC4	Propellant Thermochemical Properties
TC5	Burn Rate Switches
TC6	Tabular Burn Rate Data
TC7	Tabular Burn Rate Data (con't)
TC7.1	Plasma Guided End Burner
TC7.2	Plasma Guided End Burner (Cont'd)
TC8	Exponential Burn Rate Data
TC9	Propellant Analytical Rheology Data
TC10	Propellant Tabular Rheology Data
TC11	Propellant Tabular Rheology Data (con't)
TC12	Ablative Film Data
TC13	Propellant Friction Data
TC14	Tabular Bore Resistance Data
TC15	Barrel Shock Resistance Data
TC16	Obturator Setback Resistance Data
TC17	Obturator Friction Data

TABLE A.5 SUMMARY OF XKTC TRAVELING LIQUID CHARGE INPUT FILES

FILE NUMBER	FILE NAME
TLC2	Option Switches
TLC5	Integration Parameters
TLC6	Tube Properties
TLC6.1	Obturator Resistance
TLC6.2	Air Shock Resistance Data
TLC7	Projectile Properties
TLC7.1	Chamber Length
TLC9	Properties of Liquid Propellant
TLC9.1	Propellant Droplet Formation Data
TLC9.2	Droplet Burn Rate Data
TLC10	Initial Conditions
TLC11	Initial Cavity Parameters
TLC11.1	Initial Cavity Geometry
TLC22.1	Properties of TLC Expulsion Charge Combustion Chamber
TLC22.2	TLC Expulsion Charge Type
TLC22.3	TLC Expulsion Charge Form Function
TLC22.4	TLC Expulsion Charge Burn Rate Counter
TLC22.5	TLC Expulsion Charge Burn Rate Description
TLC22.6	TLC Expulsion Charge Thermochemistry
TLC22.7	Properties of Deterred Layer

TABLE A.6 DESCRIPTION OF INPUT FILES

File [M1] "Problem Name" (15A4) One Card	
TITLE	Problem name. May be up to 60 alphanumeric characters.

File [M2] "Control Data" (7L1,33I1) One Card	
NPRINT	T if print on logout, F otherwise.
NGRAPH	Inactive.
NDISK	T if disc write on logout, F otherwise.
DSKRD	T if disc start, F otherwise.
IBTABL	T if summarized interior ballistic data are required, F otherwise.
NFLAM	T if summary of ignition delay data required, F otherwise.
NPTABL	T if summarized pressure, pressure difference data are required, F otherwise.
NEROS	1 if erosive effect to be included in propellant combustion, 0 otherwise. If NEROS = 1, File [C2] is required.
NDYN	Inactive.
NHTW	0 if wall temperature is not updated. 1 if cubic profile update is used.
NBC(1)	Inactive.
NBC(2)	Inactive.
NRES(1)	Inactive.
NRES(2)	Inactive.
LDBED	0 if propellant beds initially uncompacted, 1 otherwise. See comment in File [M9].

JHTW	0 if heat loss to tube is neglected. 1 if heat loss is calculated by empirical correlation for fully developed turbulent flow. File [C13] is required.
LYER	Inactive.
IBRES	1 if linear interpolation of tabular data from File [C12] is used to define bore resistance. No velocity dependence is considered. 2 if the interpolated value is multiplied by $7.2V^{-0.6}$, where V is the projectile velocity (ft/sec), provided V ≥ 27 fps. 3 if the interpolated value is multiplied by (1 + 0.0004414V)/(1 + 0.005046V) where V is the projectile velocity (in/sec). 4 if the resistance is that for 1 plus resistance due to the air shock in front of the projectile. File [C12.1] is required. 5 if the resistance is that for 1 plus resistance due to Poisson deformation of the projectile. File [C12.2] is required. 6 if the resistance is that for 1 plus resistance due to the air shock plus resistance due to Poisson deformation. Files [C12.1] and [C12.2] are required. If any other value is used, IBRES will default to the value 2.
NTC	0 if traveling charge option not required. 1 if traveling charge option is in effect. When NTC = 1, NUNIN and NUNOUT (File [M3]) must not be entered as nine (default values are eight); NEL (File [M4]) must be entered as zero; NDIM (File [M3]) must not exceed KQ - 2 for a granular booster or KQ/2 - 1 for a stick booster. KQ is presently 999. Files [TC1] through [TC17] are required. 2 if end burning plasma guided charge is located in breech of chamber. Files [TC1] through [TC17] are required. In File [TC3] XIB must be entered as zero.
INHIB(1)	0 if propellant type 1 does not have a deterred layer. 1 if propellant type 1 does have a deterred layer. File [C7] is required in this case.
INHIB(2)	As per INHIB(1), but for second propellant type.
INHIB(3)	As per INHIB(1), but for third propellant type.
NXCW	0 if explicit analysis of impact-induced compaction wave not required. 1 if explicit analysis is required. In this case, the value of XIMPV (File [M6]) must be set.
NBLDWN	0 if tube blowdown analysis is not required. 1 if blowdown analysis is required. File [C17.5] is required in this case. 2 if end burning plasma guided charge is located in breech of chamber. Files [TC1] through [TC17] are required. In File [TC3] XIB must be entered as zero.

NSWSOL	0 if non-conservative form of solid-phase continuity equation is to be used. 1 if conservative form is to be used. It is recommended that this option be selected only if excessive mass defects result from the use of the non-conservative form.
KMODE	0 if kinetics option not desired. 1 if gas-phase is to be treated as a reacting, homogeneous mixture. See Files [C23.1] through [C23.9]. 2 if, in addition to treatment of gas-phase as a mixture, subsurface reactivity and/or finite difference solution of solid-phase thermal response is desired. See Files [C23.1] through [C23.9].
MODET	0 if tank gun option not desired. 1 if tank gun is desired. See Files [C25.1] through [C27].
NECH0	0 if interpretation of input and normal run desired. 1 if input data not interpreted but normal run desired. 2 if interpretation of input data with no subsequent run desired. Note: Independently of the value of NECH0, the Code prints an image of the card input file.
INBCX	0 if forward boundary is impermeable. 1 if forward boundary is permeable to mixture of combustion products. File [C29] is required. 2 if forward boundary is an inbore rocket motor. Files [C30] and [C30.1] are required.
NTLC	0 if traveling liquid charge option not required. 1 if traveling liquid charge option is required. Files [TLC2] - [TLC22.7] are required.
NFRACT	0 if analysis of propellant fracture is not required. 1 if analysis of propellant fracture is required. Files [C5.5] and [C5.6] are required.
INTRIN	0 if values of intergranular stress in File [C5.6] are non-intrinsic (dilute) averages. 1 if values are intrinsic averages.
NETG	0 if electrothermal gun option is not required. 1 if electrothermal gun option is required. Files [C31] - [C32] are required.
NFILT	0 if no solid-phase smoothing is required. 1 if porosity is smoothed 2 if solid-phase velocity is smoothed. 3 if both porosity and solid-phase velocity are smoothed.

File [M3] "Integration Parameters" (6I5,F10.0/8F10.0) Two Cards

NDIM	Number of grid points to be used in calculation. In general, NDIM must not exceed the value of KQ, currently set by a PARAMETER statement equal to 999. If perforated stick propellant is present, NDIM must not exceed KQ/2 or 499 in the current version.
NSTEP	Number of integration steps before logout. (Each step consists of a predictor followed by a corrector.) If NSTEP = 0, logout follows every predictor as well as every corrector. If NSTEP < 0, File [C1] is required with |NSTEP| pairs of data. NSTEP ≥ -10.
NDTST	Step number for disc start.
NSTOP*	Number of steps for termination.
NUNIN	Unit number for disc read. If NUNIN = 0, it is defaulted to 8.
NUNOUT	Unit number for disc logout. If NUNOUT = 0, it is defaulted to 8.
DTPRT	Time interval before logout (sec). If entered as zero, it is defaulted to 10^{10}.
TSTOP*	Time for termination (sec).
ZSTOP*	Projectile travel for termination (in).
TINT	Maximum time step (sec).
SAFE	Stability safety factor. Recommended value is 1.1 although larger values may sometimes be required.
CRIT	Stability safety factor for source terms. Recommended value is 0.05.
RZOLV	Spatial resolution factor. Recommended range of values is $0.01 \leq RZOLV \leq 0.05$. If RZOLV is entered as zero, it will default internally to 1/(NDIM - 1).
TABLIB*	Time interval for storage of summarized interior ballistic data (sec).
TABLP**	Time interval for pressure table storage (sec).

* Termination occurs at whichever of NSTOP, TSTOP or ZSTOP is first satisfied, except when NBLDWN = 1. (See File [M2]). In the latter case the projectile motion is terminated at ZSTOP and the solution is continued until whichever of NSTOP, TSTOP or PBRF (see File [C17.5]) is first satisfied.

** Table sizes are dimensioned to 500. When overflow is imminent, tables are condensed by deleting every second datum. Subsequently, storage time is doubled.

File [C1] "Logout Counters" (I6I5) One or Two Cards

N.B. File required if and only if NSTEP < 0. (See File [M3].)

NDTEP(1)	Maximum value of integration step number for which MSTEP(1) is to be used.
MSTEP(1)	Number of integration steps (predictor plus corrector count as one unit) between logout cycles.
.	
.	
.	
.	
NDTEP(|NSTEP|)*	Maximum value of integration step number for which MSTEP(|NSTEP|) is to be used.
MSTEP(|NSTEP|)	Corresponding value of number of steps between logout cycles.

* If NDTEP(|NSTEP|) is exceeded during the calculation, the value MSTEP(|NSTEP|) will be used as a default quantity.

File [M4] "File Counters" (16I5) Two Cards

NSTA	Number of entries in tube geometry table. $2 \leq NSTA \leq 10$.
JJ	Number of times at which primer discharge is specified. $0 \leq JJ \leq 40$. If II and JJ ≥ 2, Files [C8] - [C11] are required.
II	Number of positions at which primer discharge is specified. $0 \leq II \leq 40$.
NBRES	Number of entries in bore resistance table. $0 \leq NBRES \leq 20$. If NBRES ≥ 2, File [C12] is required.
NTEM	Number of entries in tube initial temperature profile. If NTEM = 0, tube temperature defaults to TEMST (see File [M5].) If NTEM $\neq 0$, File [C14] is required. $0 \leq NTEM \leq 10$.
NEL	Number of elements to characterize compactible filler between bed and projectile. If NEL = 0, projectile base is taken as right-hand boundary for computational domain. If NEL $\neq 0$, File [C18] is required. $0 \leq NEL \leq 10$.
NPROP	Number of types of propellant grains. $1 \leq NPROP \leq 3$.
NBRDS	Number of burn rate data sets to describe pressure dependence of exponent and pre-exponential factors. (See File [M10].) Note that the same value is assumed for all propellant species, if more than one are defined.

NEPS(1)	Number of entries in initial distribution of volume fraction of propellant type 1. If NEPS = 0, porosity is calculated from mass and position data given in File [M7]. If NEPS ≠ 0, File [C5] is required. Propellant types may be entered in either mode, independently of the representation of other types. $0 \leq$ NEPS(1) ≤ 10.
NEPS(2)	Number of entries for type 2.
NEPS(3)	Number of entries for type 3.
NZPT	Number of entries in table of positions for summarized pressure data. If NZPT ≠ 0, File [C23] is required. $0 \leq$ NZPT ≤ 8.
NMS(1)	Inactive.
NMS(2)	Inactive.
NWIB	Inactive.
MORE(1)	Number of additional bags of propellant of type 1. If MORE(1) > 0, File [C4] is required. $0 \leq$ MORE(1) ≤ 9.
MORE(2)	Number of additional bags of propellant of type 2. Only required if NPROP ≥ 2. Starts a new card.
MORE(3)	Number of additional bags of propellant of type 3. Only required if NPROP = 3.
NBL	Number of elements to characterize compactible filler between bed and breech. If NBL ≠ 0, File [C19.1] is required. $0 \leq$ NBL ≤ 10.

File [M5] "Properties of Ambient Gas" (8F10.0) One Card

TEMST	Initial temperature (R).
PST	Initial pressure (psi).
GMST	Molecular weight (lbm/lbmol).
GAMST	Ratio of specific heats (-).

File [M6] "General Properties of Propellant Bed" (8F10.0) One Card

TP0	Initial temperature (R).
BETA	Inactive.
BETAB	Inactive.
CE(1)	Inactive.

CE(2) Inactive.

CE(3) Inactive.

XIMPV Minimum impact velocity for initiation of explicit analysis of intergranular compaction wave (in/sec). Note that if XIMPV is entered as zero it will default to 10^8, effectively precluding the explicit analysis.

File [C2] "Erosive Burn Rate Parameters" (8F10.0) One Card

N.B. File required if and only if NEROS = 1. (See File [M2].)

CEROS Erosive burning pre-exponential factor (in^2 R/lbf).

BEROS Erosive burning exponential factor (-).

Note: The subsequent Files [M7], [C4], [C5], [M8], [M9], [M10], [C6], [M11] and [C7] are repeated, as a group for each of the NPROP (see File [M4]) types of propellant which constitute the solid-phase.

File [M7] "I-th Propellant Type, Location and Mass" (5A4,6F10.0) One Card

---

GRNAM(I) Name of propellant. Up to 20 alphanumeric characters.

ZGR(1,I) Left-hand boundary of first bag of propellant of type I (in).

ZGR(2,I) Right-hand boundary of first bag of propellant of type I (in).

WTGRA(1,I) Mass of first bag of propellant of type I (lbm). A negative value of WTGRA may be entered. In such a case, the absolute value is used to define the mass. The negative sign is used to set an internal switch which causes the computation of initial porosity for a granular charge to reflect the assumption that the propellant is packaged as a cylinder rather than filling uniformly each cross-section of the tube. Conversely, a stick charge will be given a uniform initial distribution of porosity rather than one which varies with cross-sectional area.

RHOP(I) Density of propellant type I (lbm/in^3).

RGRI(1,I) Inner radius of rear of bag (in). Only required if MODET = 1. (See File [M4].) If RGRI(1,I) is input as zero it is assumed to coincide with the inner radius of the available flow cross-section.

RGRO(1,I) Outer radius of rear of bag (in). Only required if MODET = 1. (See File [M4].) If RGRO(1,I) is input as zero it is assumed to coincide with the outer radius of the available flow cross-section.

File [C4] "Position and Mass of Additional Bags of I-th Propellant" (8F10.0) More(I) Cards

N.B. File required if and only if MORE(I) ≠ 0. (See File [M4].)

ZGR(3,I)	Left-hand boundary of second bag of propellant of type I (in).
ZGR(4,I)	Right-hand boundary of second bag of propellant of type I (in).
WTGRA(2,I)	Mass of second bag of type I (lbm).
RGRI(2,I)	Inner radius of second bag (in).
RGRO(2,I)	Outer radius of second bag (in).
ZGR(5,I)*	Left-hand boundary of third bag.
.	
.	
.	
.	
ZGR(2*MORE(I)+2,I)	Right-hand boundary of bag MORE(I)+1 (last bag).
WTGRA(MORE(I)+1)	Mass of last bag.
RGRI(MORE(I)+1)	Inner radius of last bag (in).
RGRO(MORE(I)+1)	Outer radius of last bag (in).

* Begin new card for each bag.

File [C5] "Distribution of Volume Fraction of I-th Propellant" (8F10.0) One to Three Cards

N.B. File required if and only if NEPS(I) = 0. (See File [M4].)

ZEPS(1,I)	First position relative to breech (in).
EPS0(1,I)	Corresponding volume fraction of propellant type I.
.	
.	
.	
.	
ZEPS(NEPS(I),I)	Last position.
EPS0(NEPS(I),I)	Corresponding volume fraction.

File [M8] "I-th Propellant Form Function Data" (I5,5F10.0,I5,F10.0,I5)
One Card

NFORM(I)	Form function indicator. $1 \leq \lvert NFORM(I) \rvert \leq 17$. NFORM may be entered as a negative number. In such a case, the absolute value is used to determine the form function, but the grains are taken to be stacked. This option allows granular propellant to respond as though it had the flow resistance of stick propellant.
OD(I)	Grain dimension (in). (See table below.) If OD < 0 for NFORM = 7 or 9, the grains will be treated as inhibited on the outer cylindrical surfaces up to the point of slivering.
DPERF(I)	Grain dimension (in). (See table below.)
GLEN(I)	Grain length (in). If NFORM = 14, setting GLEN = 0 will cause this granulation to be modeled as a stick.
NPERF(I)	Number of perforations (-) except for NFORM = 14 in which case NPERF is the number of slots.
SLW(I)	Grain dimension (in). (See table below.)
NFIX(I)	If 0, grains are assumed to be free to move. If 1, grains are assumed to be attached to the tube. If 2, grains are assumed to be attached to the projectile.
BONDX(I)	Strength of bond to tube or projectile (lbf). If BONDX(I) is entered as zero, it is taken to be infinite. Separation from tube or projectile occurs when absolute value of force required to maintain attachment exceeds BONDX(I).
NDUM	If NDUM = 1, File [C5.05] is required to define non-default values of drag relaxation parameters for stacked granular bed.

FORM FUNCTION PARAMETERS

NFORM	GRAIN TYPE	OD	DPERF	SLW
1	Sphere	Diameter (in)	-	-
2	Cylinder	Diameter (in)	-	-
3	Stick*	Diameter (in)	Perforation Diameter (in)	-
4	Strip*	Width (in)	Thickness (in)	-
5	Monoperforated	Diameter (in)	Perforation Diameter (in)	-
6	Monoperforated with outside inhibition	Diameter (in)	Perforation Diameter (in)	-
7	Seven Perforations	Diameter (in)	Perforation Diameter (in)	-
9	Nineteen Perforations	Diameter (in)	Perforation Diameter (in)	-
10	Hexagonal Seven-Perforation Stick*	Distance between flats (in)	Perforation Diameter (in)	-
11	Slotted stick* (single-voidage)	Diameter (in)	Perforation Diameter (in)	Slot Width (in)
12	Scroll* (single-voidage)	Width (in)	Thickness (in)	-
13	Scroll* (dual-voidage)	Width (in)	Thickness (in)	External Diameter of Scroll (in)
14	Blind slit	Diameter (in)	Diameter of slotted core (in)	-
15	Hexagonal Nineteen-Perforation	Diameter (in)**	Perforation Diameter (in)	-
16	Monolithic Grain with central port***	Port diameter at rear (in)	Port diameter at front (in)	-
17	Arbitrary Tabular****	-	-	-

* End burning is neglected for these forms. Hence GLEN (File [M8]) may be entered arbitrarily.

** Grains assumed to have rounded corners. Diameter is between opposite corners.

*** Burning is assumed to take place only on the surfaces of the internal port. Projectile afterbody may intrude into port. NFIX(I) and BONDX(I) default to 1 and 0 respectively.. If OD(I) = 0, or DPERF(I) = 0, then Files [C5.1], [C5.2] are required to define the diameter of the port as a function of position.

**** Files [C5.3], [C5.4] required if NFORM = 17.

File [C5.05] "I-th Propellant Drag Relaxation Data" (8F10.0) One Card

N.B. This file is required if and only if NDUM = 1 (See File [M8]).

RLXF(I) Exponent used to control rate of relaxation of drag of stacked granular propellant from that for stick to that for granular propellant. Default value is 1.0.

RVOLF(I) Fraction of granular flow resistance experienced by stacked granular bed in settled or loaded condition (-). Default is zero.

TUMBLE(I) Time delay for inset of tumbling of stacked granular bed (msec). Default is zero.

TSPLIT(I) Time delay for breakup of stacked granular propellant (msec).

TUMINT(I) Time interval to complete tumbling (msec).

SPLINT(I) Time interval to complete breakup. (msec).

File [C5.1] "I-th Propellant Port Diameter File Counter" (I5) One Card

N.B. File required if and only if NFORM(I) = 16 and either OD(I) = 0 or DPERF(I) = 0. (See File [M8].)

MNOP(I) Number of entries in file to define diameter of port of monolithic grain. $2 \leq MNOP(I) \leq 8$.

File [C5.2] "I-th Propellant Port Diameter" (8F10.0) One to Two Cards

N.B. File required if and only if NFORM(I) = 16 and either OD(I) = 0 or DPERF(I) = 0. (See File [M8].)

ZMNO(1,I) First axial position relative to rear surface of grain (in).

DMNO(1,I) Corresponding diameter of port (in).

.
.
.
.

ZMNO(MNOP(I),I) Last axial position.

DMNO(MNOP(I),I) Corresponding diameter.

File [C5.3] "I-th Arbitrary Form Function File Counter" (I5) One Card

N.B. File required if and only if NFORM(I) = 17. (See File [M8].)

NARBF(I) Number of sets of data in tabular description given in File [C5.4]. $2 \leq NARBF(I) \leq 20$.

File [C5.4] "I-th Arbitrary Form Function Description" (3F10.0)
NARBF(I) Cards

ARBR(1,I) First value of surface regression (in).

ARBS(1,I) First value of surface area of grain (in^2).

ARBV(1,I) First value of volume of grain (in^3).

ARBR(2,I) Second value of regression. Starts a new card.

ARBS(2,I) Second value of area.

ARBV(2,I) Second value of volume. If ARBV(2,I) < 10^{-10}, the volume will be calculated automatically from the values of area versus regression.

.
.
.

ARBV(NARBV(I),I) Last value of volume.

File [M9] "I-th Propellant Rheology" (6F10.0) One Card

GAP(I) Rate of propagation of intergranular stress in settled, loading granular bed of type I (in/sec). If propellant I consists of stick then GAP(I) is independent of the settling porosity.

GEP0(I) Porosity of settled bed for type I propellant. If LDBED = 0 (see File [M2]) and the porosity of the bed is less than GEP0(I) at any point where type I is present, GEP0(I) is automatically defaulted to the smallest value of porosity which occurs in the initial distribution. This property may be used to avoid calculating GEP0(I).

GCAP(I) Rate of propagation of intergranular stress during unloading and reloading of propellant type I (in/sec). Not required for stick propellant. If GCAP(I) < 10^{-10}, a reversible law will be used for granular propellant.

PRPYLD Inactive.

ANU(I) Poisson ratio of propellant (-). Must be specified for stick propellant. ANU(I) defaults to 0.5 internally if propellant I is granular or if ANU(I) is entered as zero.

File [C5.5] "I-th Propellant Fracture Data Counter" (I5) One Card

N.B. This file is required if and only if NFRACT = 1. (See File [M2].)

NSTRV(I) Number of sets of data in fracture characterization of File [C5.6]. $2 \leq$ NSTRV(I) ≤ 20.

File [C5.6] "I-th Propellant Fracture Characteristics" (3F10.0) NSTRV(I) Cards

N.B. This file is required if and only if NFRACT = 1. (See File [M2].)

STRV(1,I) First value of maximum intergranular stress experienced by propellant (psi). If INTRIN = 0 (File [M2]), the stress is non-intrinsic and if INTRIN = 1, the stress is understood to be an intrinsic average.

BRF(1,I) Multiplier to be applied to mass burning rate based on nominal form function when maximum stress equals STRV(1,I) (-).

RAXF(1,I) Multiplier to be applied to interphase drag and heat transfer based on nominal form function when maximum stress equals STRV(1,I) (-). If RAXF = 0, it will default to BRF.

STRV(2,I) Second value of maximum intergranular stress. Starts a new card.

.
.
.

RAXF(NTSRV(I),I) Last value of multiplier for interphase drag and heat transfer.

N.B. This table is linearly interpolated.

File [M10] "I-th Propellant Solid-Phase Thermochemistry" (8F10.0) One to Three Cards	
UPPR(1,I)	Maximum value of pressure for corresponding values of burn rate pre-exponential and exponential factors (psi).
B22(1,I)	Burning rate pre-exponential factor (in/sec-psi^n).
BNN(1,I)	Burning rate exponent (-).
.	
.	
.	
.	
UPPR(NBRDS,I)*	Maximum value for last set of burn rate data.
B22(NBRDS,I)	Corresponding pre-exponential factor.
BNN(NBRDS,I)	Corresponding exponent.
B1(I)	Burning rate additive constant (in/sec).
TEMPIG(I)	Ignition temperature (R).
KP(I)	Thermal conductivity (lbf/sec/R).
ALPHAP(I)	Thermal diffusivity (in^2/sec).
ALPHA(I)	Emissivity factor (-).

* If pressure exceeds UPPR(NBRDS,I), the corresponding values of pre-exponential and exponential factors are used as default values.

File [M11] "I-th Propellant Gas-Phase Thermochemistry" (4F10.0) One Card	
ECHEM(I)	Internal energy released in combustion (lbf-in/lbm).
GMW(I)	Molecular weight (lbm/lbmol).
GAMMA(I)	Ratio of specific heat (-).
BV(I)	Covolume (in^3/lbm).

File [C7] "I-th Propellant Deterred Layer Properties" (5F10.0) One Card

N.B. File required if and only if INHIB(I) ≠ 0. (See File [M2].)

ECHIB(I)*	Internal energy released in combustion at start of deterred layer (lbf-in/lbm).
ECHIB2(I)	Internal energy released in combustion at end of deterred layer (lbf-in/lbm).
RGFAC(I)*	Factor by which burn rate is multiplied at start of deterred layer (-).
RGFAC2(I)	Factor by which burn rate is multiplied at end of deterred layer (-).
HIBX(I)	Depth of inhibited layer (-).

* Values within deterred layer deduced by linear spacewise interpolation. Final values need not be the same as those of the undeterred propellant.

File [C8] "Igniter Thermochemistry" (8F10.0) One Card

N.B. File required if and only if II, JJ ≥ 2. (See File [M4].)

EIG	Internal energy released in combustion (lbf-in/lbm).
GMIG	Molecular weight (lbm/lbmol).
GAMIG	Ratio of specific heats (-).
VIG	Specific volume of igniter solid-phase (in^3/lbm).

File [C9] "Igniter Discharge Times" (8F10.0) One to Five Cards

N.B. File required if and only if II, JJ ≥ 2. (See File [M4].)

TPHI(1)	First time in tabular representation of igniter discharge (sec).
.	
.	
.	
.	
TPHI(JJ)	Last time.

File [C10] "Igniter Discharge Positions" (8F10.0) One to Five Cards

N.B. File required if and only if II, JJ ≥ 2. (See File [M4].)

ZPHI(1)	First position in tabular representation of igniter discharge (in).
.	
.	
.	
.	
ZPHI(II)	Last position.

File [C11] "Igniter Rate of Discharge" (8F10.0) Two to Two Hundred Cards

N.B. File required if and only if II, JJ ≥ 2. (See File [M4].)

PHI(1,1)	Igniter discharge per unit length per unit time at first position and first time (lbm/in/sec).
PHI(2,1)	Discharge at second position and first time.
.	
.	
.	
.	
PHI(II,1)	Discharge at last position and first time.
PHI(1,2)*	Discharge at first position and second time.
.	
.	
.	
.	
PHI(II,JJ)	Discharge at last position and last time.

* PHI(1,J) begins a new card, J = 1, ... ,JJ.

File [M12] "Tube Geometry" (8F10.0) One to Three Cards

ZA(1)	First axial location relative to breech (in).
RA(1)	Corresponding radius of bore (in).
.	
.	
.	
.	
ZA(NSTA)	Last axial location
RA(NSTA)	Corresponding radius

File [C12] "Bore Resistance" (8F10.0) One to Five Cards

N.B. File required if and only if NBRES ≥ 2. (See File [M4].)

BRZ(1)	First axial location. If BRZ(1) > 0, it is understood to be relative to breech (in). If BRZ(1) is entered as zero, however, all values of BRZ are understood to be relative to the initial position of the projectile.
BR(1)	Corresponding resistance exerted on projectile when base is at BRZ(1) (psi).
.	
.	
.	
.	
BRZ(NBRES)	Last location.
BR(NBRES)	Corresponding resistance.

File [C12.1] "Air Shock Data" (4F10.0) One Card

N.B. This file is required if and only if IBRES = 4 or 6. (See File [M2].)

AIRGAM	Ratio of specific heats of gas in front of projectile (-).
AIRP0	Initial pressure of gas in front of projectile (psi).
AIRT0	Initial temperature of gas in front of projectile (R).
AIRMW	Molecular weight of gas in front of projectile (lbm/lbmol).

File [C12.2] "Projectile Setback Resistance Data" (4F10.0) One Card

N.B. The file is required if and only if IBRES = 5 or 6. (See File [M2].)

PRMU	Coefficient of friction between projectile body and tube wall (-).
PRNU	Poisson ratio of projectile material (-).
PRLEN	Length of projectile (in).
PRLENC	Length of projectile in contact with wall (in). If < 10^{-10}, PRLENC defaults to PRLEN.

File [C13] "Tube Thermal Properties" (3F10.0) One Card

N.B. File required if and only if JHTW ≠ 0. (See File [M2].)

KW	Thermal conductivity (lbf/sec/R).
ALPHAW	Thermal diffusivity (in^2/sec).
ALFAW	Emissivity factor (-).

File [C14] "Tube Initial Temperature Profile" (8F10.0) One to Three Cards

N.B. File required if and only if NTEM ≠ 0. (See File [M4].)

ZW(1)	First axial location relative to breech (in).
TEMW(1)	Corresponding wall temperature (R).
.	
.	
.	
.	
ZW(NTEM)	Last location.
TEMW(NTEM)	Corresponding temperature.

File [C17.5] "Blowdown Parameters" (8F10.0) One Card

N.B. File required if and only if NBLWDN = 1. (See File [M2].)

PBRF	Value to which breech pressure must drop for termination of blowdown calculation (psi).
PBRFZ	Distance from breech at which PBRF is determined (in).
UBRF	Value to which velocity must drop for termination of blowdown calculation (in/sec).
UBRFZ	Distance from breech at which UBRF is determined (in).
CDMUZ	Discharge coefficient for muzzle discharge (-). If CDMUZ < 10^{-10}, it defaults to 1.0.

File [M13] "Projectile and Rifling Characteristics" (4F10.0) One Card

N.B. This file is not required if NTC or NTLC = 1. (See File [M2].)

ZBPR	Initial axial location of base of projectile relative to breech (in).
WTPR	Mass of projectile (lbm).
PRIN	Polar moment of inertia of projectile (lbm-in^2).
RIF	Angle of rifling(°).
ABPROJ	Base area of projectile (in^2). If ABPROJ > 10^{-10} it will be used as the propulsion area for the projectile whenever it is less than the bore area at the base.
TUBEM	Mass of recoiling parts of gun (lbm). If TUBEM is zero, recoil of the tube is not considered.

File [C18] "I-th Forward Compactible Filler Element Properties" (3F10.0),2I5) One Card

N.B. File required if and only if NEL ≠ 0. (See File [M4].) File is repeated NEL times.

XEL(I)	Position of left-hand boundary of I-th element (in). The array must be well ordered with respect to I. We require XEL(I) ≥ XEL(I-1). Forward elements are ordered so that the first is to the left.
MEL(I)	Mass of I-th element (lbm). If < 10^{-10} element is interpreted as a space. MEL(I) must be greater than 10^{-10}.
FEL(I)	Initial resistance to motion of I-th element (lbf).
NTYPE(I)	If NTYPE(I) = 0, element is treated as perfectly plastic (deformation under loading only). If NTYPE(I) = 1, element is treated as elastic. If NTYPE(I) = 2, element is treated as rigid. If NTYPE(I) = 3, element is treated as incompressible. 0 ≤ NTYPE(I) ≤ 3.
NDATA(I)	Number of pairs of entries in stress-strain table of I-th element. 0 ≤ NDATA(I) ≤ 10.

File [C19] "Constitutive Data for I-th Forward Element" (8F10.0)
One to Three Cards

N.B. File required if and only if MEL(I) > 10^{-10} and NTYPE(I) < 2. (See File [C18].) File is repeated for each element for which NDATA > 0. Files [C19], as a group, follow Files [C18], as a group.

YEL(I,1)* First engineering strain taken positive in compression (dimensionless). Must be zero.

RESEL(I,1)** Corresponding stress taken positive in compression (psi).

.
.
.
.

RESEL(I,NDATA(I)) Last engineering stress. Should exceed maximum pressure in gun.

* The array YEL must be well ordered. All entries must be in the interval [0,1].

** The array RESEL must have non-zero entries and must be non-decreasing for each element.

File [C19.1] "I-th Rear Compactible Filler Element Properties" (3F10.0,2I5)
One Card

N.B. File required if and only if NBL ≠ 0. (See File [M4].) File is repeated NBL times.

XBL(I) Position of right-hand boundary of I-th element (in). The array must be well ordered with respect to I. XBL(I) observes the opposite convention from that of XEL(I), that is XBL(I) ≤ XBL(I-1) for all I. Rear elements are tabulated so that the first is to the right.

MBL(I) Mass of I-th element (lbm). If < 10^{-10} element is interpreted as a space. MBL(I) must be greater than 10^{-10}.

FBL(I) Initial resistance to motion of I-th element (lbf).

NTYPB(I) If NTYPB(I) = 0, element is treated as perfectly plastic (deformation under loading only).
If NTYPB(I) = 1, element is treated as elastic
If NTYPB(I) = 2, element is treated as rigid.
If NTYPB(I) = 3, element is treated as incompressible.
0 ≤ NTYPB(I) ≤ 3.

NDATB(I) Number of pairs of entries is stress-strain table of I-th element. 0 ≤ NDATB(I) ≤ 10.

File [C19.2] "Constitutive Data for I-th Rear Element" (8F10.0)
One to Three Cards

N.B. File required if and only if MEL(I) > 10^{-10} and NTYPE(I) < 2. (See File [C19.1].) File is repeated for each element for which NDATB > 0. Files [C19.2], as a group, follow Files [C19.1], as a group.

YBL(I,1)* First engineering strain taken positive in compression (dimensionless). Must be zero.

RESBL(I,1)** Corresponding stress taken positive in compression (psi).

.
.
.
.

RESBL(I,NDATB(I)) Last engineering stress. Should exceed maximum pressure in gun.

* The array YBL must be well ordered. All entries must be in the interval [0,1].

** The array RESBL must have non-zero entries and must be non-decreasing for each element.

File [C23] "Positions for Pressure Table Storage" (8F10.0) One Card

N.B. File required if and only if NZPT ≠ 0. (See File [M4].)

ZPT(1) First position, relative to breech (in).

.
.
.
.

ZPT(NZPT)* Last position.

* Output consists of tables of pressure at each of the NZPT positions together with value less that at the NZPTth position.

File [C23.01] "Projectile Afterbody Pressure History Option" (16I5)
One Card

N.B. File required if and only if NZPT ≠ 0 and MODET = 1. (See File [M4].)

IZPT(1) 0 if ZPT(1) is fixed in the tube reference frame.
. 1 if ZPT(1) is fixed in the projectile afterbody
. reference frame.
.
.
IZPT(NZPT)

MODZPT 0 if gas pressure is tabulated.
1 if intergranular stress is tabulated.
2 if sum of pressure and intergranular stress is tabulated.

File [C23.1] "Kinetics Option Counters" (3I5) One Card

N.B. File required if and only if KMODE ≠ 0. (See File [M2].)

NSPEC Number of species. $1 \leq NSPEC \leq 10$.

NGASR Number of reactions occurring in the mixture of combustion products. $0 \leq NGASR \leq 10$. If NGASR > 0, File [C23.7] is required.

NSOLR Number of reactions occurring in the solid-propellant. $0 \leq NSOLR \leq 10$. If NSOLR > 0, File [C23.8] is required.

KEOS 0 if thermal energy formulation is used.
1 if total energy formulation is used.
Data as per NASA SP-273 and the present File [C23.2] is replaced by File [C23.21]. Values of ECHO are to be entered as heat of formation and not as heat released in near field combustion zone, see Files [C23.3], [C23.31], [C23.4] and [C23.41].
This option is presently confined to gas-phase species.
ECHO for chemical energy not required.

NPVAR(1) Number of data to specify composition of local products of first propellant. NPVAR may be zero, in which case the present file [C23.3] is used or it may be between 2 and 20, in which case new file [C23.31] is required.
.
.
.
.
NPVAR(NPROP) Data for last propellant.

NPVAR(NPROP+1) Data for igniter composition. Note that if NPROP is 1, this item goes in the sixth field. If it is 0, present File [C23.4] is required, otherwise we require [C23.41].

File [C23.2] "Properties of Species" (2A4,1X,A1,6F10.0) NSPEC Cards

N.B. File required if and only if KMODE ≠ 0 (See File [M2]) and KEOS = 0 (See File [C23.1]).

SPCNAM(I)	Name of species, up to 8 alphanumeric characters.
FAZE(I)	Phase of species: G = gas or vapor; L = liquid; S = solid. One alphanumeric character.
SPCV(I)	Specific heat at constant volume (lbf-in/lbm-R).
SPCP(I)	Specific heat at constant pressure (lbf-in/lbm-R).
SPBV(I)	Covolume (in^3/lbm). Only required if FAZE = G.
SPMOL(I)	Molecular weight (lbm/lbmol). Only required if FAZE = G.
SPDEN(I)	Density (lbm/in^3). Only required if FAZE = L or S.
CLOS(I)	Transfer coefficient in correlation for rate of deposition of condensed species on surface of solid propellant (sec/in^2). Only required if FAZE = L or S. If CLOS = 0, the rate of deposition is zero.

File [C23.21] "Properties of Species in NASA SP-273 Formulation" (A10,5F10.0/5E15.8/5E15.8/5E15.8) 4*NSPEC cards

N.B. The data consist of 4 cards for each of the NSPEC species.

SPCNAM(I)	Name of species I. Up to 10 characters.
TLO(I)	Lower limit of data (K).
TSW(I)	Switching point of data (K).
THI(I)	Upper limit of data (K).
SPBV(I)	Covolume (in**3/lbm).
SPMOL(I)	Molecular weight (lbm/lbmol).
A(1,I)	First NASA SP datum for specific heat. New card.
.	
.	
.	
A(5,I)	
A(6,I)	Sixth datum. New card.
.	
.	
.	
A(10,I)	

A(11,I) Eleventh datum. New card.
.
.
.
A(15,I)

N.B. TLO and THI are not presently checked when subroutine CALEOS is called. The user may want to include an appropriate test and subsequent message/action. This file is actually read by CALEOS rather than NOVSUB in order to make it easier for the user to make revisions.

N.B. The following File [C23.3] is repeated NPROP times, once for each type of solid propellant.

File [C23.3] "Composition of Propellant Near Field Combustion Products" (8F10.0) NPROP to 2*NPROP Cards

---

N.B. File required if and only if KMODE ≠ 0 (See File [M2]) and NPVAR(I) = 0 (See File [C23.1]).

ECH0(I) Chemical energy released in near field combustion (lbf-in/lbm).

Y0(I,1) Mass fraction of near field combustion products corresponding to species type 1 (-).
.
.
.
Y0(I,NSPEC) Mass fraction of near field combustion products corresponding to species type NSPEC (-).

File [C23.31] "Pressure Dependent Composition of Propellant Near Field Combustion Products" (F10.0/(8F10.0)) 1+NPROP to 1+2*NPROP cards.

N.B. File required if and only if KMODE ≠ 0 (See File [M2]) and NPVAR(I) ≠ 0 (See File [C23.1]).

ECHO(I) Chemical energy released in near field combustion (KEOS=0) or heat of formation of propellant (KEOS=1) (lbf-in/lbm).

PVAR(I,1) First value of pressure. (psi). New card.

YOVAR(I,1,1) Corresponding mass fraction of first species in near field combustion (-).
.
.
.
YOVAR(I,1NSPEC) Mass fraction of last species.

PVAR(I,2) Second value of pressure. New card.
.
.
.
YOVAR(I,NPVAR(I),NSPEC)

N.B. Inside the table range YOVAR is linearly interpolated.
Outside, the first or last set of values are used.

File [C23.4] "Composition of Igniter Discharge Combustion Products"
(8F10.0) One to Two Cards

N.B. File required if and only if KMODE ≠ 0 (See File [M2]) and
NPVAR(I) = 0. (See File [C23.1].)

ECH0(I) Chemical energy released by combustion of igniter material prior to injection (lbf-in/lbm).

Y0(I,1) Mass fraction of igniter products corresponding to species type 1 (-).
.
.
.
Y0(I,NSPEC) Mass fraction of igniter products corresponding to species type NSPEC (-).

FILE [C23.41] "Pressure Dependent Composition of Igniter Discharge Combustion Products" (F10.0/(8F10.0))
1 + NPROP to 1 + 2*NPROP cards

N.B. File required if and only if KMODE ≠ 0 (See File [M2]) and
NPVAR(I) ≠ 0. (See File [C23.1].)

ECHO(I) Chemical energy released in near field combustion (KEOS=0) or heat of formation of igniter products (KEOS=1) (lbf-in/lbm).

PVAR(I,1) First value of pressure. (psi). New card.

YOVAR(I,1,1) Corresponding mass fraction of first species in near field combustion (-).
.
.
.
YOVAR(I,1NSPEC) Mass fraction of last species.

PVAR(I,2) Second value of pressure. New card.
.
.
.
YOVAR(I,NPVAR(I),NSPEC)

File [C23.5] "Composition of Initial Ambient Gas" (8F10.0)
One to Two Cards

N.B. File required if and only if KMODE ≠ 0. (See File [M2].)

ECH0(I) Internal energy (thermal component) of ambient gas (or mixture if condensed species are initially present) (lbf-in/lbm).

Y0(I,1) Mass fraction of species 1 (-).
.
.
.
.

Y0(I,NSPEC) Mass fraction of species NSPEC (-).

N.B. The following File is repeated NPROP times, once for each type of solid propellant. Present storage limits only support the case NPROP = 1 with KMODE = 2.

File [C23.6] "Initial Composition of Solid Propellant" (8F10.0)
NPROP to 2*NPROP Cards

N.B. File required if and only if KMODE = 2. (See File [M2].)

ECH0(I) Inactive.

Y0(I,1) Mass fraction of solid propellant corresponding to species 1 (-).
.
.
.
.

Y0(I,NSPEC) Mass fraction of solid propellant corresponding to species NSPEC (-).

File [C23.61] "Composition of Traveling Charge Near Field Combustion Products" (8F10.0) One to Two Cards

N.B. File required if and only if KMODE ≠ 0 and NTC = 1. (See File [M2].)

ECHTC0 Chemical energy released in near field combustion of traveling charge (lbf-in/lbm).

YTC0(1) Mass fraction of species 1 (-).
.
.
.
.

YTC0(NSPEC) Mass fraction of species NSPEC (-).

File [C23.62] "Types of Reactions in Mixture of Combustion Prooducts" (10I5) One Card

N.B. File required if and only if KMODE ≠ 0, NGASR ≠ 0 and NTC = 1. (See Files [M2] and [C23.1].)

KRCTYP(1) If 0, reaction 1 is of the Arrhenius type and is described by File [C23.7].
. If 1, reaction 1 is of the pressure dependent type and is
. described by File [C23.71].
. If NTC = 0, KRCTYP(I) defaults to zero for all I.
.
.

KRCTYP(NGASR) Type of reaction NGASR.

File [C23.63] "Species Thermal Equilibrium Switches" (10I5) One Card

N.B. File required if and only if KMODE ≠ 0, NGASR ≠ 0 and NTC = 1. (See Files [M2] and [C23.1].)

KTEQL(1) If 0, species 1 is assumed to be in constant thermal
. equilibrium with mixture of combustion products.
. If 1, species 1 is assumed to be thermally insulated from
. mixture of combustion products. If NTC = 0, KTEQL(I)
. defaults to zero for all I.
.
.

KTEQL(NSPEC) Thermal equilibration switch for species NSPEC.

File [C23.7] "Description of Arrhenius Reactions in Mixture of Combustion Products" (8I5/8F10.0/F10.0,D10.4,F10.0,D10.4,4F10.0/F10.0) Four Cards For Each Such Reaction

N.B. File required if and only if KMODE ≠ 0, NGASR ≠ 0 and KRCTYP(I) = 0. (See Files [M2], [C23.1] and [C23.62].)

KRCNTB(1,I)* Pointer to first species acting as a reactant in reaction I.
. 0 ≤ KRCNTB ≤ NSPEC.
.
.
.

KRCNTB(4,I) Pointer to fourth species acting as a reactant in reaction I.

KPRODB(1,I)* Pointer to first species acting as a product in reaction I.
. 0 ≤ KPRODB ≤ NSPEC.
.
.
.

KPRODB(4,I) Pointer to fourth species acting as a product in reaction I.

STOIB(1,I)	Stoichiometric coefficient corresponding to first reactant species (-). Starts a new card.
STOIB(4,I)	Stoichiometric coefficient corresponding to fourth reactant species (-).
STOIB(5,I)	Stoichiometric coefficient corresponding to first product species (-).
STOIB(8,I)	Stoichiometric coefficient corresponding to fourth product species (-).
ECHB(I)	Chemical energy released by reaction (lbf-in/lbm). Starts a new card.
ARCB(I)	Pre-exponential factor in Arrhenius rate law (units yield lbmol/in^3-sec).
ARXB(I)	Temperature exponent in Arrhenius rate law (-).
AREB(I)	Activation energy in Arrhenius rate law (lbf-in/lbmol).
AROB(1,I)	Order of reaction with respect to concentration of first reactant species (-).
AROB(4,I)	Order of reaction with respect to concentration of fourth reactant species (-).
AROB(5,I)	Order of reaction with respect to concentration of gas-phase (-). Starts a new card.

* The most general reaction supported involves four reactant and four product species. At least one reactant pointer and one product pointer must be different from zero. A zero entry simply implies a reduction in generality of the reaction.

File [C23.71] "Description of Pressure-Dependent Reactions in Mixture of Combustion Products" (8I5/8F10.0/8F10.0)
Three Cards For Each Such Reaction

N.B. File required if and only if KMODE ≠ 0, NGASR ≠ 0 and KRCTYP(I) = 1. (See Files [M2], [C23.1] and [C23.62].)

KRCNTB(1,I)*	Pointer to first species acting as a reactant in reaction I. 0 ≤ KRCNTB ≤ NSPEC.
.	
.	
.	
.	
KRCNTB(4,I)	Pointer to fourth species acting as a reactant in reaction I.
KPRODB(1,I)*	Pointer to first species acting as a product in reaction I. 0 ≤ KPRODB ≤ NSPEC.
.	
.	
.	
.	
KPRODB(4,I)	Pointer to fourth species acting as a product in reaction I.
STOIB(1,I)	Stoichiometric coefficient corresponding to first reactant species (-). Starts a new card.
.	
.	
.	
.	
STOIB(4,I)	Stoichiometric coefficient corresponding to fourth reactant species (-).
STOIB(5,I)	Stoichiometric coefficient corresponding to first product species (-).
.	
.	
.	
.	
STOIB(8,I)	Stoichiometric coefficient corresponding to fourth product species (-).
ECHB(I)	Chemical energy released by reaction (lbf-in/lbm). Starts a new card.
DIAB(I)	Particle diameter, assumed constant (in).
B1B(I)	Burn rate additive constant (in/sec).
B2B(I)	Burn rate pre-exponential factor (in/sec-psi^{BNB}).
BNB(I)	Burn rate exponent (-).

* The most general reaction supported involves four reactant and four product species. At least one reactant pointer and one product pointer must be different from zero. A zero entry simply implies a reduction in generality of the reaction.

File [C23.8] "Description of Reactions in Solid Propellant" (8I5/8F10.0/F10.0,D10.4,F10.0,D10.4,4F10.0) 3*NSOLR Cards

N.B. File required if and only if KMODE ≠ 0, NSOLR ≠ 0. (See Files [M2] and [C23.1].)

KRCNTS(1,I)*	Pointer to first species acting as a reactant in reaction I. 0 ≤ KRCNTS ≤ NSPEC.
KRCNTS(4,I)	Pointer to fourth species acting as a reactant in reaction I.
KPRODS(1,I)*	Pointer to first species acting as a product in reaction I. 0 ≤ KPRODS ≤ NSPEC.
KPRODS(4,I)	Pointer to fourth species acting as a product in reaction I.
STOIS(1,I)	Stoichiometric coefficient corresponding to first reactant species (-). Starts a new card.
STOIS(4,I)	Stoichiometric coefficient corresponding to fourth reactant species (-).
STOIS(5,I)	Stoichiometric coefficient corresponding to first product species (-).
STOIS(8,I)	Stoichiometric coefficient corresponding to fourth product species (-).
ECHS(I)	Chemical energy released by reaction (lbf-in/lbm). Starts a new card.
ARCS(I)	Pre-exponential factor in Arrhenius rate law (units yield lbm/in^3-sec).
ARXS(I)	Temperature exponent in Arrhenius rate law (-).
ARES(I)	Activation energy in Arrhenius rate law (lbf-in/lbmol).

AROS(1,I)	Order of reaction with respect to concentration of first reactant species (-).
.	
.	
.	
.	
AROS(4,I)	Order of reaction with respect to concentration of fourth reactant species (-).

* The most general reaction supported involves four reactant and four product species. At least one reactant pointer and one product pointer must be different from zero. A zero entry simply implies a reduction in generality of the reaction.

File [C23.9] "Solid Propellant Thermal Response Parameters" (3I5,2D10.4,3F10.0) One Card

N.B. File required if and only if KMODE = 2. (See File [M2].)

NZC	Number of stations for analysis of thermal response of solid propellant. $0 \leq NZC \leq 21$. It is presently assumed that only one propellant region is present.
NZCBC	If 0, pyrolysis law is assumed to govern regression of surface of solid propellant. If 1, evaporative (Clausius Clapeyron) law is assumed to govern regression of surface of solid propellant.
NOFLAM	If 0, heat feedback from the gas-phase is considered according to Zel'dovitch formulism. If 1, heat feedback from the gas-phase is neglected.
AS	Pre-exponential factor in solid propellant surface regression law. If NZCBC = 0, units are in/sec. If NZCBC = 1, units are psi.
ES	Activation energy (NZCBC = 0) or heat of vaporization (NZCBC = 1) in solid propellant surface regression law (lbf-in/lbmol).
TSEN	Temperature sensitivity of propellant steady state burn rate (1/R).
TTRANS	Time interval over which external stimulus drops to zero following ignition of the surface of the propellant (sec).
PTRANS	Pressure above which thermal analysis is discontinued and steady state combustion is assumed to occur (psi).

File [C24] "Parameters to Define Mesh in Invariant Embedding Analysis" (F10.0,3I5) One Card

N.B. File required if and only if KMODE = 2. (See File [M2].)

DELX* Mesh spacing in group closest to heated surface ($sec^{1/2}$) DELX > 0.

N** Number of intervals per group.

MDELX Integer multiple by which mesh spacing increases from group to group as we move away from heated surface.

NGRP Number of groups. $1 \leq NGRP \leq 10$.

* Refers to computational coordinate $x\sqrt{\alpha}$ where x is the distance from heated surface and α is thermal diffusivity.

** $N*NGRP \leq 200$.

File [C25] "Tank Gun Option Control Data" (16I5) One Card

N.B. File required if and only if MODET = 1. (See File [M2].)

NAFT Number of pairs of data to describe projectile afterbody. NAFT may be zero. Otherwise $2 \leq NAFT \leq 10$.

JIS(1) Switch to define level of modeling of surface source term attributed to tube wall.

JIS(1)	Model
0	No source term
1	Tabular source term
2	Rate of source determined according to ignition and combustion submodels.

JIS(2) Switch to define level of modeling of surface source term attributed to centerline of tube.

JIS(3) Switch to define level of modeling of surface source term attributed to afterbody of projectile.

NENDL Number of endwalls defined by packaging of charge. $0 \leq NENDL \leq 21$.

NPRM	Number of permeability data sets. $0 \leq NPRM \leq 10$.
NRCT	Number of reactivity data sets. $0 \leq NRCT \leq 9$.
NSEGS(1)	Number of segments having different properties in tube wall surface source. $0 \leq NSEGS(1) \leq 3$. Default value is 1.
NSEGS(2)	Number of segments in centerline surface source.
NSEGS(3)	Number of segments in afterbody surface source.
KCTRL	If 0, control charge not present. If 1, control charge is present. Files [C28] - [C28.7] required.
NZCRE	Number of data to describe external geometry of ballistic control tube.
INHBCR(1)	If 0, control charge not deterred. If 1, control charge is deterred.
NABDIS	If 0, discontinuity in area at base of afterbody is represented implicitly. If 1, discontinuity in area at base of afterbody is represented explicitly as a discontinuity. File [C25.11] is required.

File [C25.1] "Geometry of Projectile Afterbody" (8F10.0) One to Three Cards

---

N.B. File required if and only if MODET = 1 and NAFT ≥ 2.
(See Files [M2] and [C25].)

ZAFT(1)*	First axial position on afterbody (in).
RAFT(1)	Corresponding radius of afterbody (in).
.	
.	
.	
.	
ZAFT(NAFT)	Last axial position.
RAFT(NAFT)	Corresponding radius of afterbody.

---

* The origin of the coordinate ZAFT is independent of that used to describe the gun tube. XKTC internally reconciles the coordinate frames by assuming that ZAFT(NAFT) coincides with ZBPR. (See File [M13].)

File [C25.11] "Spatial Resolution Factor for Analysis of Base of Afterbody as Surface of Area Discontinuity" (F10.0) One Card

N.B. This file is required if and only if MODET = 1 and NABDIS = 1. (See File ([C25].)

RZOLV2 — Spatial resolution factor (-). Recommended value is ≤ 0.01. It should be noted that this datum is completely independent of RZOLV (File [M3]). RZOLV2 is used to determine the maximum proximity of a mixture boundary to the base of the projectile.

N.B. The following Files, [C25.2] through [C26.3] are repeated, as needed, as a group for each of the three types of reactive layers whose presence is indicated by a non-zero value of JIS(I). (See File [C25].)

File [C25.2] "Thickness and Density Counters for Reactive Layer I" (4I5) One Card

N.B. File required if and only if MODET = 1 and JIS(I) ≠ 0. (See Files [M2] and [C25].)

NSTAC(I) — Number of data to describe thickness of reactive layer I. $2 \leq NSTAC(I) \leq 10$.

NRHOS(I,1) — Number of data to describe density of first segment of reactive layer I as a function of pressure. $1 \leq NRHOS(I) \leq 10$.

NRHOS(I,2) — Number of data for second segment of reactive layer I.

NRHOS(I,3) — Number of data for third segment.

File [C25.3] "Thickness of Reactive Layer I" (8F10.0) One to Three Cards

N.B. File required if and only if MODET = 1 and JIS(I) ≠ 0. (See Files [M2] and [C25].)

ZAC(1,I)* — First axial position (in).

THC(1,I) — Corresponding thickness of reactive layer (in).

.
.
.
.

ZAC(NSTAC(I),I) — Last axial position.

THC(NSTAC(I),I) — Corresponding thickness.

* When I = 1 or 2, ZAC is assumed to refer to the coordinate system used to define the tube geometry. When I = 3, ZAC is assumed to correspond to the coordinate system used to define the afterbody of the projectile. The thickness of layer I is taken to be zero outside the table range.

File [C25.31] "Segment Pointers for Reactive Layer I" (8I5) One Card

N.B. File required if and only if MODET = 1, JIS(I) ≠ 0 and NEGS(I) > 1. (See Files [M2] and [C25].)

NSG(1,I) Segment property type for axial positions between ZAC(1,I) and ZAC(2,1).

.
.
.
.

NSG(NSTAC(I)-1,I) Segment property type for axial positions between ZAC(NSTAC(I)-1,I) and ZAC(NSTAC(I),I).

NSG(NSTAC(I),I) Not used.

N.B. If Reactive Layer I consists of more than one segment, the following Files [C25.4] through [C26.21] are repeated as a group for each of the segments of the layer. The subscript pertaining to the segment is suppressed in the following discussion.

File [C25.4] "Density of Reactive Layer I" (8F10.0) One to Three Cards

N.B. File required if and only if MODET = 1 and JIS(I) ≠ 0. (See Files [M2] and [C25].)

RHOS(1,I)* Value of density at first pressure (lbm/in^3).

PRHOS(1,I) First value of pressure (psi).

.
.
.
.

RHOS(NRHOS(I),I) Last value of density.

PRHOS(NRHOS(I),I) Last value of pressure.

* Outside the table range, the first or the last value of RHOS applies. If a single value is specified, the density is taken to be constant and therefore independent of pressure. At present, case compressibility is only modeled if JIS(I) = 2. (See File [C25].)

File [C25.5] "Counter to Describe Discharge of Reactive Layer I" (2I5)
One Card

N.B. File required if and only if MODET = 1 and JIS(I) = 1.
(See Files [M2] and [C25].)

IIS(I) Number of axial positions in discharge table.
$2 \leq IIS(I) \leq 10$.

JJS(I) Number of times in discharge table. $2 \leq JJS(I) \leq 10$.

File [C25.6] "Times to Describe Discharge of Reactive Layer I" (8F10.0)
One to Two Cards

N.B. File required if and only if MODET = 1 and JIS(I) = 1.
(See Files [M2] and [C25].)

TPHIS(1,I) First time (msec).
.
.
.
.
TPHIS(JJS(I),I) Last time (msec).

File [C25.7] "Positions to Describe Discharge of Reactive Layer I"
(8F10.0) One to Two Cards

N.B. File required if and only if MODET = 1 and JIS(I) = 1.
(See Files [M2] and [C25].)

ZPHIS(1,I)* First position (in).
.
.
.
.
ZPHIS(IIS(I),I) Last position (in).

* The coordinate frame for ZPHIS is assumed to accord with that for ZAC.
(See File [C25.3].)

File [C25.8] "Rate of Discharge of Reactive Layer I" (8F10.0)
One to Thirteen Cards

N.B. File required if and only if MODET = 1 and JIS(I) = 1.
(See Files [M2] and [C25].)

PHIS(1,1,I) Rate of discharge at first position and first time (lbm/in-sec).

PHIS(2,1,I) Rate of discharge at second position and first time.

.
.
.
.

PHIS(IIS(I),1,I) Rate of discharge at last position and first time.

PHIS(1,2,I) Rate of discharge at first position and second time. Starts a new card.

.
.
.
.

PHIS(IIS(I),JJS(I),I) Rate of discharge at last position and last time.

File [C25.9] "Burn Rate Counters for Reactive Layer I" (2I5) One Card

N.B. File required if and only if MODET = 1 and JIS(I) = 2.
(See Files [M2] and [C25].)

KBRDS(I) Number of burn rate data. $1 \leq KBRDS \leq 10$.

KNHIB(I) If 0, layer I is not deterred.
If 1, layer I is deterred

KFACSF(I) If 0, the nominal surface area is used.
If $2 \leq KFACSF(I) \leq 10$, the surface area is multiplied by a value which depends on surface regression. File [C26.31] is required.

File [C26] "Burn Rate Data for Reactive Layer I" (8F10.0)
One to Three Cards

N.B. File required if and only if MODET = 1 and JIS(I) = 2.
(See Files [M2] and [C25].)

UPPRS(1,I)* First pressure limit (psi).

B22S(1,I) Value of pre-exponent for pressures less than UPPRS(1,I) (in/sec-psi^{BNNS}).

BNNS(1,I) Value of exponent for pressures less than UPPRS(1,I) (-).

.
.
.
.

UPPRS(KBRDS(I),I)* Last pressure limit (psi).

B22S(KBRDS(I),I) Value of pre-exponent for pressures less than UPPRS(KBRDS(I),I) but greater than UPPRS(KBRDS(I)-1,I).

BNNS(KBRDS(I),I) Corresponding exponent (-).

* Outside the table range the first and last values are used.

File [C26.1] "Ignition Data for Reactive Layer I" (5F10.0) One Card

N.B. File required if and only if MODET = 1 and JIS(I) = 2.
(See Files [M2] and [C25].)

B1S(I) Burn rate additive constant (in/sec).

TMPIGS(I) Ignition temperature (R).

KPS(I) Thermal conductivity (lbf/sec-R).

ALPHAS(I) Thermal diffusivity (in^2/sec).

ALFCC(I) Emissivity factor (-).

File [C26.2] "Thermochemical Data for Reactive Layer I" (8F10.0) One Card

N.B. File required if and only if MODET = 1 and JIS(I) = 1 or 2.
(See Files [M2] and [C25].)

EIGS(I) Chemical energy released during combustion (lbf-in/lbm).

GMS(I) Molecular weight of products of combustion (lbm/lbmol).

GAMAS(I) Ratio of specific heats (-).

File [C26.21] "Composition of Reactive Layer Near Field Combustion Products" (8F10.0) One Card

N.B. File required if and only if MODET = 1, KMODE = 1 and JIS(I) = 1 or 2. (See Files [M2] and [C25].)

YS0(I,1) Mass fraction of species 1 (-).

.
.
.
.

YS0(I,NSPEC) Mass fraction of species NSPEC (-).

File [C26.3] "Properties of Deterred Layer of Reactive Layer I" (5F10.0) One Card

N.B. File required if and only if MODET = 1, JIS(I) = 2 and KNHIB(I) = 1. (See Files [M2], [C25] and [C25.9].)

ECHIS(I)* Internal energy released in combustion at start of deterred layer (lbf-in/lbm).

ECHIS2(I) Internal energy released in combustion at end of deterred layer (lbf-in/lbm).

RGFAS(I)* Factor by which burn rate is multiplied at start of deterred layer (-).

RGFAS2(I) Factor by which burn rate is multiplied at end of deterred layer (-).

HIBS(I) Depth of deterred layer (in).

* Values within deterred layer deduced by linear spacewise interpolation with an allowance for compression of the reactive layer. Final values need not be the same as those of the undeterred layer.

File [C26.31] "Surface Area Multiplier for Reactive Layer I" (2F10.0) KFACSF(I) Cards

N.B. This file is required if and only if MODET = 1 and JIS(I) = 2 and KFACSF(I) ≥ 2. (See Files [M2], [C25] and [C25.9].)

DBITSF(1,I) First value of surface regression (in).

RFACSF(1,I) Corresponding surface area multiplier (-).

DBITSF(2,I) Second value of surface regression. Starts a new card.

.
.
.
.

RFACSF(KFACSF(I),I) Last value of multiplier.

File [C26.4] "Endwall Property Pointers" (6I5) NENDL Cards

N.B. File required if and only if MODET = 1 and NENDL ≠ 0.
(See Files [M2] and [C25].)

NBAGL(I) Pointer to propellant increment to which I-th endwall is attached. If NBAGL(I) = 0, the endwall is assumed to be attached to the breech of the gun. An increment may include several parallel packaged bundles of propellant.

NBAGE(I) If 0, endwall is at rear of increment.
If 1, endwall is at front of increment.

NREACT(I) Pointer to reactivity models associated with endwall. NREACT is interpreted as a four digit number. Each digit points to a different model. A zero value implies no reactivity. The digits have the following meanings

Digit	Source of Reactivity
1	Internal attached component
2	Interior of endwall
3	Exterior of endwall
4	External attached component

NPERM(I) Pointer to permeability model associated with endwall.

NPRAT(I) If 0, force on endwall is transmitted to propellant.
If 1, force on endwall is transmitted to projectile.

File [C26.5] "Permeability Model Data" (8F10.0) NPRM Cards

N.B. File required if and only if MODET = 1 and NPRM ≠ 0.
(See Files [M2] and [C25].)

PRM(I) Initial flow resistance coefficient for I-th model (-).

RUPSTR(I) Pressure differential at which rupture of endwall commences (psi).

RUPINT(I) Time interval over which rupture of endwall is completed (msec).

N.B. The following Files, [C26.6] through [C27], are repeated as a group for each of the NRCT reactivity models.

File [C26.6] "File Counters for I-th Reactivity Model" (3I5) One Card

---

N.B. File required if and only if MODET = 1 and NRCT ≠ 0.
(See Files [M2] and [C25].)

KBRDE(I) Number of data in modeled burn rate description (-). If KBRDE(I) = 0, it is assumed that tabular discharge data are specified. $0 \leq$ KBRDE(I) ≤ 10.

IGCRIT(I) Ignition criterion for modeled burn rate description. Ignition is determined by reference to VALIG(I) (File [C26.8]) as follows.

IGCRIT(I)	VALIG(I)
1	Time Delay (msec)
2	Ambient gas temperature (R)
3	Neighboring propellant temperature (R)

JRCT(I) Number of data in tabular burn rate description (-). JRCT(I) = 0 or $2 \leq$ JRCT(I) ≤ 8.

File [C26.7] "Thermochemical Data for I-th Reactivity Model" (4F10.0) One Card

---

N.B. File required if and only if MODET = 1 and NRCT ≠ 0.
(See Files [M2] and [C25].)

RHOE(I) Density (lbm/in^3).

EIGE(I) Chemical energy released during combustion (lbf-in/lbm).

GME(I) Molecular weight of combustion products (lbm/lbmol).

GAMAE(I) Ratio of specific heats of combustion products (-).

File [C26.71] "Composition of Near Field Combustion Products of I-th Reactivity Model" (8F10.0) One Card

---

N.B. File required if and only if MODET = 1, KMODE ≠ 0 and NRCT ≠ 0.
(See Files [M2] and [C25].)

YEE(I,1) Mass fraction of species 1 (-).

.
.
.
.

YEE(I,NSPEC) Mass fraction of species NSPEC (-).

File [C26.8] "Ignition Value for I-th Reactivity Model" (F10.0) One Card

N.B. File required if and only if MODET = 1, NCRT ≠ 0 and KBRDE(I) ≠ 0. (See Files [M2], [C25] and [C26.6].)

VALIG(I) Value of time delay (msec), gas temperature (R) or propellant temperature (R) in accordance with IGCRIT(I) as defined above. (See File [C26.6].)

File [C26.9] "Burn Rate Data for I-th Reactivity Model" (8F10.0) One to Three Cards

N.B. File required if and only if MODET = 1, NRCT ≠ 0 and KBRDE(I) ≠ 0. (See Files [M2], [C25] and [C26.6].)

UPPRE(1,I)* First pressure limit (psi).

B22E(1,I) Value of pre-exponent for pressures less than UPPRE(1,I) (in/sec-psi^{BNNE}).

BNNE(1,I) Value of exponent for pressures less than UPPRE(1,I) (-).

.
.
.
.

UPPRE(KBRDE(I),I)* Last pressure limit (psi).

B22E(KBRDE(I),I) Value of pre-exponent for pressures less than UPPRE(KBRDE(I),I), but greater than UPPRE(KBRDE(I)-1,I).

BNNE(KBRDE(I),I) Corresponding exponent (-).

* Outside the table range the first and last values are used.

File [C27] "Tabular Description of I-th Reactivity Model" (8F10.0) One or Two Cards

N.B. File required if and only if MODET = 1, NRCT ≠ 0, KBRDE(I) = 0 and 2 ≤ JRCT ≤ 8. (See Files [M2], [C25] and [C26.6].)

TRCT(1,I) First value of time (msec).

FLORCT(1,I) Corresponding rate of combustion (lbm/in^2-sec).

.
.
.
.

TRCT(JRCT(I),I) Last value of time.

FLORCT(JRCT(I),I) Corresponding rate of combustion.

File [C28] "Internal Properties of Control Charge Combustion Chamber"
(4F10.0) One Card

N.B. File required if and only if MODET = 1 and KCTRL ≠ 0.
(See Files [M2] and [C25].)

CDCR	Discharge coefficient for venting to gun chamber (-).
RCRI	Internal radius of bore (in).
VCR0	Initial chamber volume corresponding to zero afterbody offset (in^3).
ZCR0	Initial afterbody offset (in).

File [C28.1] "External Properties of Control Charge Combustion Chamber"
(3F10.0) NZCRE Cards

N.B. File required if and only if MODET = 1 and KCTRL ≠ 0.
(See Files [M2] and [C25].)

ZCRE(1)	First axial position relative to breechface of gun (in).
RCRE(1)	Corresponding external radius of chamber (in).
AVENT(1)	Total sidewall vent area exposed when base of afterbody is at ZCRE(1) (in^2).
ZCRE(2)	Second axial position. Starts a new card.
.	
.	
.	
.	
ZCRE(NZCRE)	Last axial position.
RCRE(NZCRE)	
AVENT(NZCRE)	

File [C28.2] "Control Charge Type" (5A4,2F10.0) One Card

N.B. File required if and only if MODET = 1 and KCTRL ≠ 0.
(See Files [M2] and [C25].)

GRNMCR	Name of propellant. Up to 20 alphanumeric characters.
WGTCR	Mass of control charge (lbm).
RHOPCR	Density of propellant (lbm/in^3).

File [C28.3] "Control Charge Form Function" (I5,4F10.0) One Card

N.B. File required if and only if MODET = 1 and KCTRL ≠ 0.
(See Files [M2] and [C25].)

NFRMCR	Form function indicator. See discussion of File [M8]. Allowable values of NFRMCR are 1, 2, 5, 6 and 7.
ODCR	Grain dimension (in). See File [M8].
DPRFCR	Grain dimension (in). See File [M8].
GLENCR	Grain length (in).
NPRFCR	Number of perforations (-).

File [C28.4] "Control Charge Burn Rate Counter" (I5) One Card

N.B. File required if and only if MODET = 1 and KCTRL ≠ 0.
(See Files [M2] and [C25].)

NBRDCR	Number of sets of values used to describe burn rate. $1 \leq NBRDCR \leq 10$.

File [C28.5] "Control Charge Burn Rate Description" (8F10.0)
One to Four Cards

N.B. File required if and only if MODET = 1 and KCTRL ≠ 0.
(See Files [M2] and [C25].)

UPPCR(1)	Maximum value of pressure for corresponding values of burn rate pre-exponential and exponential factors (psi).
B22CR(1)	Burning rate pre-exponential factor (in/sec-psi^n).
BNNCR(1)	Burning rate exponent (-).
.	
.	
.	
.	
UPPCR(NBRDCR)	Maximum value for last set of burn rate data.
B22(NBRDCR)	Corresponding pre-exponent.
BNN(NBRDCR)	Corresponding exponent.
B1CR	Burning rate additive constant (in/sec).
DELCR	Ignition delay (msec).

File [C28.6] "Control Charge Thermochemistry" (3F10.0) One Card

N.B. File required if and only if MODET = 1 and KCTRL ≠ 0. (See Files [M2] and [C25].)

ECHCR	Internal energy released in combustion (lbf-in/lbm).
GMCR	Molecular weight of combustion products (lbm/lbmol).
GAMACR	Ratio of specific heats (-).

File [C28.7] "Properties of Deterred Layer" (8F10.0) One Card

N.B. File required if and only if MODET = 1 and KCTRL ≠ 0 and INHBCR = 1. (See Files [M2] and [C25].)

ECRIB*	Internal energy released in combustion at start of deterred layer (lbf-in/lbm).
ECRIB2	Internal energy released in combustion at end of deterred layer (lbf-in/lbm).
RGFCR	Factor by which burn rate is multiplied at start of deterred layer (-).
RGFCR2	Factor by which burn rate is multiplied at end of deterred layer (-).
HIBXCR	Depth of inhibited layer (in).

* Values within deterred layer deduced by linear spacewise interpolation. Final values need not be the same as those of the undeterred propellant.

File [C29] "Forward Boundary Discharge Data" (8F10.0) One Card

N.B. File required if and only if INBCX = 1. (See File [M2].)

FBAEX	Discharge area (in^2).
FBCD	Discharge coefficient (-).
FBPMIN	Pressure required to open forward vent (psi). Discharge begins when the gas pressure exceeds FBPMIN and then continues as long as it exceeds the atmospheric value. Backflow is not considered.

File [C30] "Inbore Rocket Motor Data" (8F10.0) Two Cards

N.B. File required if and only if INBCX = 2. (See File [M2].)

RMP0	Initial mass of rocket motor propellant (lbm).
RECHEM	Chemical energy of propellant (lbf-in/lbm).
RPDEN	Density of propellant (lbm/in^3).
RGAM	Ratio of specific heats of motor combustion products (-).
RMOLW	Molecular weight of motor combustion products (lbm/lbmol).
RPOP	Operating pressure of motor (psi).
RAP0	Initial port area (in^2).
RTIG1	Delay prior to first venting from motor (msec).
RTIG2	Interval from onset of venting to operation at nominal pressure RPOP (msec).
RCDEN	Density of case material (lbm/in^3).
RCSTR	Tensile yield strength of case material (psi).

File [C30.1] "Composition of Rocket Motor Combustion Products" (8F10.0) One or Two Cards

N.B. File required if and only if INBCX = 2 and KMODE ≠ 0. (See File [M2].)

RCYEE(1)	Mass fraction of motor combustion products corresponding to species 1 (-).
.	
.	
.	
.	
RCYEE(NSPEC)	Mass fraction of motor combustion products corresponding to species NSPEC (-).

File [C31] "ETG Control Switches" (4I5) One Card

N.B. File required if and only if NETG = 1. (See File [M2].)

NETGS — Number of plasma jet data sets (-). $1 \leq NETGS \leq 10$.

MODPET(1) — If 1, propellant type 1 will have surface regression rate described by usual exponential law in accordance with data of File [M10].
If 2, propellant type 1 will have surface regression rate described by Helmholtz Law with data as given in File [C31.1].
If 3, propellant type 1 will have surface regression rate described by table of values of linear regression versus time as given in Files [C31.2] and [C31.3].
If 4, propellant type 1 will have surface regression rate described by table of value of mass burning rate versus time as given in Files [C31.2] and [C31.3].

MODPET(2) — Like MODPET(1), but applying to propellant type 2.

MODPET(3) — Like MODPET(1), but applying to propellant type 3.

N.B. The following Files [C31.3] through [C31.3] are repeated as a group for each of the NPROP propellants for which MODPET ≠ 1. (See File [C31].)

File [C31.1] "I-th Propellant Helmholtz Wiping Coefficient" (F10.0) One Card

N.B. File required if and only if NETG = 1 and MODPET(I) = 2. See Files [M2] and [C31].)

ETPR2(I) — Wiping coefficient for propellant type I (-).

File [C31.2] "I-th Propellant Tabular Regression Rate Counter" (I5) One Card

N.B. File required if and only if NETG = 1 and MODPET(I) = 3 or 4. (See Files [M2] and [C31].)

NPDAT(I) — Number of pairs of data in File [C31.3] for propellant type I (-). $1 \leq NPDAT \leq 100$.

File [C31.3] "I-th Propellant Tabular Regression Rate Data" (2F10.0)
NPDAT(I) Cards

N.B. File required if and only if NETG = 1 and MODPET(I) = 3 or 4. (See Files [M2] and [C31].)

TDOTET(1,I) First value of time (msec).

RDOTET(1,I) First value of regression rate. If MODPET(I) = 3, the value is understood to be the linear regression rate (in/sec). If MODPET(I) = 4, the value is understood to be the mass burning rate (lbm/sec).

TDOTET(2,I) Second value of time. Starts a new card.

.
.
.
.

RDOTET(NPDAT(I),I)

N.B. The data in this file are linearly interpolated within the table range. The first or last values are used outside the table range. If the rate is constant, one pair of data will suffice.

N.B. The following Files [C31.4] through [C32] are repeated as a group for each of the NETGS plasma jets. (See File [C31].)

File [C31.4] "I-th Plasma Jet File Counters" (215) One Card

N.B. File required if and only if NETG = 1. (See File [M2].)

MODPLS(I) If MODPLS(I) = 0, the plasma mixing length is assumed to be constant and the flux is described by the integrated data of Files [C31.7] and [C31.8].
If MODPLS(I) = 1, the plasma mixing length is assumed to vary in time according to a Prandtl spreading rate criterion with detailed data given by Files [C31.9] and [C32].
If MODPLS(I) = 2, the plasma mixing length is assumed to be constant and the flux is determined by the capillary model of Powell and Zielinsky.

NETDAT(I) Number of sets of data in File [C31.8] or [C32] according as MODPLS(I) = 0 or 1 respectively. $2 \leq$ NETDAT(I) ≤ 100.

File [C31.5] "Global Properties of I-th Plasma Jet" (5F10.0) One Card

N.B. File required if and only if NETG = 1. (See File [M2].)

ETTOTE(I) Total plasma energy (lbf-in).

ETTOTM(I) Total plasma mass (lbf-in).

ETDIA(I) Average capillary diameter (in). Only required if MODPLS(I) = 1.

ETAVGA(I) Average ratio of specific heats of plasma (-).

ETAVMW(I) Average molecular weight of plasma (lbm/lbmol).

File [C31.6] "Composition of I-th Plasma Jet" (8F10.0) One Card

N.B. File required if and only if NETG = 1 and KMODE ≠ 0. (See File [M2].)

YET0(I,1) Mass fraction of species 1 (-).

.
.
.
.

YET0(I,NSPEC) Mass fraction of species NSPEC (-).

File [C31.7] "I-th Plasma Jet Mixing Length Parameters in Integrated Format" (3F10.0) One Card.

N.B. File required if and only if NETG = 1 and MODPLS(I) = 0 or 2. (See Files [M2] and [C31.4].)

ETZ0(I) Distance of injection point from breech of tube (in).

ETMIXL(I) Mixing length (in).

FRIN(I) Fraction of plasma flux directed to internal voidage in cases involving dual-voidage representation of flow through propellant. $0 \leq FRIN \leq 1$.

File [C31.71] "Plasma Capillary Data" Unformatted. One Card.

N.B. This File is only required if NETG = 1 and MODPLS(I) = 2.
(See Files [M2] and [C31.4].)

XXRI	Capillary radius (m).
XXL	Capillary length (m).
NPTS	Number of pairs of data in File [C31.73]. Must not exceed 1000.
ITMAX	Maximum number of iterations for determination of plasma flux.

File [C31.72] "Stoichiometry Coefficients for Plasma Model" Unformatted. Eight Cards.

N.B. This File is only required if NETG = 1 and MODPLS(I) = 2.
(See Files [M2] and [C31.4].)

RRI(1)	First value (-).
RRI(2)	Second value. Starts a new card.
.	
.	
.	
RRI(8)	Last value.

File [C31.73] "Current History" Unformatted. NPTS Cards.

N.B. This File is only required if NETG = 1 and MODPLS(I) = 2.
(See Files [M2] and [C31.4].)

TPLAS(1)	First value of time (sec).
XIPLAS(1)	Corresponding value of current(amp).
TPLAS(2)	Second value of time. Starts a new card.
.	
.	
.	
.	
XIPLAS(NPTS)	

File [C31.8] "I-th Plasma Jet Integrated Data" (4F10.0) NETDAT(I) Cards

N.B. File required if and only if NETG = 1 and MODPLS(I) = 0.
(See Files [M2] and [C31.4].)

ETGT(1,I) First value of time (msec).

ETGE(1,I) Fraction of total energy delivered by time ETGT(1,I) (-).

ETGM(1,I) Fraction of total mass delivered by time ETGT(1,I) (-).

ETGU(1,I) Axial velocity component of plasma jet at time ETGT(1,I) (in/sec).

ETGT(2,I) Second value in time. Starts a new card.

.
.
.
.

ETGU(NETDAT(I),I).

N.B. Data in these tables are linearly interpolated within the table range. The plasma flux is assumed to be zero outside the table range.

File [C31.9] "I-th Plasma Jet Mixing Length Parameters in Detailed Format" (3F10.0) One Card

N.B. File required if and only if NETG = 1 and MODPLS(I) = 1.
(See Files [M2] and [C31.4].)

ETZ0(I) Distance of injection point from breech of tube (in).

ETPR1(I) Dimensionless spreading rate coefficient (-).

FRIN(I) Fraction of plasma flux directed to internal voidage in cases involving dual-voidage representation of flow through propellant. $0 \leq FRIN \leq 1$.

File [C32] "I-th Plasma Jet Detailed Data" (7F10.0) NETDAT(I) Cards

N.B. File required if and only if NETG = 1 and MODPLS(I) = 1.
(See Files [M2] and [C31.4].)

ETGT(1,I) First value of time (msec).

ETGE(1,I) Fraction of total energy delivered by time ETGT(1,I) (-).

ETGM(1,I) Fraction of total mass delivered by time ETGM(1,I) (-).

ETGU(1,I) Axial velocity component of plas ma jet at time ETGT(1,I) (in/sec).

ETGD(1,I) Diameter of exit plane of capillary at time ETGT(1,I) (in).
If ETGD is entered as zero, it defaults to ETDIA.
(See File [31.5].)

ETGAM(1,I) Ratio of specific heats of plasma jet at time ETGT(1,I) (-).
If ETGAM is entered as zero, it defaults to ETAVGA.
(See File [C31.5.)

ETMOL(1,I) Molecular weight of jet at time ETGT(1,I) (lbm/lbmol).
If ETMOL is entered as zero it defaults to ETAVMW.
(See File [C31.5].)

ETGT(2,I) Second value of time. Starts a new card.

.
.
.
.

ETMOL(NETDAT(I),I)

N.B. Data in these tables are linearly interpolated within the table range.
The plasma flux is assumed to be zero outside the table range.

N.B. The following Files, [TC1] - [TC17] are required only if NTC = 1 or 2 (See File [M2]).

File [TC1] "Traveling Charge Control Data" (7I5) One Card TC-Mandatory

IDEAL	Propellant burn rate indicator. 0 - Measured burn rate data. See Files [TC5] - [TC8]. 1 - Not Supported. 2 - Ideal burning with prespecified value of pressure on either side of gas/traveling charge interface or of projectile acceleration. Note the discussion of SIGMAX, MACH, APMAX in File [TC2].
NPRC	0 - Traveling charge treated as a rigid. 1 - Traveling charge treated as a continuum with analytical description of rheology. File [TC9] required. 2 - Traveling charge treated as continuum with tabular description of rheology. Files [TC10] and [TC11] required.
NPROP	Number of traveling charge increments (maximum of 20).
NWFR	Propellant Wall Friction Parameter. 0 - Friction between propellant and tube not considered. 1 - Friction due to gas film. File [TC12] required. >0 - Number of entries in velocity dependent coefficient of friction table (maximum of 10). File [TC13] required.
NBRES1	0 - Obturator resistance not given as table. >0 - Number of entries in table of resistive pressure versus travel (maximum of 10). File [TC14] required.
NBRES2	0 - Resistance due to shocked air not considered. 1 - Resistance due to shocked air considered. File [TC15] required.
NBRES3	0 - Obturator resistance not proportional to setback pressure. >0 - Number of entries in table of velocity dependent coefficient of friction of obturator (maximum of 10). Files [TC16] and [TC17] required.

File [TC2] "Mesh Parameters" (I5,F10.0) One Card TC-Mandatory

MAXDIM	Maximum number of mesh points to be used in continuum representation of traveling charge (≤ 100).
DXMIN	Minimum mesh size for continuum representation (in).

File [TC3] "General Properties" (6F10.0) One Card TC-Mandatory

DB	Diameter of tube (in) if NTC = 1 and diameter of end burning charge if NTC = 2. (See File [M2]).
XIB	Initial length of gas column (in).
PRM	Mass of projectile (lbm).
SIGMAX	Maximum value of pressure at gas/propellant interface (psi). If SIGMAX = 0, no restriction is considered. SIGMAX pertains to the reacted or the unreacted side of the flame according as NPORS(KK) = 0 or 1 respectively. (See File [TC5].)
MACH	Maximum value of Mach number of combustion products relative to regressing surface. If MACH = 0, no restriction is considered.
APMAX	Maximum value of acceleration of projectile (gravities). If APMAX = 0, no restriction is considered.

N.B. Files [TC4] through [TC13] pertain to a specific type of propellant. The sequence [TC4] through [TC13], subject to relevant contingencies, is repeated for each type of traveling charge propellant in the problem. The index KK used in the following file descriptions runs through the values 1, 2, . . . ,NPROP, where NPROP is defined in File [TC1].

File [TC4] "Propellant Thermochemical Properties" (8F10.0) One Card TC-Mandatory

XGAM(KK)	Ratio of specific heats of gas (-).
XBV(KK)	Covolume (in^3/lbm).
XMOL(KK)	Molecular weight (lbm/lbmol).
XECHEM(KK)	Chemical energy of propellant (lbf-in/lbm).
XRHOP(KK)	Density of solid propellant at zero pressure (lbm/in^3).
XCM(KK)	Mass of propellant (lbm).
XCRIT(KK)	Time delay following first exposure of increment base before combustion begins (msec).
XDEL(KK)	Time interval over which increment combustion rate increases to steady-state value (msec).

File [TC5] "Burn Rate Switches" (2I5) One Card TC-Mandatory

MNBR1(KK)
- 0 - Exponential form for measured burn rate description of propellant KK.
- 1 - Tabular form for measured burn rate description of propellant KK.
- 2 - Propellant is endburning plasma guided design

NPORS(KK)
- 0 - Measured burn rate data are given as function of pressure on reacted side of flame. Ideal burn rate value SIGMAX (see File [TC3]) pertains to reacted side.
- 1 - Measured burn rate data are given as function of pressure on unreacted side of flame. Ideal burn rate value SIGMAX pertains to unreacted side.

File [TC6] "Tabular Burn Rate Data" (2I5,F10.0) One Card TC-Contingent

N.B. File is required if and only if IDEAL = 0 and MNBR1(KK) = 1. (See Files [TC1] and [TC5].)

NBRP(KK) Number of pairs of data in KK-th tabular description of burn rate (maximum of 20).

INTD Number of table entries to use in divided difference interpolation. The same value is assumed for all propellants.

B1(KK) Burn rate additive constant for KK-th increment (in/sec).

File [TC7] "Tabular Burn Rate Data (cont'd) (2F10.0) NBRP(KK) Cards TC-Contingent

N.B. File is required if and only if IDEAL = 0 and MNBR1(KK) = 1. (See Files [TC1] and [TC5].)

PE(1,KK) First value of pressure in tabular description of burn rate of propellant KK (psi).

RP(1,KK) First value of burn rate of propellant KK corresponding to PE(1,KK) (in/sec).

.
.
.

PE(NBP(KK),KK)

RP(NBRP(KK),KK)

File [TC7.1] "Plasma Guided End Burner" (I5,F15.0) 1 card

NBRM(I) Number of sets of data to specify combustion rate. NBRM(I) must not be less than 2 or greater than 100.

EPLAS(I) Total energy of plasma to be added to surface of increment.

N.B. The subscript I indicates that as many as 20 separate increments may be defined for the endburning grain, each with distinct properties.

File [TC7.2] "Plasma Guided End Burner (Cont'd) (3F10.0) NBRM(I) cards

TBRM(1,I) First time (msec).

FBRM(1,I) Fraction of mass consumed at TBRM(1,I).

PLAS (1,I) Fraction of plasma energy delivered at TBRM(1,I).

.
.
.
.

TBRM(NBRM(I),I)

N.B. A cubic spline is fitted to these data and is then explicitly differentiated to determine a continuously varying rate as required by the code. Smooth data should be provided since the spline can give problems with data containing high order structure. The rates are taken to be zero for times less than TBRM(1,I) and are set equal to the boundary value for times greater than TBRM(NBRM(I),I) in order to allow for complete consumption of the increment in the event of imperfect integration.

It is assumed that the plasma mass can be neglected. Also, it is assumed that there is no net delivery of plasma across the surface of the grain if the rate of regression is zero.

File [TC8] "Exponential Burn Rate Data" (3F10.0) One Card TC-Contingent

N.B. File required if and only if IDEAL = 0 and MNBR1(KK) = 0. (See Files [TC1] and [TC5].)

B1(KK) Burn rate additive constant for KK-th propellant (in/sec).

B2(KK) Burn rate pre-exponential coefficient for KK-th propellant ($in/sec\text{-}psi^{BN}$).

BN(KK) Burn rate exponent for KK-th propellant (-).

File [TC9] "Propellant Analytical Rheology Data" (2F10.0) One Card TC-Contingent

N.B. File required if and only if NPRC = 1. (See File [TC1].)

XAUP(KK) Compressive wave speed at zero pressure in analytical description of propellant rheology (in/sec).

XADWN(KK) Expansion wave speed in analytical description of propellant rheology (in/sec). If XADWN(KK) is entered so that it is less than the nominal compressive wave speed, the loading value is used. By entering XADWN(KK) = 0, a reversible law is defined.

File [TC10] "Propellant Tabular Rheology Data" (I5) One Card TC-Contingent

N.B. File required if and only if NPRC = 2. (See File [TC1].)

MNSS(KK) Number of pairs of entries in tabular description of propellant rheology (maximum of 20).

File [TC11] "Propellant Tabular Rheology Data" (cont'd) (3F10.0) MNSS(KK) Cards TC-Contingent

N.B. File required if and only if NPRC = 2. (See File [TC1].)

PSTA(1,KK) First value of percent strain in tabular description of propellant rheology (-).

STRL(1,KK) Corresponding value of pressure on nominal loading (compression curve (psi)).

STRU(1,KK) Corresponding value of pressure on nominal unloading (expansion curve (psi)).

.
.
.
.

PSTA(MNSS(KK),KK)

STRL(MNSS(KK),KK)

STRU(MNSS(KK),KK)

File [TC12] "Ablative Film Data" (2F10.0) One Card TC-Contingent

N.B. File required if and only if NWFR < 0. (See File [TC1].)

VISLYR(KK) Viscosity of gas film used to lubricate propellant (lbm/in-sec).

DELYR(KK) Thickness of film.

File [TC13] "Propellant Friction Data" (8F10.0) One to Three Cards
TC-Contingent

N.B. File required if and only if NWFR > 0. (See File [TC1].)
All propellants are assumed to have the same number of data NWFR.

AMUV(1,KK) First value of velocity of propellant (in/sec).

AMU(1,KK) Corresponding coefficient of friction on tube (-).

.
.
.
.

AMUV(NWFR,KK) Last value of velocity (in/sec).

AMU(NWFR,KK) Corresponding coefficient of friction (-).

File [TC14] "Tabular Bore Resistance Data" (8F10.0) One to Three Cards
TC-Contingent

N.B. File required if and only if NBRES1 ≠ 0. (See File [TC1].)

BRX(1) First value of projectile travel (in).

BR(1) Corresponding value of resistive pressure due to obturator (psi).

.
.
.
.

BRX(NBRES1) Last value of projectile travel (in).

BR(NBRES1) Corresponding value of resistive pressure (psi).

File [TC15] "Barrel Shock Resistance Data" (4F10.0) One Card
TC-Contingent

N.B. File required if and only if NBRES2 ≠ 0. (See File [TC1].)

AIRGAM Ratio of specific heats of air (-).

AIRP0 Pressure of air in barrel (psi).

AIRT0 Temperature of air in barrel (R).

AIRMW Molecular weight of air in barrel (lbm/lbmol).

File [TC16] "Obturator Setback Resistance Data" (3F10.0) One Card TC-Contingent

N.B. File required if and only if NBRES3 ≠ 0. (See File [TC1].)

PRMB	Mass of projectile ahead of midpoint of obturating band (lbm).
ELB	Length of bearing section of obturating band (in).
ANU	Poisson's ratio of obturating band (-).

File [TC17] "Obturator Friction Data" (8F10.0) One to Three Cards TC-Contingent

N.B. File required if and only if NBRES3 ≠ 0. (See File [TC1].)

BMUV(1)	First value of velocity of projectile (in/sec).
BMU(1)	Corresponding value of coefficient of friction between obturator and tube (-).
.	
.	
.	
.	
BMUV(NBRES3)	Last value of velocity of projectile (in/sec).
BMU(NBRES3)	Corresponding coefficient of friction (-).

N.B. The following Files [TLC2] - [TLC22.7] are required if and only if NTLC = 1 (See File [M2]).

File [TLC2] "Option Switches" (3I5) One Card TLC-Mandatory

KIN1	If 0, traveling liquid propellant is assumed to convert to droplets instantaneously upon discharge into region where cavity is not mechanically stabilized. If 1, propellant converts to droplet form according to finite kinetic law which depends on slip velocity at propellant/cavity interface in region where cavity is not mechanically stabilized. File [TLC9.1] is required.
KIN2	If 0, droplets are assumed to burn instantaneously upon formation. If 1, droplets are assumed to burn according to finite rate kinetic law which depends on pressure. File [TLC9.2] is required. Solutions based on KIN2 will only be valid if the ratio of specific heats and the molecular weight are not expected to vary, and provided that droplets are not swept back into the booster region.
NXPEL	If 0, a TC expulsion charge is not located in the projectile base. If 1, a TC expulsion charge is located in the projectile base and Files [TLC22.1] - [TLC22.7] are required.

File [TLC5] "Integration Parameters" (I5,2F10.0) One Card TLC-Mandatory

NMSHLC	Number of mesh points assigned to traveling liquid charge. Must be at least 6 unless NCAV = 0 (See File [TLC11]). Suggested value is 11.
DZMNLC	Minimum mesh spacing in traveling liquid charge (in).
TOLP	Convergence tolerance for iterative determination of fluxes between lumped parameter regions (10^{-6} lbm^2/sec^2). Default value is 1.0. Suggested value is 0.01.

N.B. The value of 2 * NMSHLC must not exceed 95.

File [TLC6] "Tube Properties" (2I5,F10.0) One Card TLC-Mandatory

NBRES1	If 0, obturator resistance is neglected. If > 0, NBRES1 is the number of tabular entries used to define the obturator resistance as a function of travel. NBRES1 must not be greater than 8. File [TLC6.1] is required in this case.
NBRES2	If 0, resistance due to shocked air in front of projectile is neglected. If 1, resistance due to shocked air is considered. File [TLC6.2] is required in this case.
DB	Diameter of gun tube (in).

File [TLC6.1] "Obturator Resistance" (8F10.0) One or Two Cards TLC-Mandatory

N.B. File required if and only if NBRES1 > 0.

BRZ(1)	First value of projectile travel (in).
BR(1)	Corresponding value of obturator resistance (psi).
.	
.	
.	
.	
BRZ(NBRES1)	Last value of projectile travel (in).
BR(NBRES1)	Corresponding value of bore resistance (psi).

File [TLC6.2] "Air Shock Resistance Data" (8F10.0) One Card TLC-Mandatory

N.B. File required if and only if NBRES2 = 1.

AIRP0	Initial pressure of gas in barrel (psi).
AIRT0	Initial temperature of gas in barrel (R).
AIRGAM	Ratio of specific heats of gas in barrel (-).
AIRMW	Molecular weight of gas in barrel (lbm/lbmol).

File [TLC7] "Projectile Properties" (8F10.0) One Card TLC-Mandatory

PRM	Projectile mass (lbm).
ZPR0	Initial location of projectile base with respect to entrance of gun tube (in).

N.B. This datum does not take into account the possible presence of an afterbody used to stabilize the traveling liquid charge. The base of the afterbody is located a distance ZCAV(NCAV) - ZCAV(1) behind the projectile base. (See File [TLC11.1].) Accordingly, even if ZPR0 is positive, it is possible that the data base may represent the afterbody as intruding into the booster combustion chamber. The analysis of the combustion chamber by XKTC is only performed to the base of the afterbody. Errors will occur if the afterbody intrudes into the chamber and the chamber diameter differs from that of the tube.

ZVENT	Projectile travel after which traveling liquid charge begins to vent rearwards from mechanically stabilized region.
RHOCAV	Density of afterbody material (lbm/in^3).
PCAV	Pressure at which traveling liquid charge separates from base of projectile (psi).

File [TLC7.1] "Chamber Length" (F10.0) One Card TLC-Mandatory

CHAMLN	Distance from breech to entrance of tube (in).

File [TLC9] "Properties of Liquid Propellant" (8F10.0) One Card TLC-Mandatory

RHOL	Density of liquid propellant at one atmosphere (lbm/in^3).
BUL1	Bulk modulus of liquid propellant at one atmosphere (psi).
BUL2	Derivative of bulk modulus with respect to pressure at one atmosphere (-).
EFL	Chemical energy released in combustion (lbf-in/lbm).
GAML	Ratio of specific heats of products of combustion (-).
GML	Molecular weight of products of combustion (lbm/lbmol).
BVL	Covolume of products of combustion (in^3/lbm).

File [TLC9.1] "Propellant Droplet Formation Data" (8F10.0) One Card TLC-Contingent

N.B. This file is required if and only if KIN1 = 1.

DROP	Diameter of propellant droplets (in). This datum applies to both the traveling and the booster increments.
WIPE	Coefficient of proportionality between rate of droplet formation and slip velocity for traveling liquid charge in mechanically unstabilized region (lbm/in).

File [TLC9.2] "Droplet Burn Rate Data" (8F10.0) One Card TLC-Contingent

N.B. This file is required if and only if KIN2 = 1.

B1	Additive burn rate constant (in/sec).
B2	Burn rate pre-exponential factor ($in/sec/psi^{BN}$).
BN	Burn rate exponent (-).

File [TCL10] "Initial Conditions" (8F10.0) One Card TLC-Mandatory

PSTG	Initial pressure of gas (psi).
PSTLT	Initial pressure of traveling charge (psi).
TEMST	Initial temperature (R).
GAMST	Ratio of specific heats of initial ambient in TLC (-).
GMOLST	Molecular weight of initial ambient in TLC (lbm/lbmol).

N.B. GAMST and GMOLST are not required by RLPTC.

File [TLC11] "Initial Cavity Parameters" (2I5) One Card TLC-Mandatory

NCAV	Number of tabular data used to describe initial configuration of cavity. Maximum of 50. If NCAV = 0, it is understood that there is no traveling liquid charge present. The subsequent data of this file are not required.
MECH	If 0, cavity is not mechanically stabilized and its behavior is governed by the Taylor principle. If 1, cavity is stabilized and its geometry is taken to be frozen directly behind the projectile into the configuration defined by the initial data.

File [TLC11.1] "Initial Cavity Geometry" (3F10.0) NCAV Cards
TLC-Contingent

N.B. This file is required if and only if NCAV > 0.

ZCAV(1)	First axial location for definition of initial cavity geometry (in). Starts a new card. The cavity defined by these data must formally extend to the projectile base. Zero values of RCAV may be used to represent sections of the traveling liquid charge which fill the cross-section of the tube. It is always understood that ZCAV(NCAV) corresponds to the base of the projectile. This latter assumption is always enforced internally to the code by adding a suitable value to the values of ZCAV(I), I = 1, . . . ,NCAV.
RCAV(1)	Corresponding radius of cavity (in).
THKV(1)	Thickness of mechanically stabilizing layer (in). Only used if MECH = 1. If THKV > 0, it is understood that RCAV refers to the exterior of the surface. The thickness is measured in the radial direction rather than normal to the surface of the stabilizing layer.
ZCAV(2)	Second axial location. Starts a new card.
.	
.	
.	
.	
THKV(NCAV)	

File [TLC22.1] "Properties of TLC Expulsion Charge Combustion Chamber"
(8F10.0) One Card TLC-Contingent

N.B. This file is required if and only if NXPEL = 1.

CDCR(2)	Discharge coefficient for venting to traveling charge region (-).
ACRI(2)	Venting area (in^2).
VCR0(2)	TC expulsion charge chamber volume (in^3).
PSTCR(2)	Initial Pressure (psi).
TSTCR(2)	Initial Temperature (R).
DELPST(2)	Pressure differential between expulsion charge combustion chamber and forward end of TC to initiate venting (psi). Once ventholes open, they stay open.

File [TLC22.2] "TLC Expulsion Charge Type" (5A4,2F10.0) One Card
TLC-Contingent

N.B. This file is required if and only if NXPEL = 1.

GRNMCR(2) Name of propellant. Up to 20 alphanumeric characters.

WGTCR(2) Mass of TC expulsion charge (lbm).

RHOPCR(2) Density of propellant (lbm/in^3).

File [TLC22.3] "TLC Expulsion Charge Form Function" (I5,4F10.0) One Card
TLC-Contingent

N.B. This file is required if and only if NXPEL = 1.

NFRMCR(2) Form function indicator. See discussion of File [M8]. Allowable values of NFRMCR are 1, 2, 5, 6, and 7.

ODCR(2) Grain dimension (in).

DPRFCR(2) Grain dimension (in).

GLENCR(2) Grain dimension (in).

NPRFCR(2) Number of perforations (-).

File [TLC22.4] "TLC Expulsion Charge Burn Rate Counter" (2I5) One Card
TLC-Contingent

N.B. This file is required if and only if NXPEL = 1.

NBRDCR(2) Number of sets of values used to describe burn rate. $1 \leq NBRDCR \leq 10$.

INHBCR(2) If 0, propellant is not deterred.
If 1, propellant is deterred and File [TLC22.7] is required.

File [TLC22.5] "TLC Expulsion Charge Burn Rate Description" (8F10.0)
One to Four Cards TLC-Contingent

N.B. This file is required if and only if NXPEL = 1.

UPPCR(1,2) Maximum value of pressure for corresponding values of burn rate pre-exponential and exponential factors (psi).

B22CR(1,2) Burning rate pre-exponential factor (in/sec-psi^n).

BNNCR(1,2) Burning rate exponent (-).

.
.
.
.

UPPCR(NBRDCR(2),2) Maximum value for last set of burn rate data.

B22(NBRDCR(2),2) Corresponding pre-exponent.

BNN(NBRDCR(2),2) Corresponding exponent.

B1CR(2) Burning rate additive constant (in/sec).

DELCR(2) Ignition delay (msec).

File [TLC22.6] "TLC Expulsion Charge Thermochemistry" (8F10.0) One Card
TLC-Contingent

N.B. This file is required if and only if NXPEL = 1.

ECHCR(2) Internal energy released in combustion (lbf-in/lbm.)

GMCR(2) Molecular weight of combustion products (lbm/lbmol).

GAMACR(2) Ratio of specific heats (-).

File [TLC22.7] "Properties of Deterred Layer" (8F10.0) One Card
TLC-Contingent

N.B. This file is required if and only if NXPEL = 1 and INHBCR(2) = 1.

ECRIB(2)*	Internal energy released in combustion at start of deterred layer (lbf-in/lbm).
ECRIB2(2)	Internal energy released in combustion at end of deterred layer (lbf-in/lbm).
RGFCR(2)	Factor by which burn rate is multiplied at start of deterred layer (-).
RGFCR2(2)	Factor by which burn rate is multiplied at end of deterred layer (-).
HIBXCR(2)	Depth of inhibited layer (in).

* Values within deterred layer deduced by linear spacewise interpolation Final values need not be the same as those of the undeterred propellant.

INTENTIONALLY LEFT BLANK.

NO. OF COPIES	ORGANIZATION
2	DEFENSE TECHNICAL INFORMATION CENTER DTIC DDA 8725 JOHN J KINGMAN RD STE 0944 FT BELVOIR VA 22060-6218
1	HQDA DAMO FDT 400 ARMY PENTAGON WASHINGTON DC 20310-0460
1	OSD OUSD(A&T)/ODDDR&E(R) R J TREW THE PENTAGON WASHINGTON DC 20301-7100
1	DPTY CG FOR RDA US ARMY MATERIEL CMD AMCRDA 5001 EISENHOWER AVE ALEXANDRIA VA 22333-0001
1	INST FOR ADVNCD TCHNLGY THE UNIV OF TEXAS AT AUSTIN PO BOX 202797 AUSTIN TX 78720-2797
1	DARPA B KASPAR 3701 N FAIRFAX DR ARLINGTON VA 22203-1714
1	US MILITARY ACADEMY MATH SCI CTR OF EXCELLENCE MADN MATH MAJ HUBER THAYER HALL WEST POINT NY 10996-1786
1	DIRECTOR US ARMY RESEARCH LAB AMSRL D D R SMITH 2800 POWDER MILL RD ADELPHI MD 20783-1197

NO. OF COPIES	ORGANIZATION
1	DIRECTOR US ARMY RESEARCH LAB AMSRL DD 2800 POWDER MILL RD ADELPHI MD 20783-1197
1	DIRECTOR US ARMY RESEARCH LAB AMSRL CI AI R (RECORDS MGMT) 2800 POWDER MILL RD ADELPHI MD 20783-1145
3	DIRECTOR US ARMY RESEARCH LAB AMSRL CI LL 2800 POWDER MILL RD ADELPHI MD 20783-1145
1	DIRECTOR US ARMY RESEARCH LAB AMSRL CI AP 2800 POWDER MILL RD ADELPHI MD 20783-1197
	ABERDEEN PROVING GROUND
4	DIR USARL AMSRL CI LP (BLDG 305)

NO. OF COPIES	ORGANIZATION
1	CHAIRMAN DOD EXPLOSIVES SAFETY BOARD ROOM 856-C HOFFMAN BLDG 1 2461 EISENHOWER AVE ALEXANDRIA VA 22331-0600
1	US ARMY BALLISTIC MISSILE DEFENSE SYS CMD ADVANCED TECH CTR PO BOX 1500 HUNTSVILLE AL 35807-3801
1	DEPT OF THE ARMY OFC OF THE PRODUCT MANAGER 155MM HOWITZER M109A6 PALADIN SFAE AR HIP IP R DE KLEINE PICATINNY ARSENAL NJ 07806-5000
3	PM ADVANCED FIELD ARTILLERY SYS SFAE ASM AF E J SHIELDS PICATINNY ARSENAL NJ 07801-5000
1	PM ADVANCED FIELD ARTILLERY SYS SFAE ASM AF Q PICATINNY ARSENAL NJ 07801-5000
2	COMMANDER PRODUCTION BASE MODERNIZATION AGENCY ARDEC AMSMC PBM A SIKLOSI L LAIBSON PICATINNY ARSENAL NJ 07806-5000
1	PEO ARMAMENTS PM TMAS AMCPM TMA PICATINNY ARSENAL NJ 07806-5000
1	PEO ARMAMENTS PM TMAS AMCPM TMA 105 PICATINNY ARSENAL NJ 07806-5000
1	PEO ARMAMENTS PM TMAS AMCPM TMA 120 PICATINNY ARSENAL NJ 07806-5000
1	PEO ARMAMENTS PM TMAS AMCPM TMA AS H YUEN PICATINNY ARSENAL NJ 07806-5000
2	COMMANDER ARDEC AMSTA AR CCH V C MANDALA E FENNELL PICATINNY ARSENAL NJ 07806-5000
1	COMMANDER ARDEC AMSTA AR CCH T L ROSENDORF PICATINNY ARSENAL NJ 07806-5000
1	COMMANDER ARDEC AMSTA AR CCS PICATINNY ARSENAL NJ 07806-5000
1	COMMANDER ARDEC AMSTA AR AEE J LANNON PICATINNY ARSENAL NJ 07806-5000
11	COMMANDER ARDEC AMSTA AR AEE B A BEARDELL D DOWNS S EINSTEIN S WESTLEY S BERNSTEIN J RUTKOWSKI B BRODMAN P OREILLY R CIRINCIONE P HUI J OREILLY PICATINNY ARSENAL NJ 07806-5000

NO. OF COPIES	ORGANIZATION
5	COMMANDER ARDEC AMSTA AR AEE WW M MEZGER J PINTO D WIEGAND P LU C HU PICATINNY ARSENAL NJ 07806-5000
1	COMMANDER ARDEC AMSTA AR AES S KAPLOWITZ PICATINNY ARSENAL NJ 07806-5000
1	COMMANDER ARDEC AMSTA AR HFM E BARRIERES PICATINNY ARSENAL NJ 07806-5000
1	COMMANDER ARDEC AMSTA AR FSA F LTC R RIDDLE PICATINNY ARSENAL NJ 07806-5000
1	COMMANDER ARDEC AMSTA AR FSC G FERDINAND PICATINNY ARSENAL NJ 07806-5000
1	COMMANDER ARDEC AMSTA AR FS T GORA PICATINNY ARSENAL NJ 07806-5000
1	COMMANDER ARDEC AMSTA AR FS DH J FENECK PICATINNY ARSENAL NJ 07806-5000

NO. OF COPIES	ORGANIZATION
3	COMMANDER ARDEC AMSTA AR FSS A R KOPMANN B MACHEK L PINDER PICATINNY ARSENAL NJ 07806-5000
1	COMMANDER ARDEC AMSTA AR FSN N K CHUNG PICATINNY ARSENAL NJ 07806-5000
2	DIRECTOR BENET WEAPONS LAB AMSTA AR CCB RA G A PFLEGL AMSTA AR CCB S F HEISER WATERVLIET NY 12189-4050
2	COMMANDER US ARMY RSRCH OFC TECH LIB D MANN PO BOX 12211 RESEARCH TRIANGLE PARK NC 27709-2211
1	DIRECTOR US ARMY RSRCH OFC AMXRO MCS K CLARK PO BOX 12211 RESEARCH TRIANGLE PARK NC 27709-2211
1	DIRECTOR US ARMY RSRCH OFC AMXRO RT IP LIBRARY SERVICES PO BOX 12211 RESEARCH TRIANGLE PARK NC 27709-2211

NO. OF COPIES	ORGANIZATION
1	COMMANDER USACECOM R&D TECH LIB ASQNC ELC IS L R MYER CENTER FORT MONMOUTH NJ 07703-5301
1	COMMANDANT US ARMY AVIATION SCHOOL AVIATION AGENCY FORT RUCKER AL 36360
1	PM US TANK AUTOMOTIVE CMD FIGHTING VEHICLE SYS SFAE ASM BV WARREN MI 48397-5000
1	PM ABRAMS TANK SYS SFAE ASM AB WARREN MI 48397-5000
1	DIRECTOR HQ TRAC RPD ATCD MA FORT MONROE VA 23651-5143
1	COMMANDER US ARMY BELVOIR RSRCH DEVELOPMENT CTR STRBE WC FORT BELVOIR VA 22060-5006
1	DIRECTOR US ARMY TRAC ATRC L MR CAMERON FORT LEE VA 23801-6140
1	COMMANDANT US ARMY CMD & GENERAL STAFF COLLEGE FORT LEAVENWORTH KS 66027
1	COMMANDANT US ARMY SPECIAL WARFARE SCHOOL REV AND TRNG LIT DIV FORT BRAGG NC 28307

NO. OF COPIES	ORGANIZATION
1	COMMANDER RADFORD ARMY AMMUNITION PLANT AMSTA AR QA HI LIB RADFORD VA 24141-0298
2	COMMANDANT US ARMY FIELD ARTILLERY CTR & SCHOOL ATSF CO MW E DUBLISKY ATSF CN P GROSS FORT SILL OK 73503-5600
1	COMMANDANT US ARMY ARMOR SCHOOL ATZK CD MS M FALKOVITCH ARMOR AGENCY FORT KNOX KY 40121-5215
1	US ARMY EUROPEAN RSRCH OFC USARDSG UK BOX 65 FPO NY 09510-1500
2	COMMANDER NSSC SEA 62R SEA 64 WASHINGTON DC 20362-5101
1	COMMANDER NASC AIR 954 TECH LIB WASHINGTON DC 20360
4	COMMANDER NATL RSRCH LAB TECH LIB CODE 4410 K KAILASANATE J BORIS E ORAN WASHINGTON DC 20375-5000
1	OFC OF NAVAL RSRCH CODE 473 R S MILLER 800 N QUINCY ST ARLINGTON VA 22217-9999

NO. OF COPIES	ORGANIZATION
1	OFC OF NAVAL TECH ONT 213 D SIEGEL 800 N QUINCY ST ARLINGTON VA 22217-5000
9	COMMANDER NSWC T C SMITH K RICE S MITCHELL S PETERS J CONSAGA C GOTZMER R BERNECKER TECH LIB CODE 730 INDIAN HEAD MD 20640-5000
4	COMMANDER NSWC CODE G30 GUNS & MUNITIONS DIV CODE G32 GUNS SYS DIV CODE G33 T DORAN CODE E23 TECH LIB DAHLGREN VA 22448-5000
5	COMMANDER NAWC CODE 388 C PRICE T BOGGS CODE 3895 T PARR R DERR INFO SCIENCE DIV CHINA LAKE CA 93555-6001
1	COMMANDING OFC NAVAL UNDERWATER SYS CTR CODE 5B331 TECH LIB NEWPORT RI 02840
1	OLAC PL TSTL D SHIPLETT EDWARDS AFB CA 93523-5000

NO. OF COPIES	ORGANIZATION
3	AL LSCF J LEVINE L QUINN T EDWARDS EDWARDS AFB CA 93523-5000
1	WL MNAA B SIMPSON EGLIN AFB FL 32542-5434
1	WL MNME ENERGETIC MATERIALS BRANCH 2306 PERIMETER RD STE 9 EGLIN AFB FL 32542-5910
1	WL MNSH R DRABCZUK EGLIN AFB FL 32542-5910
2	NASA LANGLEY RSRCH CTR M S 408 W SCALLION D WITCOFSKI HAMPTON VA 23605
1	CENTRAL INTEL AGENCY OFC OF THE CENT REF DISSEM BRNCH ROOM GE 47 HQS WASHINGTON DC 20502
1	CENTRAL INTEL AGENCY J BACKOFEN NHB ROOM 5N01 WASHINGTON DC 20505
2	HQ DNA D LEWIS A FAHEY 6801 TELEGRAPH RD ALEXANDRIA VA 22310-3398
1	DIRECTOR SANDIA NATL LAB ENERGETIC MAT & FLUID MECH DEPT 1512 M BAER PO BOX 5800 ALBUQUERQUE NM 87185

NO. OF COPIES	ORGANIZATION
1	DIRECTOR SANDIA NATL LAB COMBUSTION RSRCH FACILITY R CARLING LIVERMORE CA 94551-0469
1	DIRECTOR SANDIA NATL LAB G A BENEDITTI 8741 PO BOX 969 LIVERMORE CA 94551-0969
2	DIRECTOR LAWRENCE LIVERMORE NATL LAB L 355 A BUCKINGHAM M FINGER PO BOX 808 LIVERMORE CA 94550-0622
2	DIRECTOR LOS ALAMOS SCIENTIFIC LAB T3 D BUTLER M DIV B CRAIG PO BOX 1663 LOS ALAMOS NM 87544
1	BATTELLE TWSTIAC V LEVIN 505 KING AVENUE COLUMBUS OH 43201-2693
1	BATTELLE PNL M C C BAMPTON PO BOX 999 RICHLAND WA 99352
1	INST OF GAS TECH D GIDASPOW 3424 S STATE ST CHICAGO IL 60616-3896
1	INST FOR ADVANCED TECH T KIEHNE THE UNIV OF TX AT AUSTIN 4030 2 W BRAKER LN AUSTIN TX 78759-5329

NO. OF COPIES	ORGANIZATION
2	CPIA JHU H J HOFFMAN T CHRISTIAN 10630 LITTLE PATUXENT PKWY STE 202 COLUMBIA MD 21044-3200
1	BRIGHAM YOUNG UNIV DEPT OF CHEMICAL ENGNRG M BECKSTEAD PROVO UT 84601
1	JET PROPULSION LAB CA INST OF TECH L D STRAND MS 125 224 4800 OAK GROVE DR PASADENA CA 91109
1	CA INST OF TECH 204 KARMAN LAB MAIN STOP 301 46 F E C CULICK 1201 E CALIFORNIA ST PASADENA CA 91109
3	GA INST OF TECH SCHOOL OF AEROSPACE ENGNRG B ZIM E PRICE W STRAHLE ATLANTA GA 30332
1	MA INST OF TECH DEPT OF MECH ENGNRG T TOONG 77 MASSACHUSETTS AVE CAMBRIDGE MA 02139-4307
2	UNIV OF IL DEPT OF MECH INDUSTRY ENGNRG H KRIER R BEDDINI 144 MEB 1206 N GREEN ST URBANA IL 61801-2978
1	UNIV OF MA DEPT OF MECH ENGNRG K JAKUS AMHERST MA 01002-0014

NO. OF COPIES	ORGANIZATION
1	UNIV OF MI DEPT OF MECH ENGNRG E FLETCHER MINNEAPOLIS MN 55414-3368
3	PENN STATE UNIV DEPT OF MECH ENGNRG V YANG K KUO G SETTLES UNIVERSITY PARK PA 16802-7501
1	RENSSELAER POLYTECHNIC INST DEPT OF MATHEMATICS TROY NY 12181
1	STEVENS INST OF TECH DAVIDSON LAB R MCALEVY III CASTLE POINT STATION HOBOKEN NJ 07030-5907
1	RUTGERS UNIV DEPT OF MECH & AEROSPACE ENGNRG S TEMKIN UNIV HEIGHTS CAMPUS NEW BRUNSWICK NJ 08903
1	UNIV OF SOUTHERN CA MECH ENGNRG DEPT 0HE200 M GERSTEIN LOS ANGELES CA 90089-5199
1	UNIV OF UT DEPT OF CHEM ENGNRG A BAER SALT LAKE CITY UT 84112-1194
1	WASHINGTON STATE UNIV DEPT OF MECH ENGNRG C CROWE PULLMAN WA 99163-5201
1	AFELM THE RAND CORP LIBRARY D 1700 MAIN ST SANTA MONICA CA 90401-3297

NO. OF COPIES	ORGANIZATION
1	ARROW TECH ASSOC INC W HATHAWAY PO BOX 4218 S BURLINGTON VT 05401-0042
3	AAI CORP J HEBERT J FRANKLE D CLEVELAND PO BOX 126 HUNT VALLEY MD 21030-0126
1	ALLIANT TECHSYSTEMS INC R TOMPKINS 7225 NORTHLAND DR BROOKLYN PARK MN 55428
1	TEXTRON A PATRICK 2385 REVERE BEACH PKWY EVERETT MA 02149-5900
1	GENERAL APPLIED SCIENCES LAB J ERDOS 77 RAYNOR AVE RONKONKAMA NY 11779-6649
1	GENERAL ELECTRIC CO TACTICAL SYS DEPT J MANDZY 100 PLASTICS AVE PITTSFIELD MA 01201-3698
1	IITRI M KLEIN 10 W 35TH ST CHICAGO IL 60616-3799
4	HERCULES INC RADFORD ARMY AMMO PLANT L GIZZI D WORRELL W WORRELL C CHANDLER RADFORD VA 24141-0299

NO. OF COPIES	ORGANIZATION
2	HERCULES INC ALLEGHENY BALLISTICS LAB W WALKUP T F FARABAUGH PO BOX 210 ROCKET CENTER WV 26726
1	HERCULES INC AEROSPACE R CARTWRIGHT 100 HOWARD BLVD KENVILLE NJ 07847
1	HERCULES INC HERCULES PLAZA B M RIGGLEMAN WILMINGTON DE 19894
1	MBR RSRCH INC MOSHE BEN REUVEN 601 EWING ST STE C 22 PRINCETON NJ 08540
1	OLIN CORP BADGER ARMY AMMO PLANT F E WOLF BARABOO WI 53913
3	OLIN ORDNANCE E KIRSCHKE A GONZALEZ D WORTHINGTON PO BOX 222 ST MARKS FL 32355-0222
1	OLIN ORDNANCE 10101 9TH ST NORTH ST PETERSBURG FL 33716
1	PAUL GOUGH ASSOC INC P GOUGH 1048 SOUTH ST PORTSMOUTH NH 03801-5423
1	PHYSICS INTL LIB H WAYNE WAMPLER PO BOX 5010 SAN LEANDRO CA 94577-0599

NO. OF COPIES	ORGANIZATION
2	PRINCETON COMBUSTION RSRCH LAB INC N MER N MESSINA PRINCETON CORP PLAZA 11 DEERPARK DR BLDG IV STE 119 MONMOUTH JUNCTION NJ 08852
1	SAIC M PALMER 1410 SPRING HILL RD SUITE 400 MCLEAN VA 22102
1	SOUTHWEST RSRCH INSTITUTE J RIEGEL 6220 CULEBRA RD PO DRAWER 28510 SAN ANTONIO TX 78228-0510
1	SVERDRUP TECH INC J DEUR 2001 AEROSPACE PKWY BROOK PARK OH 44142
3	THIOKOL CORP ELKTON DIV R WILLER R BIDDLE TECH LIB PO BOX 241 ELKTON MD 21921-0241
3	VERITAY TECH INC E FISHER R SALIZONI J BARNES 4845 MILLERSPORT HWY EAST AMHERST NY 14501-0305
1	UNIV PROPULSION CO H MCSPADDEN 25401 N CENTRAL AVE PHOENIX AZ 85027-7837
1	SRI INTL PROPULSION SCIENCES DIV TECH LIB 333 RAVENWOOD AVE MENLO PARK CA 94025-3493

NO. OF COPIES	ORGANIZATION
1	KELLER CONSULTING INC G KELLER 265 CHARLOTTE ST NO 10 ASHEVILLE NC 28801-1400
1	PRIMEX E STEINER DIR LARGE CAL R & D PO BOX 127 RED LION PA 17356
	ABERDEEN PROVING GROUND
17	DIR USARL AMSRL WM B A HORST W OBERLE AMSRL WM BC P PLOSTINS B GUIDOS AMSRL WM BD M BUNDY T MINOR T COFFEE C LEVERITT L M CHANG J COLBURN P CONROY M NUSCA A BRANT M MCQUAID B FORCH C CHABALOWSKI AMSRL WM TB D KOOKER

INTENTIONALLY LEFT BLANK.

REPORT DOCUMENTATION PAGE

Form Approved
OMB No. 0704-0188

1. AGENCY USE ONLY *(Leave blank)*	2. REPORT DATE	3. REPORT TYPE AND DATES COVERED
	February 2001	Final, March 1986 - December 1987

4. TITLE AND SUBTITLE
Interior Ballistics Modeling: Extensions to the One-Dimensional XKTC Code and Analytical Studies of Pressure Gradient for Lumped Parameter Codes

5. FUNDING NUMBERS
CR: DAAK11-85-D-0002

6. AUTHOR(S)
Paul S. Gough

7. PERFORMING ORGANIZATION NAME(S) AND ADDRESS(ES)
Paul Gough Associates
1048 South Street
Portsmouth, NH 03801-5423

8. PERFORMING ORGANIZATION REPORT NUMBER
ARL-CR-460

9. SPONSORING/MONITORING AGENCY NAMES(S) AND ADDRESS(ES)
U.S. Army Research Laboratory
ATTN: AMSRL-WM-BD
Aberdeen Proving Ground, MD 21005-5066

10.SPONSORING/MONITORING AGENCY REPORT NUMBER

11. SUPPLEMENTARY NOTES
Point of contact for this report is Mr. Paul J. Conroy, U.S. Army Research Laboratory, ATTN: AMSRL-WM-BD, Aberdeen Proving Ground, MD 21005-5066.

12a. DISTRIBUTION/AVAILABILITY STATEMENT
Approved for public release; distribution is unlimited.

12b. DISTRIBUTION CODE

13. ABSTRACT*(Maximum 200 words)*

We describe a number of extensions to the XNOVAKTC (XKTC) code, a model of interior ballistics phenomena based on a numerical solution of the governing equations for one-dimensional, multi-phase flow. We also present some analytical formulations for the pressure gradient in a gun in a form suitable for incorporation into a lumped parameter interior ballistics model.

In XKTC, the flow resistance formula for stacked-granular propellant is extended to account for the increase in drag due to tumbling of the grains as the bed expands. The code is also extended to permit the analysis of the consequences of propellant fracture, with fracture taken to be dependent on the local maximum intergranular stress. An explicit representation of the impact induced granular compaction wave as a surface of discontinuity is encoded to support the fracture analysis.

The analytical formulas for the pressure gradient include the effects of tube geometry and several aspects of the structure of the two-phase flow. The results are in a closed form with the breech and base pressure explicitly related to the spacemean pressure. Results are presented for both granular and stick propelling charges.

14. SUBJECT TERMS	15. NUMBER OF PAGES
interior ballistics, multi-phase flow, Lagrange formulation	171
	16. PRICE CODE

17. SECURITY CLASSIFICATION OF REPORT	18. SECURITY CLASSIFICATION OF THIS PAGE	19. SECURITY CLASSIFICATION OF ABSTRACT	20. LIMITATION OF ABSTRACT
UNCLASSIFIED	UNCLASSIFIED	UNCLASSIFIED	UL

INTENTIONALLY LEFT BLANK.

USER EVALUATION SHEET/CHANGE OF ADDRESS

This Laboratory undertakes a continuing effort to improve the quality of the reports it publishes. Your comments/answers to the items/questions below will aid us in our efforts.

1. ARL Report Number/Author ARL-CR-460 (POC: Conroy) Date of Report February 2001

2. Date Report Received _____

3. Does this report satisfy a need? (Comment on purpose, related project, or other area of interest for which the report will be used.) _____

4. Specifically, how is the report being used? (Information source, design data, procedure, source of ideas, etc.) _____

5. Has the information in this report led to any quantitative savings as far as man-hours or dollars saved, operating costs avoided, or efficiencies achieved, etc? If so, please elaborate. _____

6. General Comments. What do you think should be changed to improve future reports? (Indicate changes to organization, technical content, format, etc.) _____

CURRENT ADDRESS

_____
Organization

_____
Name E-mail Name

_____
Street or P.O. Box No.

_____
City, State, Zip Code

7. If indicating a Change of Address or Address Correction, please provide the Current or Correct address above and the Old or Incorrect address below.

OLD ADDRESS

_____
Organization

_____
Name

_____
Street or P.O. Box No.

_____
City, State, Zip Code

(Remove this sheet, fold as indicated, tape closed, and mail.)

(DO NOT STAPLE)

DEPARTMENT OF THE ARMY

OFFICIAL BUSINESS

NO POSTAGE
NECESSARY
IF MAILED
IN THE
UNITED STATES

BUSINESS REPLY MAIL
FIRST CLASS PERMIT NO 0001,APG,MD

POSTAGE WILL BE PAID BY ADDRESSEE

DIRECTOR
US ARMY RESEARCH LABORATORY
ATTN AMSRL WM BD
ABERDEEN PROVING GROUND MD 21005-5066